NTNU – Trondheim
Norwegian University of
Science and Technology

Physiological Function of Cyanobacterial Methionine Sulfoxide Reductase

Jhonne Anderson Uy

Biotechnology
Submission date: May 2015
Supervisor: Martin Frank Hohmann-Marriott, IBT

Norwegian University of Science and Technology
Department of Biotechnology

Abstract

Methionine is a sulfur-containing amino acid which is susceptible to oxidation by Reactive Oxygen Species (ROS). Oxidation of methionine could lead to protein denaturation; with methionine itself turning into methionine sulfoxide (MetSO), a radical which further damages other cellular components. To prevent these damages, the cell uses antioxidizing enzymes which reduce MetSO back to methionine. These enzymes are called methionine sulfoxide reductase (MSR). MSR is divided into two types which correspond to each MetSO diastereomers. The first type is MSRA which shows specificity towards S-MetSO, while the second is MSRB to R-MetSO. These MSR genes are highly conversed and widely distributed amongst the animal and plant kingdom, suggesting their importance in the repair of oxidative damage. The cyanobacterium, *Synechocystis* PCC 6803 (PCC 6803), contains two MSRA (slr1795 and sll1394) and one MSRB. The function of these MSRs for this organisms' physiology, however, is still poorly defined. The main objective of this research was to therefore characterize MSRs functionality in PCC 6803. In order to do so, two mutant strains lacking either the slr1795 or sll1394 MSRA were generated. These mutant strains were then exposed to moderate and high-light intensity experiments with ROS promoting plate conditions to induce oxidative stress. Parameters such as growth rate and doubling time, degree of pigmentation, chlorophyll and carotenoid levels, and colonial morphology were quantified to determine the effect of MSRAs partial absence on the cells' physiology.

Analysis of the experiments revealed that partial absence of MSRA did not necessarily affect the cells overall survivability against oxidative damage; mainly because of the cells many layers of defense against ROS. However, the data gathered from the experiments seem to indicate that the mutant strains were experiencing more stress in comparison to the wild type. In particular, the Δsll1394 strain displayed elevated stress levels on two experiments; the first one being in the high-light experiment, and the second on chlorophyll and carotenoid measurements. Strains exposed to high-light and grown on glucose displayed a decrease in cell density and enter a lag time after 100 hours of incubation, before being able to recover again. Deletion of the sll1394 gene seem to prolong this lag time, suggesting slower repair of the damaged done by ROS. In addition, the Δsll1394 strain also had higher levels of carotenoid in comparison to the other two strains, indicating more sensitivity towards high-light. In summary, the gathered results only gave an initial insight of MSRAs repair and protective functionalities in PCC 6803. Further experiments, such as generation of a double deletion strain, are needed to give a more detailed analysis.

Sammendrag

Methionin er en svovelholdig aminosyre som er følsom for oksidasjon av reaktive oksygenarter (ROS). Oksidasjon av metionin kan føre til denaturering av proteiner; der selve metionin blir til metioninsvoveloksid (MetSO), et radikal som videre skader andre cellulære komponenter. For å forhindre disse skadene, benytter cellen antioksiderende enzymer som reduserer MetSO tilbake til Methionin. Disse enzymene er kalt for metioninsvoveloksidreduktase (MSR). MSR er delt inn i to typer som samsvarer med hvert sitt MetSO diastereomerer. Den første typen er MSRA som viser spesifisitet mot S-MetSO, mens den andre er MSRB til R-MetSO. Disse MSR genene er sterk bevart og svært utbredt blant dyre- og planteriket, noe som tyder på deres betydning i reparasjon av oksidasjonsskade. Cyanobacterium, Synechocystis PCC 6803 (PCC 6803), inneholder to MSRA (slr1795 og sll1394) og ett MSRB enzym. Likevel er den fysiologiske funksjonen til disse enzymene fremdeles dårlig definert for denne organismen. Hovedmålet med denne forskningen var derfor å karakterisere MSRs funksjonalitet i PCC 6803. For å kunne gjøre dette, ble to mutantstammer som mangler enten slr1795 eller sll1394 MSRA generert. Disse mutantstammene ble deretter utsatt for moderate og sterkt lysintensitet eksperimenter med ROS framkallende platevilkår for å indusere oksidasjonsstress. Parametere som veksthastighet og fordoblingstid, grad av pigmentering, klorofyll og karotenoid nivåer, og kolonimorfologi ble kvantifisert for å bestemme konsekvensen av MSRAs delvis fravær på cellens fysiologi.

Analysen av eksperimentene viste at delvis fravær av MSRA ikke nødvendigvis påvirket cellenes generelle overlevelsesevne mot oksidasjonsskade. Dette var hovedsakelig på grunn av cellenes mange lag av forsvar mot ROS. Likevel har samlet data fra forsøkene tydet på at mutantstammene opplevde mer stress i forhold til villtypen. Spesielt Δsll1394 har vist forhøyet stressnivå på to eksperimenter, med den første i sterkt lyseksperimentet, og den andre på klorofyll og karotenoid målingene. Stammene utsatt for sterkt lys og dyrket på glukose viste en nedgang i celletettheten, og gikk inn en stasjonærperiode etter 100 timers inkubasjon, før den kunne vokse igjen. Delesjon av sll1394 genet så ut til å forlenge denne stasjonærperioden, noe som tyder på langsommere reparasjon av skadene gjort av ROS. I tillegg, hadde Δsll1394 stammen også høyere nivåer av karotenoid i forhold til de to andre stammer, noe som indikerer mer sensitivitet mot sterkt lys. For å oppsummere, de innsamlede resultatene ga en første innsikt av MSRAs reparasjon og beskyttende funksjoner i PCC 6803. Videre eksperimenter som for eksempel generering av en dobbel delesjons stamme, må utføres for å gi en mer detaljert analyse.

Acknowledgements

People often say no man is an island; that a helping hand is always a welcome sight. The same could be said with the completion of this project. I would like to extend my gratitude to the Institute of Biotechnology and to the people of Photosynlab for their support during the duration of this Master's project. To my advisor, Professor Martin F. Hohmann-Marriott, I would like to thank you for introducing me to the fascinating world of photoautotrophs; and for your constant guidance throughout the project. You have always managed to motivate me when everything seems to be going wrong in the lab. Your enthusiasm for science and overall curiosity is something I would like to have in the future. I would also like to thank PhD student Jacob Lamb, for always giving me clever tips. It was always a fun surprise to learn simple yet efficient alternative lab techniques from you.

I would also like to thank my lab mates and friends for being there to listen and share their thoughts when laboratory work became overwhelming. I would certainly miss the small fun conversations we've had, and our after-school activities. The challenges in life always have a way in bringing people together, and that's good.

Finally and most importantly, I would like to my mom for always being there, for always encouraging me to pursue what I want in life and for constantly challenging me to reach new heights. You will always be my inspiration in life, and the foundation of my wisdom.

Contents

Chapter 1: Introduction

1. Photosynthesis

1.1) Introduction

Much of life in its present form would not have been possible during the early stages of life on our planet, with Earth being in a different state. The atmosphere of the early Earth was anoxic, the temperature was too hot, and the radiation levels lethal (Kasting, 1993). Nevertheless, life emerged, but it was not until the emergence of photosynthetic organisms around 2.0 Ga that life started to bloom. These organisms contributed to the slow but steady rise of oxygen levels in the planet (Holland, 2006). This event, alongside other planetary changes (Barley, 2005), eventually triggered the great oxygenation period around 2.2-2.3 Ga, forming the ozone layer and giving way to the development of more complex organisms. Truly, the emergence of these organisms and photosynthesis had a great impact in the development of life here on Earth.

Photosynthesis is basically the conversion of light energy into chemical energy. In oxygenic photoautotrophs as plants, algae and cyanobacteria, this mainly involves the use of light as an energy source, carbon dioxide (CO_2) as a carbon source, and water (H_2O) as an electron donor; producing glucose and oxygen (O_2) as byproducts.

$$6CO_2 + 6H_2O \rightarrow C_6H_{12}O_6 + 6O_2$$

In plants, this process occurs within the chloroplasts, which contain the thylakoids and the stroma. The thylakoids are disc like membrane-bound components were the light dependent reactions occur (Stanier and Cohen-Bazire, 1977). This is where light is captured and energy is generated in the form of ATP and NADPH. These two energy carriers are used to power the production of glucose through the Calvin cycle in the stroma, the fluid surrounding the thylakoids.

Cyanobacteria are the progenitors of chloroplasts. Cyanobacteria also possess thylakoids that mediate the light-dependent reactions. Carbon fixation in cyanobacteria occurs in the cytoplasm, which is equivalent to stroma of chloroplasts.

1.2) Light Reaction

Photosynthesis can be functionally divided into two main parts: the light reaction and the dark reaction, which compromises the so called Calvin Cycle. In the light reaction, photons of light are first captured by chlorophyll, alongside other pigments, within a light-harvesting antenna complex. Captured light energy is then delivered to reaction centers which power the transfer of electrons throughout the electron transport chain.

1.2.1) Reaction Centers

Reaction centers are large complexes consisting of proteins, pigments and cofactors necessary for electron transport. Two types of reaction centers can be found within the electron transport chain of plants and cyanobacteria, Photosystem I (PSI) and Photosystem II (PSII). Each contain a primary electron donor chlorophyll which reduces a nearby primary electron acceptor upon excitation. This will start a chain of redox events ultimately ending in the production of ATP and NADPH. The process was first proposed by R. Hill and F. Bendall (1960) and it can be schematically visualized as the Z-scheme.

1.2.2) The Z-scheme

The Z-scheme is a schematic representation of the photosynthetic process, in which the sequence of redox midpoint potentials of all electron carriers is indicated. The Z-pattern arises from the presence of two photochemical reactions (Blankenship, 2014). The first photochemical process occurs in PSII when light energy excites the primary donor chlorophylls, P680 to P680*. These chlorophylls then transfer an electron to the primary acceptor, pheophytin. The lost electrons are then replaced by the photolysis of water by an oxygen evolving complex, thus reducing the cationic $P680^{+}$ back to its' non-ionic ground state.

From pheophytin, the electrons are first transferred to a tightly bound plastoquinone A molecule (Q_A) before being transferred to a more loosely bound variant, plastoquinone B (Q_B). The difference is that Q_A can only transfer one electron at a time, while Q_B can receive two electrons, before it leaves PSII and becomes part of the PQ pool. During the reduction and oxidation of plastoquinol, protons are transferred from the stroma/cytosol into the thylakoid lumen (Pospíšil, 2009). Electrons are then carried to a protein complex called cytochrome ***b_6f*** *complex* which catalyzes the electron transfer from plastoquinol to another electron carrier, plastocyanin. The cytochrome ***b_6f*** *complex* also acts as a proton pump and thereby contributes to the proton gradient between the thylakoid lumen and the stroma or cytoplasm. These protons are later used to power the phosphorylation of ADP to ATP by ATP synthase.

The second photochemical process occurs in PSI and is similar to PSII. It too has a set of primary donor chlorophylls, P700 which absorbs light in the 700 nm range. Once excited, PSI passes electrons to an early electron acceptor, Chlorophyll A_0, before getting reduced back by electrons from plastocyanin. The electron then travels from A_0 to the next electron acceptor, phylloquinone A_1, followed by iron-sulfur clusters (Fx,Fa,Fb) and ferredoxin (Fd). Ferredoxin facilitates the transfer of electrons to ferredoxin-NADP+ reductase (FNR); the enzyme that reduces $NADP^{+}$ to NADPH.

2. Reactive Oxygen Species

Reactive oxygen species (ROS) are unstable and reactive molecules generated as byproducts of oxygen reduction or energization. ROS are produced during the light-dependent reactions in photosynthesis (Latifi *et. al.,* 2008). ROS are very strong oxidizing agents which interact and damage proteins, lipids and nucleic acids, which in turn, can generate other radicals that further damage the cell.

Oxygen while being in its ground state will contain two unpaired spin-aligned electrons on its pi antibonding orbital (Fig 1.1). Because of its chemical structure, it is only able to take up one electron at a time (spin-restriction); and is considered a weak electron acceptor which cannot fully oxidize lipids, amino acids and nucleic acids (Krieger-Liszkay, 2004; Imlay, 2003). However, partial reduction or over excitation of oxygen will cause it to be unstable; eventually causing the formation of ROS. Singlet oxygen ($^1O_2$), superoxide anion (O_2^-), hydrogen peroxide (H_2O_2) and hydroxyl radical (OH·) are four notable ROS which have distinct effects within the cell. (Latifi *et. al.*, 2008).

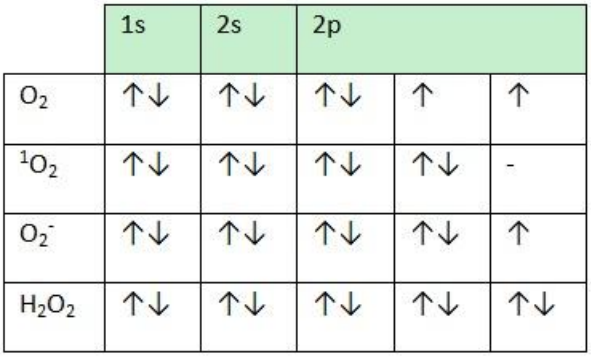

Figure 1.1 - Molecular orbital of oxygen with corresponding electron configuration and spin: O_2 is shown on its' ground triplet-state on the 2p orbital, $^1O_2$ with an energized single-state, O_2^- with an extra electron, and $H_2O_2$with two extra electrons. From Imlay, 2003.

2.1) Singlet Oxygen

Singlet oxygen is generated during high-light intensity exposure, wherein collected energy from harvested light exceeds its utilization during carbon fixation. Transfer of excitation energy from pigments within the light harvesting complexes or reaction centers to oxygen will cause one of oxygen's unpaired electrons to reverse its spin. This leads to the removal of oxygen's spin restriction making it highly reactive, and thus damage cellular components within its vicinity (Krieger-Liszkay, 2004; Latifi *et. al.*, 2008).

2.2) Superoxide Anion

The univalent reduction of O_2 in PSI causes it to be negatively charged with an unpaired electron, thus forming superoxide anion (O_2^-). This mostly occurs during high-light intensity when O_2 is used as an electron acceptor instead of NADP. This reaction was observed in chloroplast by Mehler in 1951, and was therefore named Mehler reaction.

O_2^- can also be formed when O_2 accidentally collides with en electron during its transfer in between enzymes and secondary substrates (Imlay, 2003). An example would be a collision between O_2 and an electron during transfer from ferredoxin to FNR.

2.3) Hydrogen Peroxide and Hydroxyl Radical

Disproportionation of O_2^- by superoxide dismutase will eventually yield hydrogen peroxide (H_2O_2) and O_2; wherein H_2O_2 is safely converted to H_2O by catalases and peroxidases. Reduced enzymatic activity or complete inactivation of these enzymes however, may cause H_2O_2 build-up (Latifi *et. al.*, 2008).

The hydroxyl radical (OH·) is generated through a process called the Fenton Reaction. For example, the reduction of the iron clusters by O_2^- would release Fe^{2+}, which then cuts the oxygen bonds in H_2O_2 producing OH· and OH^- as a product (Imlay, 2003; Castano *et. al.,* 2004).

$$H_2O_2 + Fe^{2+} \rightarrow OH^- + FeO^{2+} + H^+ \rightarrow Fe^{3+} + OH^- + OH$$

2.4) Oxidative Stress in Cyanobacteria

Oxidative stress mainly occurs when an organisms antioxidative defense mechanism fail to cope with the generated ROS or radicals, therefore leading to cellular damage or even death (Latifi *et. al.*, 2008). In cyanobacteria, this specially occurs during high-light intensity situations wherein light-energy harvested exceeds the energy requirements of carbon fixation.

One example of oxidative stress would be the photoinhibition of PSII. A study by Nishiyama et al., 2004 suggest that although $^1O_2$ does not directly damage PSII, it inhibits its repair during severe light intensity. It does so by inhibiting the translational elongation of *psb*A mRNA which encodes for the D1 protein; a photochemical reaction center in PSII (Allakhverdiev, 2004). A more recent study also indicates that $^1O_2$ also targets the Mn complex in oxygen evolving species of PSII (Murata *et. al.,* 2007).

O_2^-, alongside H_2O_2, is known to target iron-sulfur clusters within a cell. One specified target group are cysteine molecules which can either be oxidized to its sulfenic form, and or further oxidized to its sulfinic form. Sulfenic cysteine can react with other cysteine molecules forming disulfide bridges which can compromise certain protein/enzymes (Imlay, 2003). Another target group is methionine residues which can be oxidized to methionine sulfoxide (Tarrago *et. al*, 2009).

Last but not least, enzymes containing iron clusters are inactivated by O_2^- by its oxidization of one of the iron atoms in the enzymes' active site (Imlay, 2003). O_2^- can also oxidize, and thereby, inactivate catalase and peroxidase which safely reduces H_2O_2 to H_2O.

2.5) Defense against Oxidative Stress

Since ROS are generated as a part of the photosynthetic activity, cyanobacteria are in constant need to defend themselves against oxidative stress. For this, several mechanisms have been developed to either scavenged ROS with antioxidizing agents/ enzymes, or to prevent its' initial generation.

2.5.1) Energy Dissipation

The energy dissipation in photoautotrophs is a preventive measure wherein excess light-energy is converted into something unharmful, thus preventing the generation of ROS. In plants, excess light energy is dissipated as heat by non-photochemical quenching (NPQ) of the light-harvesting complexes (LHCII) in PSII. NPQ is a two-step process wherein in, (1) carotenoids are first modified in order to absorb light energy better, (2) and that LHCII undergoes a conformational change that redirects light-energy towards the converted carotenoids instead of chlorophyll a/b, therefore preventing its use (Szabó *et. al.,* 2005).

Although cyanobacteria lack LHCII, Latifi *et. al.,* 2008 did a review which suggests three mechanisms in which cyanobacteria can also perform energy dissipation. The first mechanism resembles NPQ of LHCII in plants, in the way that cyanobacteria produce orange carotenoid proteins (OCP) to quench excitation energy in its phycobilisomes (Kirilovsky, 2007). The second mechanism involves synthesis of high-light inducible proteins (HLIP), alongside CAB-like proteins which absorb and dissipate light energy (Latifi *et. al.,* 2008; Havauex *et. al.,* 2003). A last mechanism is triggered when cyanobacteria undergo an iron starvation and starts producing CP43, a Chl-binding protein which dissipitates energy within a complex it forms with PSI.

2.5.2) Antioxidants

Another defense mechanism photoautotrophs can utilize is the synthesis of antioxidants which can directly react with ROS. Due to their chemical structure, they can quench ROS by electron donation, thereby turning into an intermediate radical that can be safely reduced back to their initial states by other antioxidants or enzymes (Maeda *et. al.,* 2005). Carotenoids are one good example of an antioxidant. In addition for their role in the NPQ of LHCII/phycobilins, they have also been known to quench excited molecules such as singlet oxygen (Blankenship, 2014). In this manner, it serves as both an energy dissipater and an antioxidant.

Organic chemical compounds such as α-Tocopherols may also act as antioxidants. α-Tocopherols function by either directly reacting with ROS thereby minimizing damage, or by obstructing a free radical chain reaction that has been set off by ROS. One example would be lipid peroxidation, wherein OH· reacts with polyunsaturated fatty acids (PUFA) thus producing lipid peroxyl radicals (LOO·). Unless scavenged, LOO· will react with other PUFA to produce more of itself, setting off the chain reaction (Maeda *et. al.,* 2005). Interaction with radicals turn α-Tocopherols to a stable radical that can be safely converted back to its original state by other antioxidants

2.5.3) Enzymatic Defense

In general, three main types of enzymes can be found in photoautotrophs that play an important role against oxidative stress. These are superoxide dismutase (SOD), catalases or peroxidases. SOD is an enzyme that catalyses the disproportion of O_2^- to H_2O_2. Three types of SOD can be found in cyanobacteria, Fe-containing SOD (FeSOD), Mn-containing SOD (MnSOD) and copper-zinc SOD (Cu/ZnSOD); of which, the FeSOD is found to be the most distributed among the species (Touchy and Vermaas, 1999).

Once O_2^- has been converted to H_2O_2, it is then further converted to water and oxygen by either catalases or peroxidase. The difference between the two lies in their catalytic activity; catalase only converts H_2O_2, while peroxidase uses a multitude of substrates (Latifi *et. al.,* 2008). In plants, the most common one is ascorbate-peroxidase; while in cyanobacteria these are glutathione-peroxidase and thiol-dependant peroxidase.

3. Synechocystis sp. PCC 6803

Synechocystis sp. PCC 6803 (PCC 6803) is a non-nitrogen fixing spherical cyanobacterium found in freshwater (Ikeuchi and Tabata, 2001). Amongst all the species of cyanobacteria, it is considered as convenient model organism for the molecular and physiological study of photosynthesis for three reasons: (1) it has the capability to perform phototrophic, mixotrophic and heterotrophic metabolism (Rippka *et. al.,* 1979), making it possible to expose it against various conditions and parameters; (2) it can naturally incorporate exogenous DNA through homologous recombination (Grigorieva and Shestakov, 1982), which facilitates the generation of mutants (3) due to its evolutionary relationship with chloroplasts, it is a model for the chloroplast in higher plants. PCC 6803 was the also first photoautotroph to have its genome fully sequenced and made public in Cyanobase by Kaneko and colleagues in 1996. This opened the door in transcriptomics and proteomics studies (Ikeuchi and Tabata, 2001).

4. Methionine Sulfoxide Reductase

4.1) Introduction

Protein oxidation by ROS can lead to the breakage of polypeptide backbone and/or oxidation of the amino acid side chains, which may result in protein denaturation. Of all amino acid side chains, the ones of cysteine (Cys) and methionine (Met) are the most susceptible to oxidation because of their sulfur residues, which display a high reactivity with ROS (Tarrago *et. al.*, 2009).

The oxidation of Cys can lead to two possible outcomes, with the first one being its conversion to its sulfonic or sulfinic form. The other outcome is the oxidation of its thiol group which leads to the formation of disulfide bonds with a neighboring Cys amino acid.

Methionine oxidation occurs when this amino acid receives an extra oxygen molecule on its sulfur residue, converting Met into methionine sulfoxide (MetSO). Due to its chemical configuration and the location wherein the oxygen molecule reacts, MetSO has a R-MetSO and S-MetSO diastereomers. Both of which can be further irreversibly oxidized to methionine sulfone in the presence of strong oxidants (Hoshi and Heinemann, 2001). Despite being susceptible to oxidation, both cysteines and methionines oxidized forms can be reduced back to their initial state by enzymes or antioxidant proteins. Cys oxidized form can be reduced by thioredoxins, glutaredoxins, and sulfiredoxin, while MetSO is reduced by methionine sulfoxide reductase (MSR) (Davies, 2005).

4.2) MSRA and MSRB

Two types of MSR which correspond to each MetSO diastereomers can be found in almost every organism. The first type is MSRA which show specificity towards S-MetSO, while MSRB to R-MetSO. Tarrago *et.al.,* 2009 reviewed thoroughly the structural differences between the two reductase families, and their genetic distribution across photosynthetic and non-photosynthetic organisms. In particular with cyanobacteria, the difference between the MSR A and B lies in the amount of cysteine residues they have in their active sites. MSRA has two to three cysteine residues, with one being catalytic, while MSRB only has one.

4.2.1) MSR Catalytic Function

Despite the differences in their active sites, both MSR A and B almost follow the same mechanism in reducing MetSO back to Met. In MSRA, the process is divided into 3 major steps: (1) reduction of the sulfur in MetSO by the catalytic cysteine in MSR, thus releasing Met and turning itself into a sulfenic intermediate; (2) formation a disulfide bond between the resolving cysteine and another cysteine residue within the active site, and the release of H_2O; (3) reduction of the disulfide bond by reductants, such as thioredoxin (Lowther *et. al.,* 2000; Boschi-Muller *et. al.,* 2008). Since most MSRB generally have one catalytic cysteine residue, it cannot form disulfide bonds once it reduces MetSO. Instead, it is directly reduced by either thioredoxins or glutaredoxins (Fig 1.2). It is important to note that these reductants are important in maintaining MSRs catalytic activity. This connection is demonstrated by the finding that, thioredoxin, thioredoxin reductase and NADPH, are often coupled with MSRA in most cellular redox systems (Hoshi and Heinemann, 2001; Kumar *et. al.,* 2002).

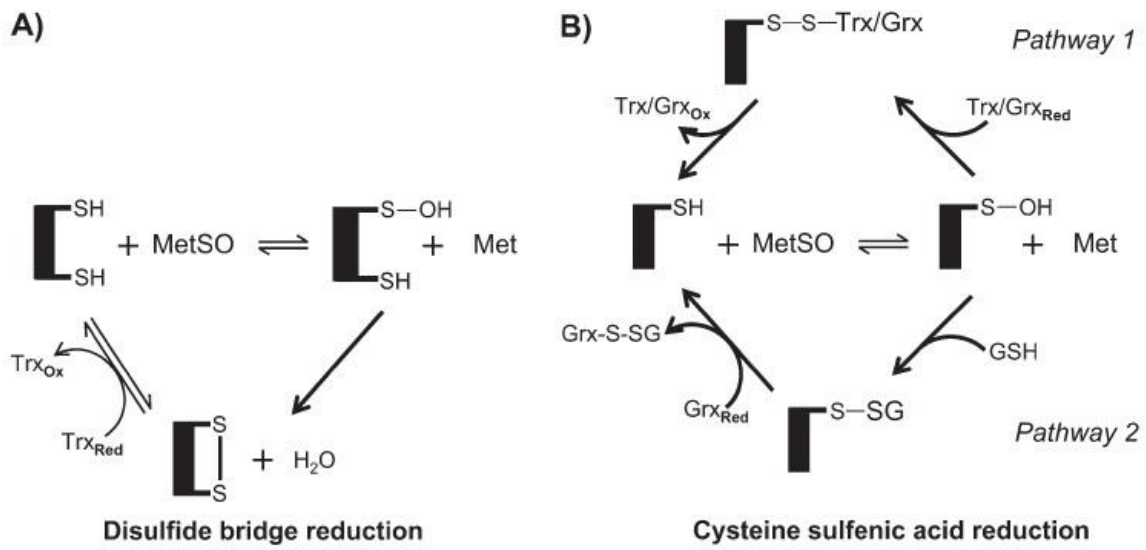

Figure 1.2 - MSRs catalytic pathways: (A) describes MSR with two or more cysteine residues reduce MetSO. This type of catalytic pathway is mostly present on MSRAs. This mainly involves the attack on the methionine radical, formation of an intermediate disulfide bridge between the intermolecular cysteine residues, and reduction of the bridge through thioredoxin or other cofactor systems. (B) Shows the catalytic pathway for MSR containing a singular cysteine residue; mostly present in MSRB. In here, the sulfide bridge intermediate step is skipped, and the resolving cysteine is directly reduced by cofactor systems. From Tarrago *et. al,* (2009).

5. Aim of Research

Methionine oxidation by ROS can lead to protein degradation; and further oxidation of other cellular components by the oxidized methionine radical, methionine sulfoxide. Methionine sulfoxide reductase can reversible reduce MetSO back to methionine; thus playing a crucial role in the protection against ROS and the restoration of biological systems from oxidative damage. Despite being highly conserved and widely distributed amongst organisms, MSRs physiological function has not been defined in the cyanobacterium PCC 6803. The aim of this project is to determine MSRs functionality in PCC 6803s physiology. PCC6803 contains three MSR encoding genes; two for MSRA and one for MSRB. Molecular techniques will be used to delete the two MSRA genes, sll1394 and slr1795, individually. Growth experiment with various stress conditions will be performed with the mutant strains to characterize the lack of MSRA in the cells' physiology.

Chapter 2: Materials and Methods

1. Introduction

The projects' workflow can be divided into three parts. The first is heavily based on molecular biological techniques, and is mainly focused on vector generation, amplification, and sequencing. The second focuses on the microbiological techniques, in the sense that the transformation and phenotyping of the primary organism, *Synechocystis* sp. PCC 6803 (PCC 6803) were performed here. The third and last part involves the tools and methods used to analyze the acquired data. If not noted otherwise, all methods that were used in this project were followed by the standardized protocols in Photosynlab website. http://unitedscientists.org/labs/norway/NTNU/PhotoSynLab/wiki/table-of-contents-2

2. Vector generation and Amplification

2.1) Vector Editor

Vector designing was performed using a plasmid-map tool called VectorEditor; wherein the different components of the vectors such as the backbone, the flanking regions of PCC 6803, and the antibiotic cassettes (kanamycin, chloramphenicol, and spectinomycin) were positioned. In addition, pLitmus28i was used as the template plasmid for the design (Fig 2.1). Once the initial designing was done, the forward and reverse primers were ordered.

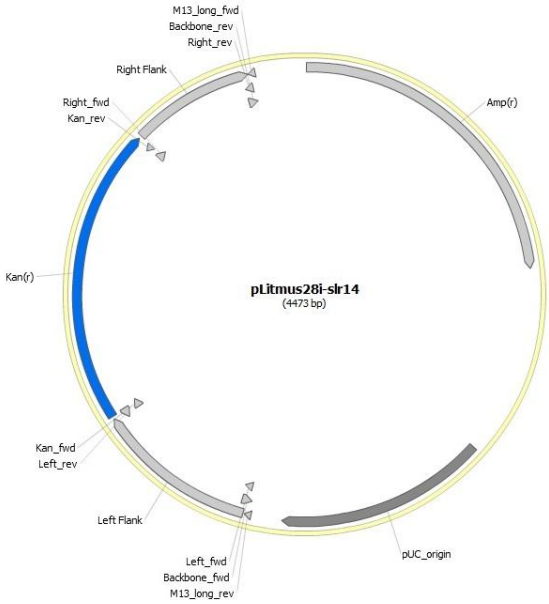

Figure 2.1 - Vector design of slr1795: Contains the vector backbone from plitmus28i (with an ampicillin resistance cassette and origin of replication), together with the kanamycin insert, and the flanking regions from PCC6803. Also displays the corresponding primers for each component.

2.1.1) slr1795 and sll1394 Flanking Regions

The flanking regions for the MSRA genes (slr1795 and sll1394) were generated by searching for the target gene sequences on Cyanobase, and then adding 1000 nucleotides (nt) on each side. The forward primers were generated 200-500 nt upstream and downstream from the target sequence, while the reverse primers were 20-100 nt within the start and end of the target sequence itself (Fig 2.2).

CCAGTAACTACGAACCCTGTGGTTTGACCCAAATGATTGGTCTGCGTTATGGGGCCGTTCCGGTGGTGCGGGGAGTAGGCGGTTTGGTAAATACTGT
TTTCGACCGGGATTATGACCAGAACCATCCCCCGGAGAAACGTAATGGTTTTGTTTTCTATCAACCGGATGAGTATGCCCTGGAAACGGCCCTCAGT
CGGGCGATCGCCTTGTATAAGGATGATCCCGTGGCTTTTAAAACCTTGGCCTTGCAGGGCATGGCCTACGACTACTCTTGGAATAAACCAGGGCTCC
AATATGTGGAAGCCTACGAATACATCCGGGCTTAACACCTCGGGTTTGTAACAGTTTCGTTACACTAGTTCAGAGGCGGAGTCAAAGCAGTTGGTCA
AAGCTTCGTTCAGTATTATCCGCACTTAGATAAATAACAACAACTTAAGCATTATGGGATTCTTCGATTTATTCGGTAAAAAAACTGCCATGGTTGC
CCCCAATGAAGCATTACCCGGGCGATCGGCCACTATGCCCGTGCCAGATAAGCATTTTGTCAACGGCAATCCTCTCAAAGCTCCCTTTCCCCAGGGA
ATGGAAACGGCTCTGTTTGGTTTAGGCTGTTTTTGGGGAGCAGAACGCAAATTTTGGCAAATACCTGGAGTTTACAGCACCGCTGTTGGTTATGCGG
CTGGTTATACCCCCAATCCCACTTACCAAGAAGTTTGTACGGGTATGACTGGCCATAACGAAGTGGTTTTAGTAGCCTTTGATCCCCAGCAAGTGAG
TTACGACCAATTGCTCAAAGTCTTTTGGGAAAGCCATAACCCTACCCAGGGCATGCGCCAGGGCAATGATGTGGGTACCCAATACCGCTCTGGCATT
TACACCTATTCCGAAGCCCAACAACAGGCCGCTTTGGCATCGAAGCAAGCCTATCAGCAAGCTCTGCAACAGGCAGGCTACGGGGAAATTACCACGG
AAATTTTACCAGCCCCGGATTTTTATTACGCTGAAGACTATCACCAACAATATTTGGCGAAAAACCCCAATGGTTACTGCGGTTTGGGGGGCACTAA
TGTGGCCTGCCCCATTGGCACAGAAGTTTCCCTGGGAGCTTAGTTAGGTTGGCGAGCAAAATCCTGTTATTAGGTTCAGCGGGGCAAGTGGGACGAG
AATTAGCCATTCCTTTGTCCTGTTTTGGTTCAGTGCAAGAAGCAACTAGGGCTAGCTTTGATTTGGCCCAGCCGGATGTCTTAGGGGAGAAAATTCG
TGCTTTTGCCCCGGACATTATTGTCAACTCCGCGGCCTATACTGCTGTGGACAGGGCCGAAACAGAACCGGAATTAGCCTACGCAGTTAACGCCCTT
GCTCCCCAGGCGATCGCCAAAGTGGCCAAGGAAATCGGTGCCTATGTGGTGCATATTTCCACTGACTATGTGTTTGATGGTAGCCAGAGTTCTCCCT
ACCGAGAAACGGATGCCACCAATCCCCTCGGGGTTTATGGCCAAAGCAAATTCCAGGGGGAA

Figure 2.2 - sll1394 gene sequence: The gene sequence displaying the slr1394 sequence in green, the left flanking region in blue, and the right flank in orange text. The primers are highlighted and underlined.

2.2) Primers

The primers used for this project were designed to have overhangs that overlap with the neighboring primers. This was required for the assembly of the different components afterwards. The primers were ordered from Sigma-Aldrich.

Table 2.1 - Sequence primers: Shows the primers, and their sequences, that were used for the construction of the sll1394 and slr1795 vectors.

slr1795	
Left Flank Forward	TCCTTCTCCGTGGGCTTAT
Left Flank Reverse	CCCTATGTGTTGGTCCATGATT
Right Flank Forward	GGACTGATGAGAAAGCTACCC
Right Flank Reverse	GCGGCTCTACCAAGTTACAA
Backbone Forward	GGAAACAGCTATGACCATGTCCTTCTCCGTGGGC

Backbone Reverse	TCCCAGTCACGACGCGGCTCTACCAAGTTACAA
Sequence Forward	ATAGTGGGCTTTGGCTAACTAC
Sequence Reverse	CCGCCAGGTGAAGGTATTT

sll1394	
Left Flank Forward	CAGCTATGACCATGTACGAACCCTGTGGTTTGAC
Left Flank Reverse	ACACAACGTGGCGGCCGCGCCCGGGTAATGCTTCAT
Right Flank Forward	ATTGGTTGTAGCGGCCGCCGCTGAAGACTATCACCAACAA
Right Flank Reverse	TTCCCAGTCACGACGAGAACTCTGGCTACCATCAAA
Backbone Forward	GGAAACAGCTATGACCATGTACGAACCCTGTGGTTTGAC
Backbone Reverse	GGTTTTCCCAGTCACGACGAGAACTCTGGCTACCATCA
Sequence Forward	CGTAGGCTAATTCCGGTTCTG
Sequence Reverse	TATTGGAGCCCTGGTTTATTCC

2.3) PCR Amplification and Gel Electrophoresis

PCR amplification was done using Phusion® High-Fidelity DNA Polymerase from New England Biolabs (NEB). We used Phusion in a "touchdown protocol" which offers a higher specificity than standard PCR protocol. Touchdown PCR uses a cycle program which starts on a temperature above the initial annealing temperature, and then gradually decreases until it reaches (or drops below) the primers melting point (https://www.neb.com/faqs/1/01/01/what-is-touchdown-pcr). The program ran for 16 cycles ending with a final elongation step for 5 min before it ends in storage temperature.

The PCR mix that used was:

Filtered water	31 uL
Buffer	10 uL
Forward Primer	2.5 uL
Reverse Primer	2.5 uL
dNTP	1 uL
Template	1 uL
Enzyme	0.5 uL
Total	48.5 uL

Gel electrophoresis ran with 20% Gel Green (GG) agarose gel for 40 min with 80V, or for 60 minutes with 60V.

2.4) PCR Purification

Purification of PCR products was done using QIAquick PCR purification kit (QIAGEN, Germany). The method is spin-column based having a silica membrane, which binds and eludes DNA depending on the salt concentration of the buffers used (QIAGEN, 2015). Purification was necessary to remove all unwanted enzymes, buffers, impurities, etc that may disrupt fragment assembly afterwards.

2.5) Nanodrop and Fragment Assembly

The concentrations of the purified PCR products were attained by using Nanodrop (Thermo Scientific, USA). Assembly was done using NEBs Gibsons Assembly Master Mix kit. The process involved the ligation of overlapping DNA fragments in an isothermal reaction containing a variety of enzymatic processes (NEB, 2012). Optimization required 2-3 fold concentration of fragments for a 50-100 ng plasmid backbone. Once the concentration of each fragments were calculated, the total amount of these was within 0.2-1 pmoles. Assembled vectors were then sent to GATC (Germany) for sequencing in order to validate that the inserts were ligated with the vector backbone.

2.5.1) sll1394 vector

Due to technical difficulties with the assembly of the different vector fragments, only the sll1795 vector was produced in this manner described above (2.1 to 2.5). The sll1394 was designed and then ordered from Sigma-Aldrich. This vector design contained the flanking regions for the sll1394 gene which also included a restriction site (Not1) between the left flank, and the right flank. Digestion by Not1-HF opened up the vector and made it convenient to ligate a pre-amplified kanamycin cassette. Similar to the Gibsons Assembly, the method was optimized by having 2-3 folds of fragments per backbone. Kanamycin cassette insertion was confirmed by PCR amplification with the flanking regions + the cassette with the sll1394 Sequence Forward and Sequence Reverse primers. Confirmation of this restriction patterns on agarose gel was carried out.

2.6) Vector Amplification

Constructed vectors were amplified by Heat-Shock transformation into DH5a competent cells. The process starts with 100 uL of DH5a being thawed on ice for 5-10 min. Once no longer frozen, the constructed vector is added, and the mixture is incubated on ice for 30 min. The cells are then heat-shocked on a 37^{o}C water bath for 2 min, and are incubated on ice again for 3 min.

The transformed cells were then amplified on 2 mL LB media on a 37^{o}C shaker for 90 min. Following amplification, the cells were concentrated through spinning, and transformants were selected by plating

100 uL of resuspended cultures on selective-plates with their corresponding antibiotic cassettes. The transformants were then incubated for 37^{o}C overnight. The following morning, the transformation efficiency is calculated.

2.6.1) Transformation Efficiency

An extra culture was transformed with 1 ng of plasmid DNA in parallel with the heat-shock transformation. This culture serves as a positive control and is later used to calculate the transformation efficiency of the competent cells.

Transformation efficiency is calculated by counting the number of colony forming units (cfu) per ng of DNA. The usual concentration for this is 100 uL per 2 mL of culture, as described above (2.6). This results in a 1/20 dilution, or 50 pg of DNA per X number of cfu. For example: if there are 500 cfu after incubation overnight, the equation would be: **500 cfu/ 50 pg** which give us 10 cfu/pg DNA. Converted to ug, that would be around 10 x 10^6 cfu/ug DNA.

Transformation efficiency is expected to be around 2-8 x 10^6 or more.

2.7) Mini prep and Sequencing

Plasmid isolation from transformants was done using a Wizard® Plus SV Minipreps DNA Purification System (Promega, USA). The system is divided into 4 parts: Cellular lysis, plasmid binding, washing, and plasmid elution. Similar to the DNA purification kit, this system is also spin-column based with a DNA binding membrane.

Once the plasmid has been harvested, 5 uL of 80-100 ng/uL of plasmid DNA along with 5 uL of 5 pmol of primer is sent to GATC for sequencing. This step is necessary in order to verify that the plasmid has the right inserts. Alternatively, if the sequence is already known, the vector can be digested by the Not1-HF enzyme and then the restriction pattern is analyzed by gel electrophoresis to confirm if the different inserts are present.

2.8) Changing of Antibiotic Cassettes

Changing of antibiotic cassettes is done to construct independent versions of a mutant strain in PCC 6803. Furthermore, having different antibiotic resistance versions is also of advantage for generating PCC 6803 strains in which different genes have been deleted. Changing the antibiotic resistance

cassettes is done by digesting a pre-existing vector with Not1-HF restriction enzyme to cut and release the old antibiotic cassette. Incubation time on the warm bath (37°C) was around 60-90 min. Samples were then purified using the QIAquick PCR purification before ligation of the new antibiotic cassette.

Plasmid	30 uL
Buffer (CutSmart)	3.5 uL
Not1-HF	1.5 uL
Total	**35 uL**

T4 DNA ligase was used for ligation. Similar to the Gibsons assembly, inserts also had a threefold concentration for every pmol of vector backbone. Incubation time of 12-16 hours at 5°C (refrigerator), or 3-4 hours on the bench are required.

In total, four types of vectors were produced in this manner before transformation into PCC6803: sll1394 + kanamycin (94Kan), sll1394 + chloramphenicol (94Chl), slr1795 + kanamycin (95Kan), and slr1795 (95Chl). A third type of vector containing the spectinomycin (Spec) antibiotic cassette was supposed to be included in the project. However due to Specs length (1000+bp), it proved to be difficult to integrate it with the pre-existing vector. Constructing the Spec vector was then abandoned after several trials, and due to time constraints.

3. Transformation into PCC 6803 and Phenotyping

For microbiological work, it was important that every procedure was performed in a sterile environment, usually on a sterile bench that has been sterilized with 70% ethanol. The tools should also be sterile, either through flaming or through autoclavation beforehand. Wearing of sterile gloves was mandatory during all microbiological procedures to avoid contamination.

3.1) Starter Culture

Before PCC 6803 could be transformed with DNA, a starter culture was needed; as actively growing cells have higher transformation efficiency than stagnant/slowly growing cells on agar plates. For preparing a starter culture, a plate containing PCC 6803 wild type strain (WT) was transferred to a falcon tube containing BG11. Once fully dissolved, the mixture was then added into an Erlenmeyer flask containing 200-300 mL of BG11. The set-up culture was then connected to an air-pump device, placed in a 30°C incubator with access to light, and was incubated for 3-4 days (Fig 2.3).

Figure 2.3 - 500 ml Erlenmeyer flask with 300 ml of BG11: Standard set-up for establishing a starter culture for PCC 6803.

3.2) Transformation into PCC 6803

From the starter culture, another culture was grown overnight on 200 mL of BG11 + 1 mL of glucose with an OD_{730} of 0.25. The cells were then centrifuged (2500 g) the following morning, and were resuspended to an OD_{730} of 5. A mixture of cells (0.5 mL) and constructed vectors (30-45 uL) were then made on sterile test tubes. The samples were incubated for 6 hours, with mixing after the first 3 hours, in a 30^{o}C incubator. After incubation, the cells were placed on a sterile filter on BG11 plates containing glucose + Atrazine, and then grown overnight.

The following morning, the transformants were selected by placing the filter on a new BG11 containing the corresponding antibiotic to the transformed vector this time. The transformants were then incubated for 3 weeks or until visible colonies were seen (Fig 2.4).

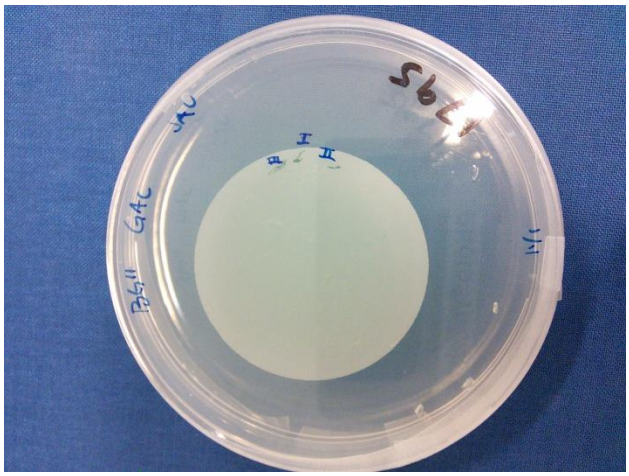

Figure 2.4 - BG11 plate with a nanopore filter: The filter allows easy transfer of the transformed mutant strains from a post transformation plate, to a selective BG11 plate containing antibiotics as seen on this image. The plate contains glucose, atrazine and chloramphenicol.

3.2.1) Transformation with PCR Fragments

Of the four types of generated vectors, only the 94Kan and 95Kan were successfully transformed into PCC 6803. After several rounds of troubleshooting and trying to transform 94Chl and 95Chl, it was concluded that the backbone of these two vectors, may have been the reason why it kept failing. As a last attempt, a PCR fragment containing the flanking regions and the Chl cassette was produced from the existing vectors; and was amplified to 400-500 ng/ul. These were then successfully transformed into PCC6803 shortly after.

3.3) Colony PCR

Colony PCR was done to verify which of the strains has been transformed and segregated (i.e. no copies of the wild type gene are present); and to determine which candidate was best suited for phenotyping. This was done by choosing and re-plating 3-4 colonies from each of the mutant strains. Once enough of the new strains have grown, they were used as templates for PCR. Primers from each side of the flanking region were used in combination to amplify the presence of the flanking regions and the presence of the antibiotic resistance cassettes (Fig 2.5).

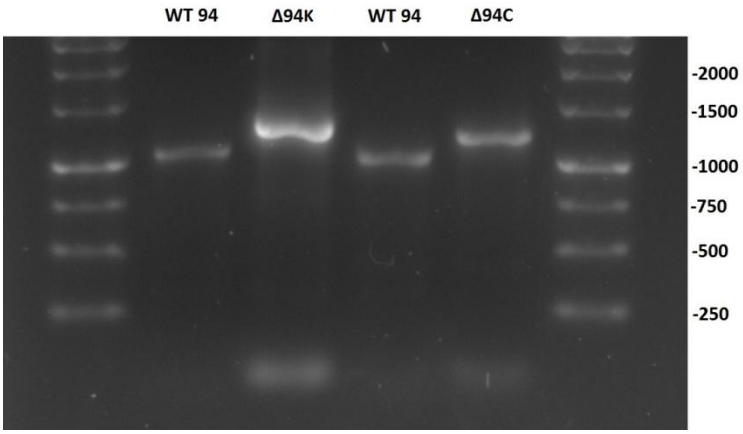

Figure 2.5 - Gel electrophoresis bands for the flanking regions + sll1394 gene/ Kan or Chl inserts: WT94 is the wild type containing the sll1394 gene, and is about 1071 bp. 94K is a Δsll1394 strain with the Kan insert, ca. 1346 bp. 94C is also Δsll1394 strain but with the Chl insert, ca. 1226 bp.

3.4) Phenotyping by Spot Testing

For quantitatively assessing the growth of cultures, spot testing was done by diluting the culture strains to an OD_{730} of 1.0 from a starter culture. These were further diluted by a factor of 10 for 3-5 more times. The dilution series were then spotted on a plate with 2-3 repetitions for each culture. The dilutions and replicates are done in order to reliably measure cellular density.

Data was collected by taking daily images of the growth cultures for 7 days, then on the 10th day, and lastly on the 14th day. The images were then processed with a program that aligns images on top of each other, and progressively calculate the cellular density of marked colonies. Once the calculations were done, the data acquired was plotted in LibreOffice (See also 4. Data Analysis for detailed description).

3.5) Photosensitizers

Photosensitizers were used to ensure ROS generation, and further compromise the cells defense mechanism against ROS, when exposed to light conditions. Photosensitizers can react in two ways: 1) by transferring a charge to a substrate thereby making it unstable; 2) through transfer of excitation energy, as described in Chapter 1: 2.1) Singlet Oxygen (Castano *et. al.*, 2004). Rose bengal (RB) and methyl viologen (MV) were used in this project.

3.5.1) Rose Bengal

Rose bengal promotes singlet oxygen generation by energy transfer to oxygen when illuminated. Light can excite rose bengal. As a consequence, energized triplet state of rose bengal can be generated. When interacting with oxygen, triplet state rose bengal is efficient in generating singlet oxygen states (Castano, 2004, Krieger-Liszkay, 2004, and Latifi *et al.*, 2008). RB is able to diffuse through the thylakoid lumen, thus generally affecting PSII where most oxygen is generated as a byproduct of H_2O photolysis (Fig 2.6) (Nishiyama et. al., 2004).

3.5.2) Methyl Viologen

Methyl viologen acts as an electron acceptor and generates ROS through electron transfer to oxygen. This mainly occurs in PSI where MV disrupts the electron transfer from ferredoxin to ferredoxin NADP reductase (Fujii *et. al.,* 1990). Transfer of an electron to O_2 generates the superoxide anion (encircled in red on Fig 2.6), and possibly, hydrogen peroxide and hydroxyl radical.

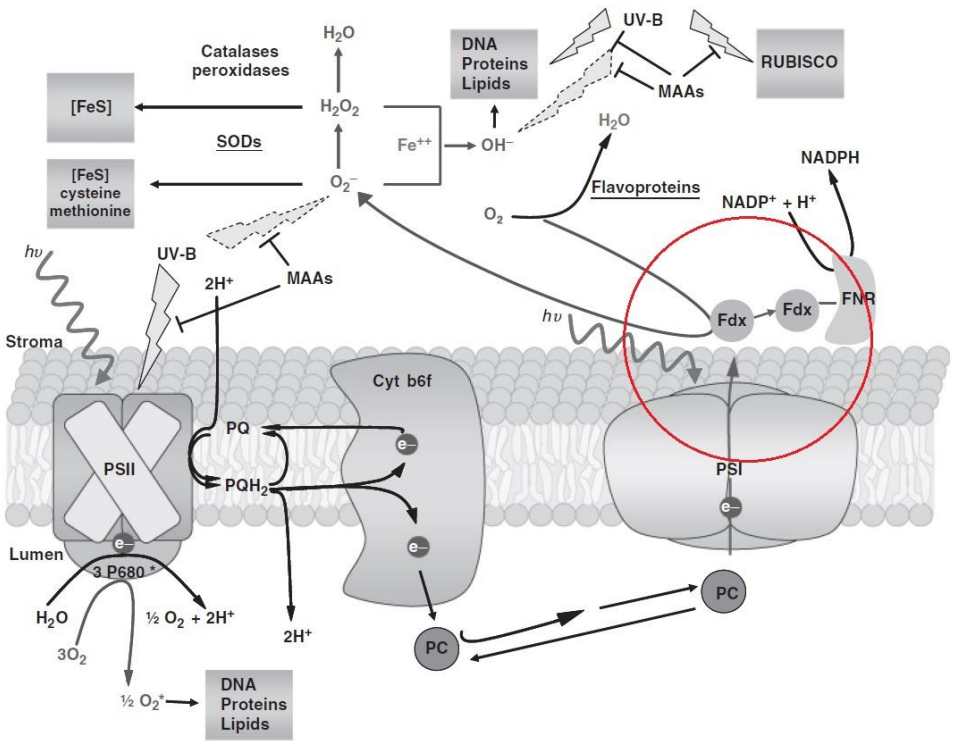

Figure 2.6 - Reactive Oxygen Species generation: Shows reduction or energization of triplet oxygen results in the production of ROS. Singlet oxygen is produced in PSII when O_2 receives energy input from photosensitized chlorophyll. Reduction of O_2 in PSI (encircled in red), results in the generation of superoxide anion; which is disproportionated to O_2 and hydrogen peroxide by SOD. Hydrogen peroxide can be safely converted to H_2O and O_2 by catalase and peroxidase. However, hydrogen peroxide, in the presence of high iron concentration, can also be converted to a hydroxyl radical through a process called, the Fenton reaction.

3.5.3) DCMU

DCMU is a herbicide that is used to inhibit the photosynthetic activity. It does so by binding to plastoquinone B (Q_B) binding pocket, thereby interrupting the electron transfer from Q_A and the rest of the electron transport chain. In PCC 6803, this can be seen as an indirect way of preventing ROS generation during high light intensity conditions.

3.6) Growth Experiment on The Mutant Strains Δsll1394 and Δslr1795

Mutant strains of Δsll1394 and Δslr1795 were cultured with the wild type to check for phenotypic differences. Parameters such as the growth rate, the doubling time, and the pigmentation of the three strains were assessed. The experiment was divided in two parts with varying light intensities, incubation temperature, and exposure time. The plate conditions were the same however.

3.6.1a) Moderate Light Intensity Experiment

The first set of cultures was exposed to **150 microeinsteins (µE m^{-2} s^{-1})** of light on room temperature for 14 days. In addition to this, a separate batch was grown in a quasi-dark environment (wrapped in aluminum foil, with the sides exposed to light as PCC 6803 cannot grow in complete darkness with glucose as a carbon source) (Fig 2.7). Cultures were taken from plates, and spotted with two replicates having an OD_{730nm} of 1.0, 0.1, 0.01, 0.001 and 0.0001 for each strain (WT, Δsll1394 and Δslr1795). Measurements were taken daily for 7 days, then on the 10th day and lastly on the 14th day.

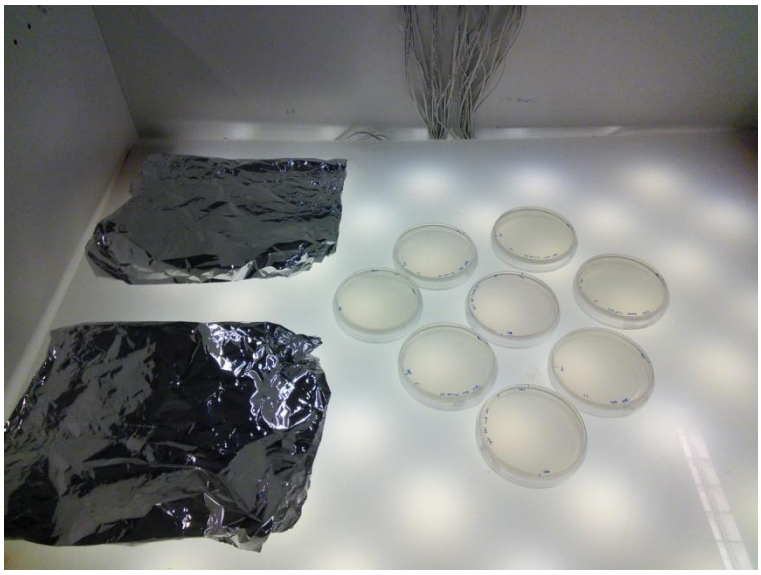

Figure 2.7 - The light cabinet with culture strains: This is where the light and quasi-dark conditions (left side) were performed for 14 days. Plates are re-shuffled everyday to create varying light intensities for each plate condition.

3.6.1b) High-Light Intensity Experiment

In order to gather more data and increase the likelihood of inducing more oxidative damage, a second set of experiment was done under high-light conditions >300 µE m^{-2} s^{-1} (Hihara *et. al.,* 2001). Unlike the first experiment, however, strains were pre-cultured in liquid BG11 first, in order to have them actively growing, before they were spotted on plates (Fig 2.8). During the high-light experiment, cells experienced ca**. 1500 µE m^{-2} s^{-1}** of light, in a 30°C incubator for 7 days. As in the moderate light environment, a separate set of cultures was grown in a quasi-dark environment (Fig 2.9). Different to the moderate light experiment, cultures were spotted with 3 replicates with an OD_{730nm} of 1.0, 0.1, and 0.01 in the high-light experiment.

Figure 2.8 - Starter cultures: shows the starter cultures for the Δslr1795 strain (left), Δsll1394 strain (middle), and the wild type (right). Light has been minimized to prevent the mutant strains from getting stressed earlier than the wild type.

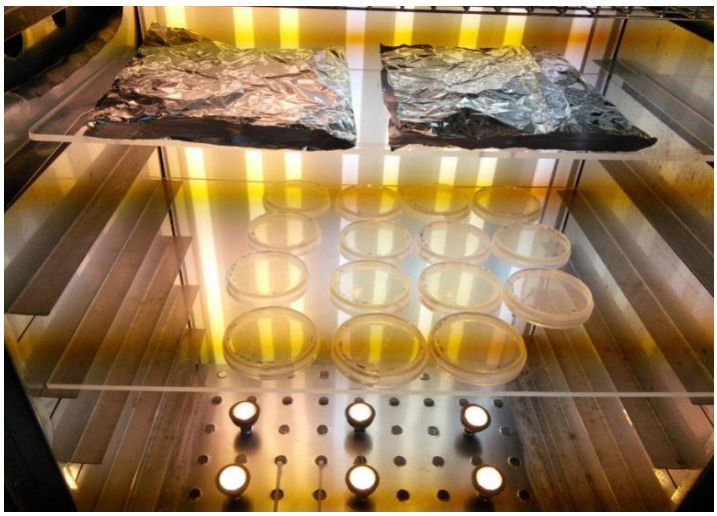

Figure 2.9 - The incubator cabinet with high light intensity: Light conditions are placed on the middle of the incubator, while the quasi-dark conditions are on top. The plates are shuffled everyday to have a varying light intensity.

3.6.2) Plates Conditions

Aside from BG11 and glucose (Glu), RB and MV, and the herbicide DCMU were used to both promote ROS generation, and inhibit photosynthesis. Unlike the growth experiment performed on the wild type, as described in 3.4) Phenotyping by Spot testing, the concentrations used for this experiment were slightly below the lethal level of RB and MV (2uM determined by Nishiyama *et. al.,* 2004; Maeda *et. al.,* 2005).

Light conditions	**Dark conditions**
BG11	Glucose
MV/RB (0.1 uM/1.0 uM)	Glucose + DCMU
Glucose	Glucose + DCMU + RB/MV (0.1 uM/1.0 uM)
Glucose + MV/RB (0.1 uM/1.0 uM)	Glucose + DCMU + RBMV (0.1 uM/1.0 uM)
Glucose + DCMU	
Glucose + DCMU + RB/MV (0.1 uM/1.0 uM)	

Each condition and the initial effects are listed below:

Conditions	Effects
BG 11	- Strains are photosynthethically active.
BG11 + Glucose (GLU)	- Electrons are supplied by glucose in PETC. - Photosystem II (PSII) is down-regulated.
DCMU	- Blocks the electron transport from phytoquinone A to B in PSII. - Protects the strains from generating (ROS) as a consequence.
BG11 + Glucose+ DCMU (GDCMU)	- PSII is down-regulated. - In addition, strains are protected from ROS.
Rose Bengal (RB)	- Promotes singlet oxygen generation. - Singlet oxygen damages proteins and lipids.
Methyl Viologen(MV)	- Promotes superoxide anion generation. - Hydrogen peroxide and hydroxyl radical can also be generated as by products. -Damages DNA and amino acid residues such as methionine.
BG11 + Glucose + RB (GRB)	- PSII is down-regulated. - Singlet Oxygen can still be generated
BG11 + Glucose + MV (GMV)	- PSII is down-regulated. - Superoxide anion, hydrogen peroxide and hydroxyl radical can still be generated through an undefined electron cycle pathway.
BG11 + Glucose + DCMU + RB (GDRB)	- PSII is down-regulated. - PSII is protected.

	- Expected less generation of ROS.
BG11 + Glucose + DCMU + MV (GDMV)	- PSII is down-regulated. - PSII is protected. - Superoxide anion, hydrogen peroxide and hydroxyl radical can still be generated through an undefined electron cycle pathway.

4. Data Analysis

Agar plates were imaged by a camera to document growth of PCC 6803 wild type and mutant strains. To quantify growth on these plates, a suite of custom programmed and interfaced imaging tools and programs were used. In addition, a statistical package (R-grofit) was used to obtain growth parameters (lag time and growth rate) of the imaged plates.

Due to having slightly different parameters, the data acquired from the moderate light experiment and the high-light intensity experiment, were measured in two different ways. Nevertheless, image capture and cell density calculation remained the same for both.

4.1) Photo Imager and Python scripts

Photo Imager is a custom built photo booth to take digital pictures of bacterial cells on agar plates. A set of Python scripts and the image manipulation package IMOD (University of Boulder, USA) was used to align images on top of each other, and progressively calculate the cellular density of marked colonies. The data acquired once the calculations were done, were then plotted on either LibreOffice or veusz.

4.2) R and grofit

R is the statistical calculating program that was used to assess the lag phase, exponential phase and stationary phase of the growth curves that were generated by processing the data (see 4.1). R makes use of a package called *grofit*. (See Table 2.2). Grofit was designed to analyze the growth parameters: lag phase (λ), growth rate (mμ) and amplitude (A). Standard errors between the raw data and the fitted data are also calculated. Once calculations were done, R-grofit provides the fitted data from the raw data.

Table 2.2 - Raw data and Fit Data: displays the fitted data and the raw data of PCC 6803 strains grown in BG11. Time is displayed in hours, while data is displayed as relative cell density.

Time	Raw Data	Fit Data
42.1016666667	21.2910787533	20.2924707147
64.4883333333	35.0787177938	35.7531572646
90.5355555556	71.6931630021	78.2485414061
113.924444444	187.8701252788	175.4169950977
144.23	497.6978977568	497.8285099744
162.118888889	782.535420708	788.3356351857
256.621666667	1122.4672005183	1306.5298869779
328.515555556	1527.5557138913	1312.205643389

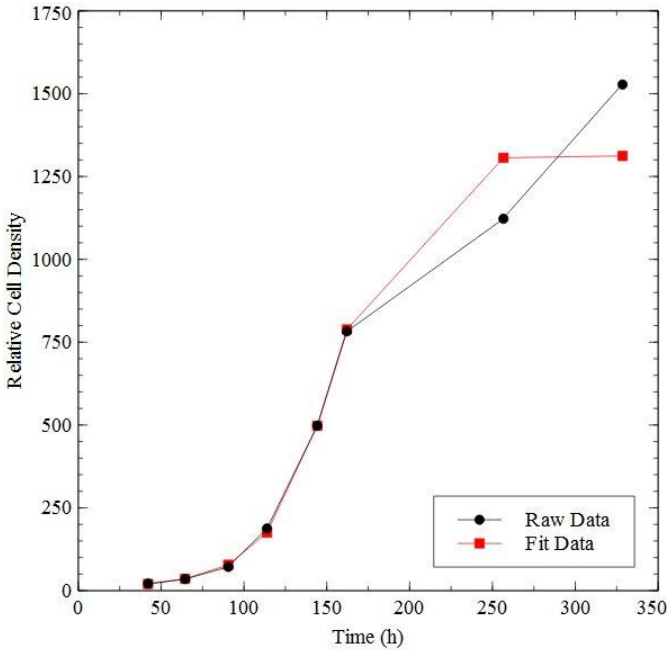

Figure 2.10 - Growth curve of the raw data and fit Data: displays the growth curve of the wild type PCC 6803 which was grown in BG11. The raw data collected was ran though grofit to obtain the fitted data.

4.3) Spectroscopy

In order to estimate if strains experienced oxidative stress, indicators of stress such as higher amount of carotenoids, and lower amounts of chlorophyll and phycobilins were determined semi-quantitatively. Relative chlorophyll, carotenoid and phycobilin levels were estimated with Hitachi U-3010 spectrometer. The instrument also includes an integrated sphere which decreases light scatter.

Chapter 3: Results

1. Introduction

The main aim for this project was to characterize the functionality of methionine sulfoxide reductase (MSR) in aiding in *Synechocystis* sp. PCC 6803s (PCC 6803) defense against oxidative stress caused by ROS. In order to do this, mutant strains lacking either sll1394 or slr1795 genes were generated. Both genes code for MSRA which reduces S-methionine sulfoxide that can be generated by hydrogen peroxide and hydroxyl radical, back to methionine. A third gene coding for MSRB exists in PCC 6803 but its function was not characterized during the duration of this project.

The mutant strains, together with the wild type, were exposed to various conditions to characterize the effect of the lack of MSR on the cells physiology. Growth curves with two different light intensities and several different chemical plate conditions, such as inhibitors of PSII and promoters of oxidative stress, were evaluated. Parameters such as growth rate, doubling time and pigmentation were then calculated. Chlorophyll and carotenoid levels were also determined with absorption spectra to investigate the strains' stress response to high-light intensity.

2. Growth Experiment on PCC 6803

Prior to the initial experiment with the generated mutant strains, an extra experiment was done to determine the wild types' ability to grow in the presence of rose bengal (RB) and methyl viologen (MV). Inhibitory and lethal concentrations of RB and MV were determined by adapting the concentrations used by Nishiyama *et. al.*, 2004, and Maeda *et. al.*, 2005. For this experiment, the concentrations were: 0 uM, 0.5 uM, 1 uM, 5 uM, 10 uM and 20 uM for both RB and MV. Cultures were spotted with 3 replicates of OD_{730nm} 1.0, 0.1, 0.01, 0.001 and 0.0001. The experiment lasted for 14 days, exposing the culture strains to **150 microeinsteins ($\mu E\ m^{-2}\ s^{-1}$)** of light at room temperature. Measurements were taken daily for 7 days, then on the 10th day and lastly on the 14th day. The results were as follows:

Table 3.1 - Growth experiment for the wild type PCC6803: a) displays the data measured on the 10th day while b) on the 14th. Concentration levels of either MV or RB are in uM. The + sign indicates cell growth, while - indicates cell death. The "+" sign indicates visible spots from the dilution series. X indicates no growth. On a) no observable growth after 5 uM of MV and 10 uM of RB; on b) 10 uM for both MV and RB.

a)

10 days	**0 uM**	**0.5 uM**	**1 uM**	**2 uM**	**5 uM**	**10 uM**	**20 uM**
MV	++	++	++	+	X	X	X
RB	++	+++	++++	+++	+	X	X

b)

14 days	**0 uM**	**0.5 uM**	**1 uM**	**2 uM**	**5 uM**	**10 uM**	**20 uM**
MV	+++	+++	+++	++	+	X	X
RB	+++	+++	++++	+++	+	X	X

3. Moderate Light Intensity Experiment

Once the data from the different plate conditions grown in **150 microeinsteins (µE m^{-2} s^{-1})** of light were acquired, an overall growth curve was made to give an overview of the summed growth for all the three strains (wild type, Δsll1394 and Δslr1795). This helped in getting a general idea of how different each strains growth was, in comparison to one another (Fig 3.1).

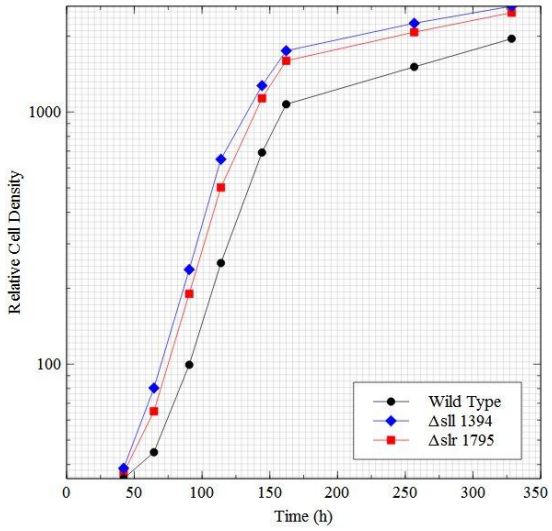

Figure 3.1 - Logarithmic growth curves of all three strains: The wild type data points are indicated as black circles, Δsll1394 as diamonds, and Δslr1795 as squares. Each display the averaged growth points of all the dilution replicates within their corresponding strain. Curves are plotted against the relative cell density on the y-axis, and time represented as hours, on the x-axis.

To quantitatively assign growth parameters, R and the program package grofit, were used. Colonies containing the same dilution replicates (either to an OD_{730nm} of 0.01, 0.1, 1.0) within each strain, were averaged out, and then ran through the program to get the lag phase (λ), growth rate (mμ) and amplitude phase (A) for each growth curve.

Table 3.2 - R and grofit measurements: Displays the lag phase (λ), growth rate (mμ) and Amplitude (A) for each growth curve on each averaged colony dilution (represented as optical density, OD). Error from the raw data and fit data is also shown below each parameter.

Parameters	**Wild Type**			**Δsll1394**			**Δslr1795**		
	OD 0.01	**OD 0.1**	**OD 1.0**	**OD 0.01**	**OD 0.1**	**OD 1.0**	**OD 0.01**	**OD 0.1**	**OD 1.0**
Amplitude (A)	7.18	7.37	7.71	7.6	7.81	7.95	7.51	7.71	7.92
A error	0.09	0.13	0.011	0.07	0.06	0.05	0.1	0.074	0.05
Growth Rate (mμ)	**0.03594**	**0.03499**	**0.03591**	**0.04038**	**0.04106**	**0.04165**	**0.03909**	**0.03847**	**0.03995**
mμ error	0.002	0.004	0.003	0.002	0.002	0.001	0.02	0.002	0.001
Lag phase/ Lambda (λ)	-29.76	-33.51	-49.02	-38.84	-37.86	-50.24	-35.91	-40.45	-50.29
λ error	8.82	18.4	16.5	5.41	4.29	4.16	7.47	5.45	4.2

3.1) Doubling Time

From the gathered data on tolerance against MV and RB (see 3. Moderate Light experiment), the doubling time was calculated from the growth rate (mμ) for each of the OD on each strain. These were then averaged to get the strains' reported doubling time (Table 3.2). In addition to this, the standard error for each averaged doubling time was also calculated.

$$Dt = \frac{Log\ (2)}{m\mu}$$

3.1.1) Light Condition

The total doubling time for the wild type and the mutant strains on different plate conditions specified on Chapter 2: 3.6.2.) Plates conditions, were collected (Table 3.3) in order to provide an overview on which plate conditions affect the strains doubling time. This also made it possible to see whether there was a difference in the doubling time between the wild type and the mutant strains. For this experiment, the strains displayed a notable decrease in doubling time on plates containing RB, with the exception of plates with RB + DCMU.

Table 3.3 - Light condition measurements: Shows the doubling time (h) difference for each strain grown in different plate conditions for the culture batch exposed to 150 µE m^{-2} s^{-1} of light. Standard Error (Std. Err) for the doubling times is shown (in blue) right next to each plate condition.

	BG11	Std. Err	MV_0.1uM	Std. Err	MV_1uM	Std. Err	RB_0.1uM	Std. Err	RB_1uM	Std. Err
Wild Type	19.47	0.17	21.46	0.36	18.18	0.3	9.32	0.51	10.64	0.58
Δsll1394	16.9	0.15	12.96	0.26	14.9	0.32	10.67	1.22	11.54	0.64
Δslr1795	17.7	0.19	13.83	0.16	16.77	1.37	9.59	0.8	10.96	0.51

	GLU	Std. Err	GMV_0.1uM	Std. Err	GMV_1uM	Std. Err	GRB_0.1uM	Std. Err	GRB_1uM	Std. Err
Wild Type	26.4	0.4	23.82	0.3	inconclusive	inconclusive	10.36	0.54	7.44	1.27
Δsll1394	12.8	0.62	12.74	0.26	inconclusive	inconclusive	9.59	0.24	10.42	0.87
Δslr1795	16.6	0.23	15.56	0.26	inconclusive	inconclusive	10.92	0.15	11.79	0.42

	GDCMU	Std. Err	GDMV_0.1uM	Std. Err	GDMV_1uM	Std. Err	GDRB_0.1uM	Std. Err	GDRB_1uM	Std. Err
Wild Type	21.42	1.57	22.36	1.82	21.07	2.18	22.48	1.03	28.41	0.28
Δsll1394	22.91	0.41	17.41	1.09	18.3	1.04	20.21	0.43	20.91	2.03
Δslr1795	20.77	1.14	19.25	1.28	20.42	2.4	23.87	1.16	22.16	2.15

3.1.2) Dark Condition

As previously stated, a second batch of the strains was also grown covered in foil. This was to stimulate heterotrophic growth wherein PCC 6803 mostly metabolizes glucose in minimal light conditions. Dark conditions are thought to reduce the generation of oxidative stress.

Table 3.4 - Dark condition measurements: Shows the doubling time (h) difference for each strain grown in different plate conditions contained in the quasi-dark environment with 150 µE m^{-2} s^{-1} of light. Standard Error (Std. Err) for the doubling times is shown (in blue) right next to each plate condition.

	GLU	Std. Err	GDCMU	Std. Err	GDMV_0.1uM	Std. Err	GDMV_1uM	Std. Err
Wild Type	20.82	0.63	27.32	1	21.85	3.87	19.47	0.17
Δsll1394	18.88	0.19	24.68	0.49	22.57	2.99	16.9	0.15
Δslr1795	17.14	0.26	27.33	0.67	23.78	1.13	17.7	0.19

	GDRB_0.1uM	Std. Err	GDRB_1uM	Std. Err	GMVRB_0.1uM	Std. Err	GMVRB_1uM	Std. Err
Wild Type	26.89	1.25	29.62	0.58	16.76	0.32	17.08	0.65
Δsll1394	22.91	0.67	23.49	0.59	16.7	0.44	15.07	0.28
Δslr1795	18.68	0.52	17.12	1.9	15.86	1.39	13.8	0.53

4. High-Light Intensity Experiment

Processing the acquired data for this experiment, cultures on **1500 µE m^{-2} s^{-1}** of light, required a different analysis compared to the analysis of the moderate light experiments. In both sets of experiments, the overall growth for each strain was recorded by imaging and processing of the imaging data. Replicates with corresponding OD for each strain were also averaged (see appendix). The difference, however, was that it was not possible to use R and grofit for calculating growth parameters in high-light conditions. This was due to the fact that some strains lack enough data points at the exponential phase of the growth curve, and some strains underwent a "death and re-growth", characterized by a dip in apparent cell density around 110 hours (h). To represent this data, growth curves were plotted to determine there was a significant difference between the investigated strains. Growth curves not represented here can be found in the appendix.

4.1) High-Light Light Condition

Majority of the growth curves on plates without glucose and/or DCMU, had little to no difference between the growth rates in the exponential phase. However, addition of glucose appears to give the Δsll1394 strain a slight growth advantage compared to the other two strains. This was most observable around 50-70 hours when the other two strains appear to have a decrease in recorded cell density (Fig 3.2)

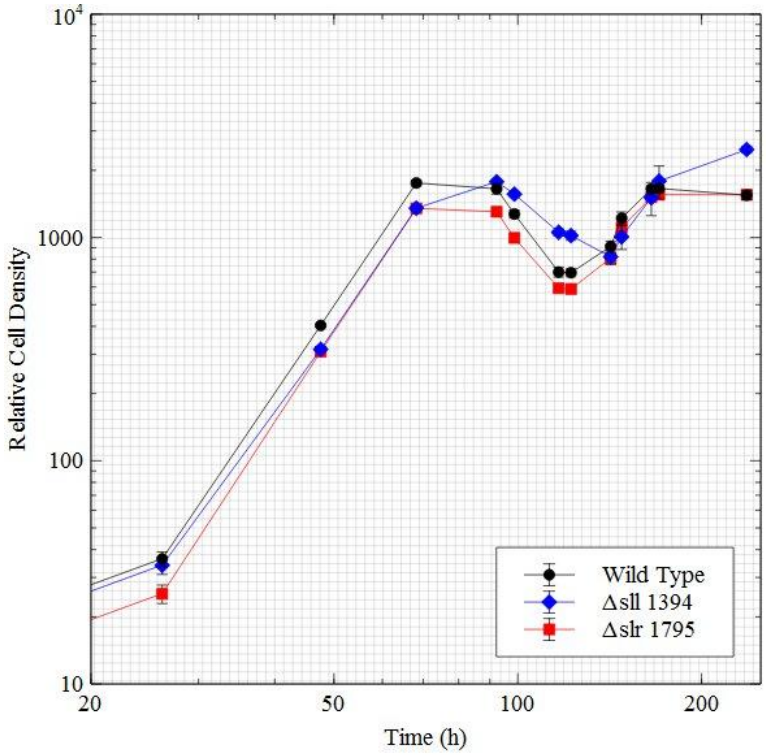

Figure 3.2 - Growth curves with decreased in recorded cell density and recovery: Shows the exponential growth from 20-70 h, and eventual decrease in the apparent cell density and the recovery phase after 100 h for all three strains. Wild type data points are in marked with circles, Δsll1394 with diamonds, and Δslr1795 with squares. The growth curve is from strains grown in glucose + 0.1 uM of MV.

4.1.1) Δsll1394

As seen in the moderate light experiments, the mutant strain Δsll1394 seem to grow better in some plate conditions on/after 50 hours in the presence of glucose. Addition of DCMU, however, cancels this growth advantage. Δsll1394 also displayed a rather interesting growth recovery in comparison to the wild type and Δslr1795 after ca. 100 hours on the MV plate. For the other three plates, this growth recovery occurs after 170 h (Fig 3.4).

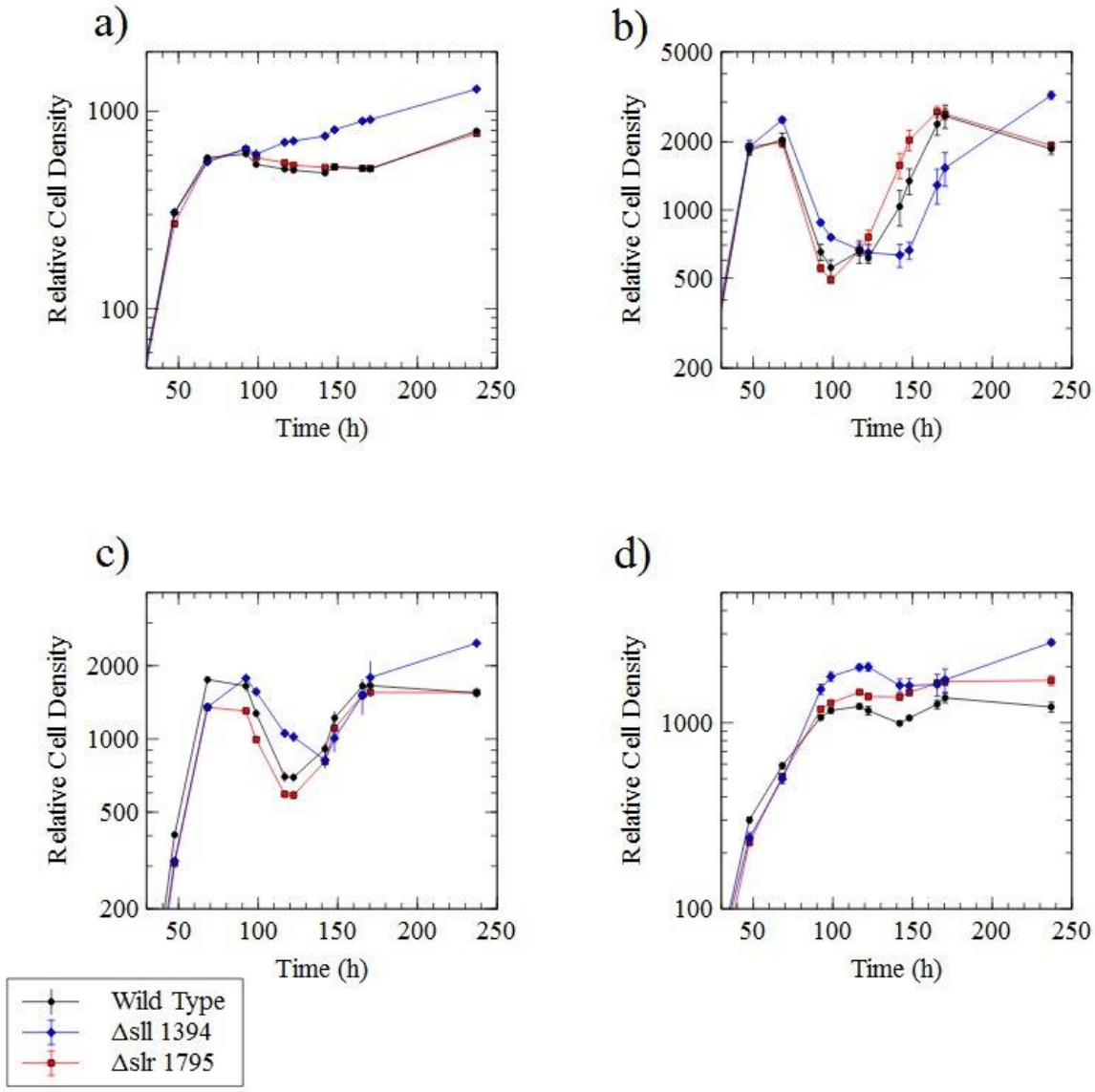

Figure 3.4 - Δsll1394s growth recovery on 4 plates: Data points are plotted against the relative cell absorbance on the y-axis, and time per hour (h) on the x-axis. (a) shows Δsll1394s growth curve on 1.0 uM of MV, (b) BG11 + glucose, (c) on glucose + 0.1 uM of MV, and (d) on glucose + 0.1 uM of RB.

4.1.2) Self-shading

At high-light conditions, ring formation of plated cells was observed on plate conditions with glucose and glucose + DCMU (GDCMU). Strains on GDCMU displayed this phenotype most intensely and did not have a decrease in apparent cell density and the recovery phase behavior observed in other conditions. The arrangement of cells in rings, however, produces a larger variation in the determined cell densities. (Fig 3.4). One particular plate condition worth mentioning is the glucose + DMCU + 0.1 uM of RB plate. Plate inspection after ca. 180 hours, revealed that the wild type was greatly inhibited while the mutant strains were able to grow by establishing rings; with Δsll1394 displaying a denser level of pigmentation. Spectra show very spread data points which most likely included noise (Fig 3.5).

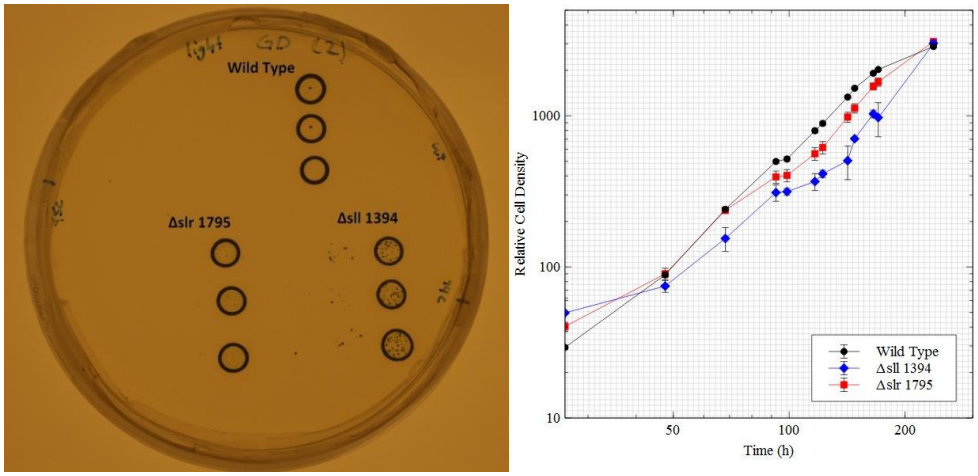

Figure 3.4 - Image plate and spectrum of colonies with ring formation: shows an example of strains grown in high light condition with DCMU. Strains exhibit ring formations, where dark external rings are formed (left). Generated graphs display continuous growth of all three strains after 50-70 h; where strains supposedly start dying on plate conditions without DCMU.

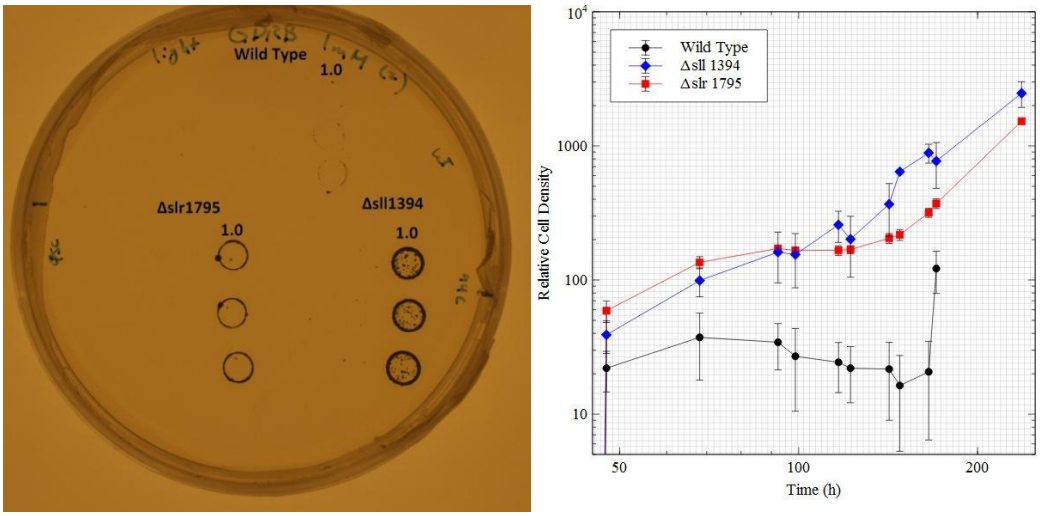

Figure 3.5 - Image plate and spectra of colonies grown on glucose and DCMU: strains grown Glu + DCMU + 1.0 uM of RB after 250 h of incubation (left). Graphs reveal widely spread error bars.

4.2) High-Light Dark Condition

Due to the slow growth because of being covered in quasi-darkness, majority of the colonies under $OD_{730\ nm}$ 1.0 had unreliable growth curves, and thus were not used during analysis of PCC 6803s cellular physiology. Unlike the cultures grown fully exposed to light, the quasi-dark cultures did not have the decrease in recorded cell density-and-recovery phase. Most, if not all, also had very little difference in the growth curves. One exception is at the glucose + 0.1 uM of MV and RB plate where the wild type started dying around 100 hours, while the other two strains remained stationary (Fig 3.6).

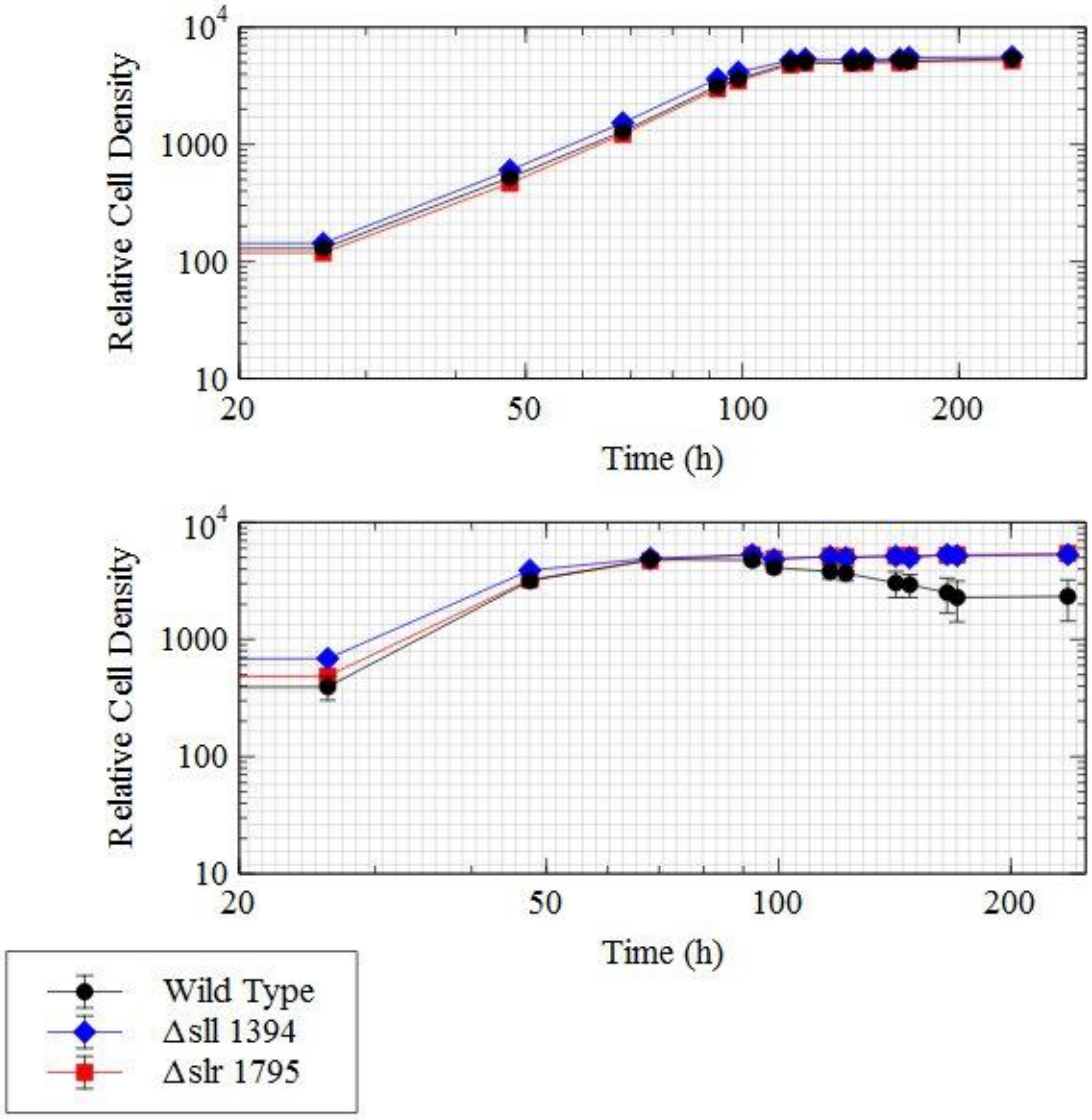

Figure 3.6 - Growth curves of strains grown in dark conditions: (top) Represents the growth curves for most of the plates grown in the quasi-dark environment under the high-light. (bottom) Growth curves of strains grown in glucose + 0.1 uM of MV and RB; also in quasi-dark and under high-light.

5. Chlorophyll and Carotenoid levels

Photoautotrophs experiencing oxidative stress caused by high-light, would increase the production of carotenoids to quench the light harvesting complexes, and act as antioxidants against generated ROS. Therefore, another parameter that was determined in addition to the growth parameters, were chlorophyll (Chl) and carotenoid levels. Four types of culture sets were chosen for each strain: starting from the least pigmented colonies on the MV_0.1 plate; to having slightly green pigmentation on the

GLU plate, and moderate pigmentation on the RB_0.1 plate; and finally colonies that exhibited ring formation on the GDMV_0.1 plate (Fig 3.7). Colonies grown under these conditions were scrapped off entirely from the agar plates and diluted with BG11 on the 18th of growth, and then used to record absorption spectra. Samples were not diluted to 0.3-0.6 OD_{730nm} before analysis.

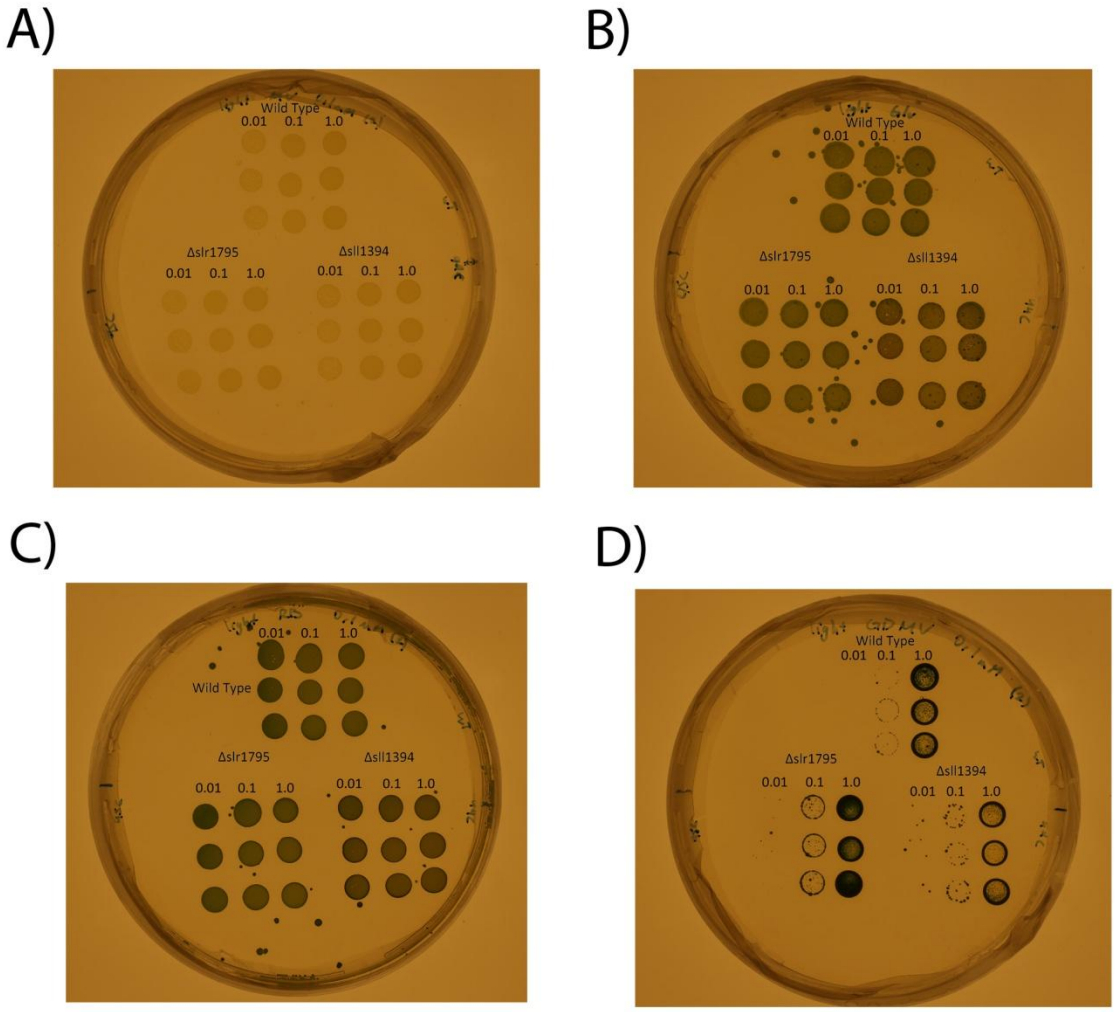

Figure 3.6 - Image plates with strains showing varying degree of pigmentation: Each culture for each strain has three replicates, and are marked with their corresponding optical densities at 730 nm (after scraping off the entire colony). The first plate (A) contains 0.1 uM of MV, and has the least pigmented colonies; (B) is a glucose plate which has slightly green pigmented colonies; (C) contains 0.1 uM of RB with moderately pigmented colonies that appear greener than the ones on glucose plate; (D) contains Glu + DCMU and 0.1 uM of MV, and display colonies that form a ring.

5.1) Absorption Spectra

Absorption Spectra were determined between 400 nm and 750 nm. Chlorophyll α (Chl α) absorbs light at around 435 nm and 680 nm, carotenoids (CAR) at ca. 480 nm and phycobilins (PHY) at ca. 500 nm (Niedzweidzki and Blankenship, 2010). All the spectra were normalized to the chlorophyll α absorption peak at 680 nm = 1.

5.1.1) Spectra on MV_0.1

The culture set taken from this plate condition had the least pigmentation. Spectras reveal a lot of noise, up to 4 in absorbance. All strains seem to have the same similar distribution of peaks, indicating similar pigmentation and stress levels (Fig 3.8).

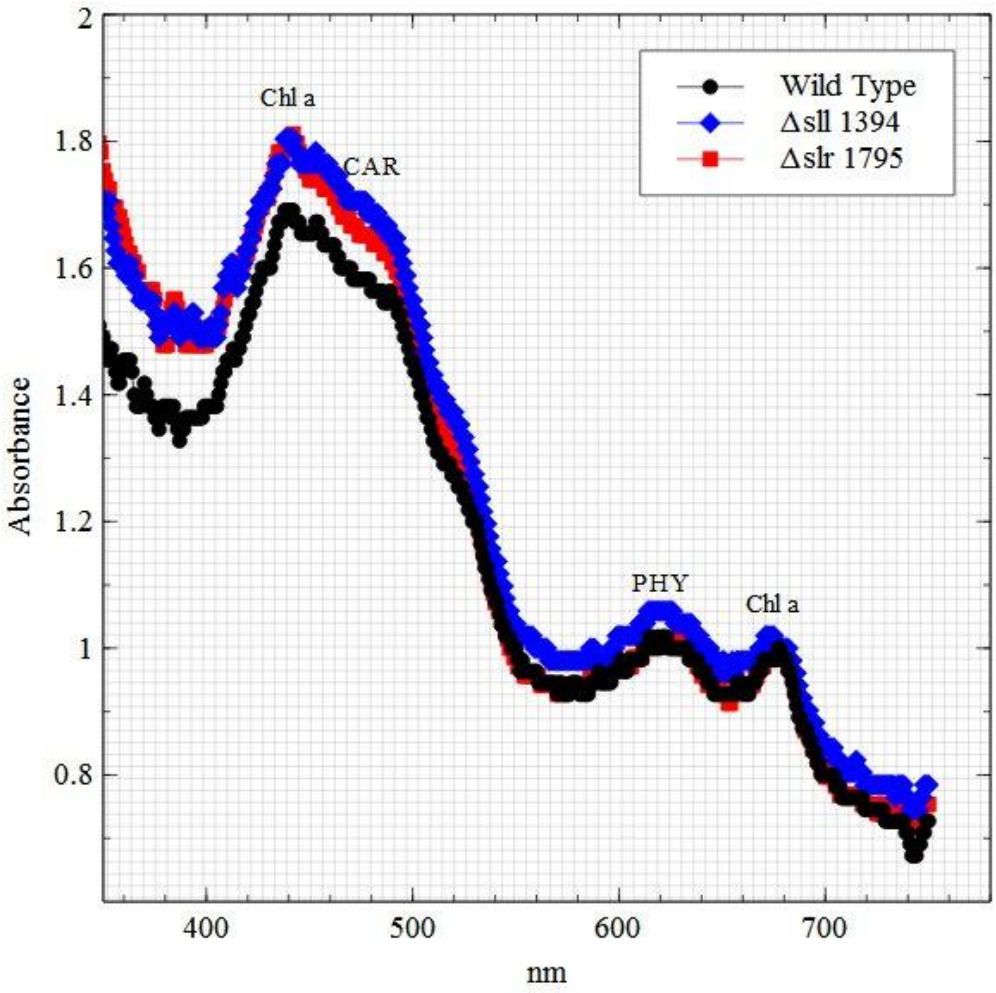

Figure 3.8: Absorption spectrum of very lightly pigmented cultures grown with 0.1 uM of MV plates.

5.1.2) Spectra on GLU

Colonies on the glucose media appeared to be greener when compared to the colonies on plates containing 0.1 uM of MV. The Δsll1394 strain seems to have more carotenoids present in the spectra, in comparison to the other two strains. This is can be seen by the small difference in the maximum absorbance between Δsll1394s carotenoid peak (480 nm) and the Chl α (435 nm) peak. This suggests more carotenoid is present in this particular strain (Fig 3.9). The Δsll1394 strain also has the highest OD value when normalized at 730 nm, indicating less pigmentation per cell basis.

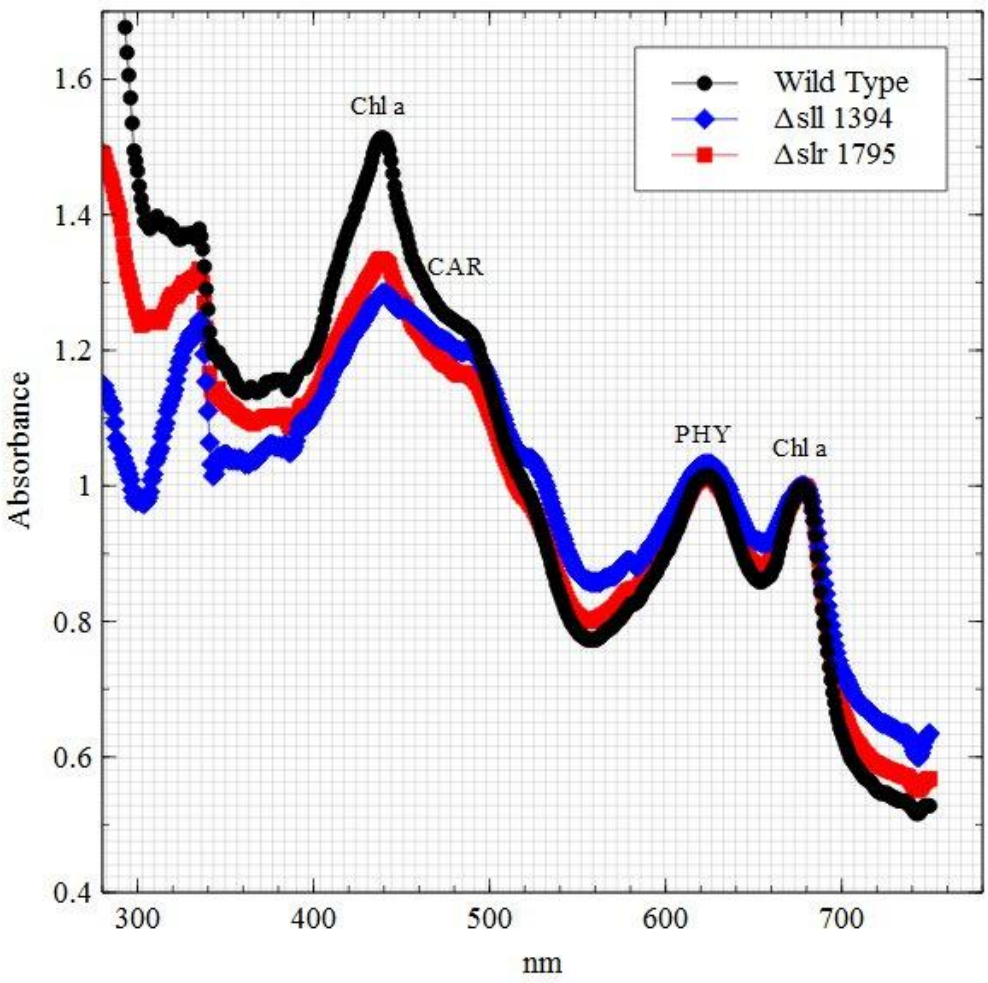

Figure 3.9: Absorption spectrum of slightly pigmented cultures grown in glucose plates.

5.1.3) Spectra on RB_0.1

Colonies on RB at a concentration of 0.1 uM, appear more dark green in colorization in comparison to the strains grown in glucose plates. Again, the Δsll1394 strain seems to contain more carotenoids than the other two strains. Spectras also reveal that all strains have a lower OD at 730 nm compared to the Chl α peak (680 nm) indicating a higher degree of pigmentation than observed on glucose plates.

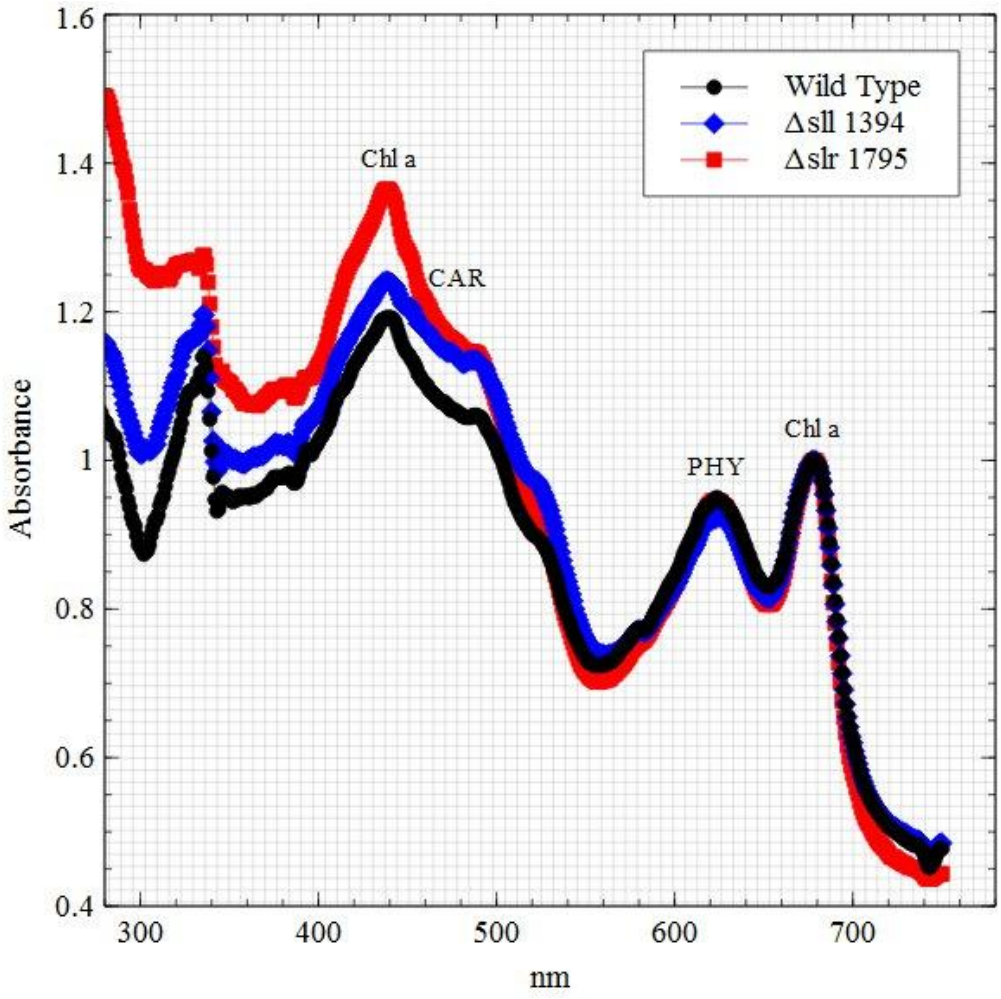

Figure 3.10: Absorption spectrum of moderately pigmented cultures grown in 0.1 uM of RB plates.

5.1.4) Spectra on GDMV_0.1

In contrast to the colonies on glucose, MV at a concentration of 0.1 uM, and RB at a concentration of 0.1 uM plates, the colonies on glucose + DCMU + 0.1 uM of MV display a slightly thicker outer ring. The colonies plated with an $OD_{730\ nm}$ of 1.0, also contained scattered pigmentation inside the ring; with exception of the Δsll1795 strain. Cultures on Δsll1795 appear to have a denser pigmentation at the center of the colony compared to the two strains.

In the 680 nm-normalized spectra, the OD at 730 nm is highest in the Δslr1795 strain, indicating overall lower pigmentation in this strain compared to wild type. The same parameter also indicates less pigmentation for the strain Δsll1394 compared to the wild type. The wild type also appears to have lower chlorophyll to carotenoids ratio than the Δsll1394 strain.

There is also a clear difference in the absorption spectra between the Δsll795 strain and the other two strains. The Δsll1795s carotenoid maximum absorbance is close to the Chl α (435 nm) peak, indicating a high content of carotenoids (Fig 3.11). The Δslr1795 strain also has a lower phycobilin to chlorophyll ratio that the other two strains under these conditions.

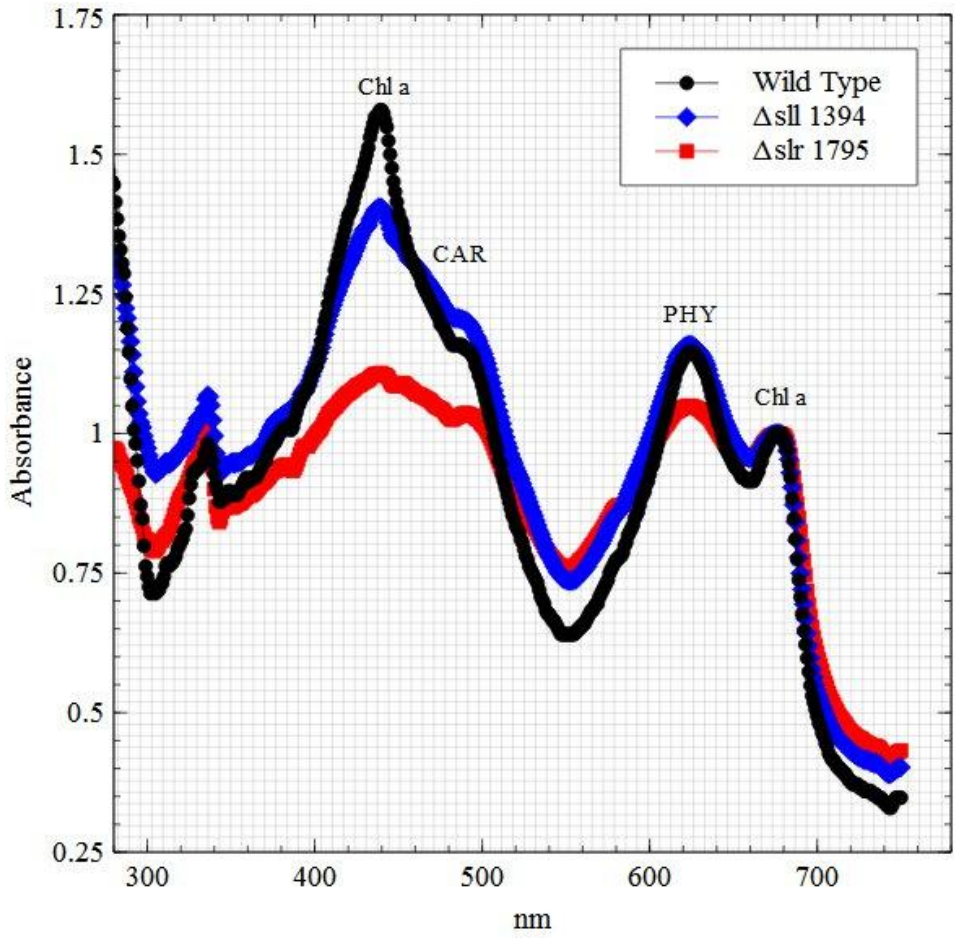

Figure 3.11: Absorption spectrum of cultures that show ring formation, grown in 0.1uM of GDMV plates.

6. Summary

Data gathered from the experiments seem to indicate that the deletion of either MSRA gene, did affect PCC6803s physiology in terms of growth and carotenoid levels. In the moderate light experiment, the mutant strains had a shorter doubling time in comparison to the wild type when grown in the presence of light. Between the two mutant strains, Δsll1394 has a shorter doubling time than Δsll1795 in the presence of glucose. Strains grown in quasi-dark in moderate light experiment show no significant difference in doubling time for all strains, with the exception of strains grown on glucose + 0.1 uM of MV and RB.

In the high-light experiment, strains displayed a decrease in cell density and in the recovery phase when grown in high-light and in the presence of glucose. The Δsll1394 strain displayed a slight growth advantage between 50-70h in comparison to the other two strains in the presence of glucose; but it also displayed a longer lag time after 100h. The strains grown in quasi-darkness did not exhibit this apparent decrease in cell density and recovery behavior. Most strains, if not all, also had very little difference in the growth curves. One exception is at the glucose + 0.1 uM of MV and RB plate where the wild type started dying around 100h, while the other two strains remained stationary.

Another observation of strains exposed to high-light, is the ring formation of plated cells on plate conditions with glucose and glucose + DCMU (GDCMU). Strains on GDCMU displayed this phenotype most intensely and did not have a decrease in apparent cell density and the recovery phase behavior observed in other conditions.

Spectra measuring chlorophyll and carotenoids levels in response to oxidative stress in high light were also measured. Inspection of three plates with varying pigmentation (from least pigmented to moderate pigmentation) and an extra plate with ring forming colonies by absorption spectra revealed that the mutant strains had an elevated level of carotenoids in comparison to the wild type.

7. Other Observations

7.1) Wild Type Growth Experiment

Prior to the moderate and high-light experiments, a growth experiment which exposed the PCC6803 wild type to increasing concentrations of MV and RB was performed. Analysis of the plates showed that cultures grown in the presence of rose bengal had more visible spotted colonies, in comparison to the control plate with 0 uM of RB. The plate containing 0.5 uM of RB, for example, had two visible colonies; while the plate with 1.0 uM of RB had four visible colonies growing.

7.2) New Mutants Adapted to High Light

Inspection of the plates after long exposures to high-light (>21 days) showed that one plate seemed to contain new colonies which seem to have adapted to high-light. In the presence of glucose and 1 uM of MV, all three strains (wild type, Δsll1394, and Δslr1795) seem to have these new high-light adapted colonies.

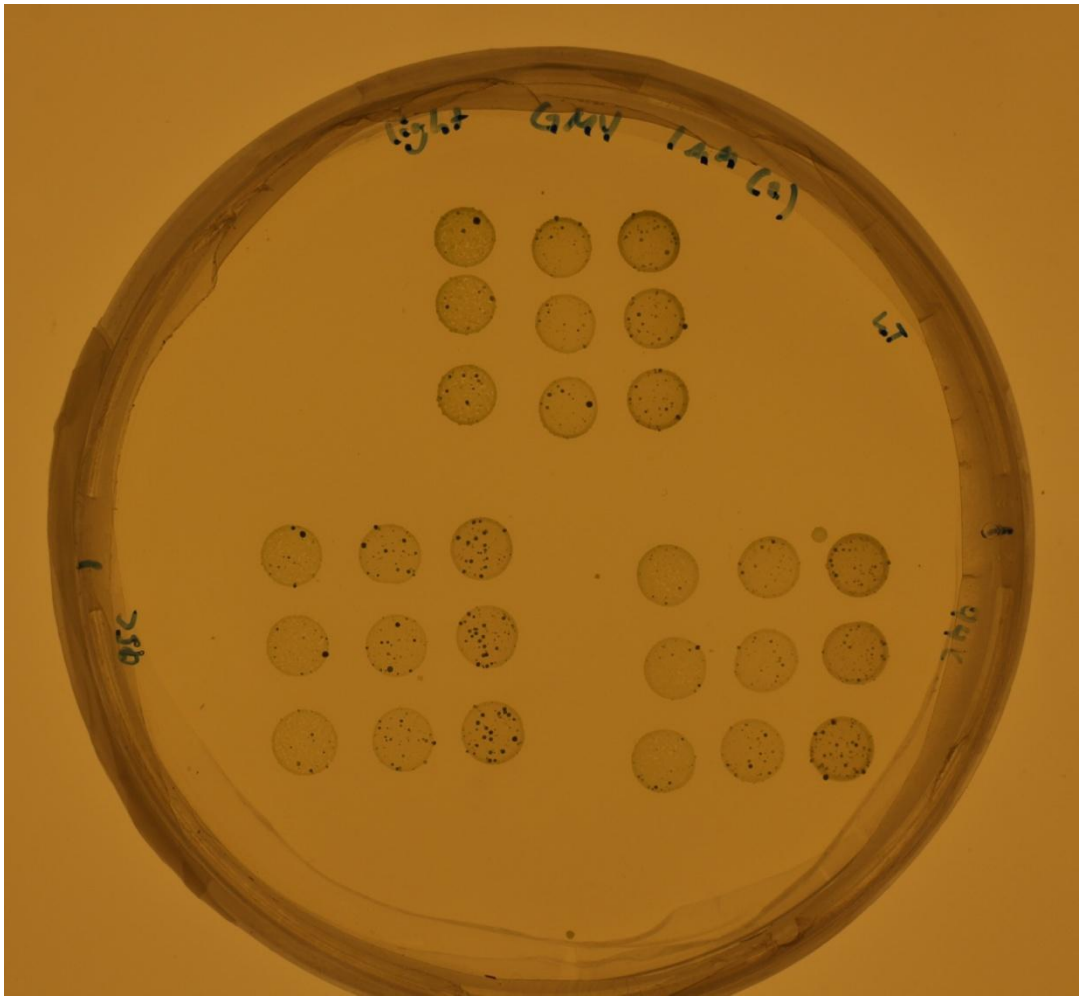

Figure 3.12 - Image plate with new mutant strains: shows new colonies (black spots) growing on top of the previous spotted colonies after 21 days. The new colonies seem to be a new form of mutant strains adapted to high-light.

Chapter 4: Discussion

1. Introduction

The primary objective of this thesis was to determine methionine sulfoxide reductases (MSR) functionality in the cellular physiology of *Synechocystis* sp. PCC 6803 (PCC 6803); as MSRs have been shown to have functionality in combating oxidative stress (Laugier *et. al.,* 2010; Tarrago *et. al.,* 2009). We tested the hypothesis that MSRs also have this functionality in PCC 6803. Genes encoding for the two families of within MRS are present in PCC 6803, one coding for MSRB and two coding for MSRA variants.

Two mutant strains lacking either the MRSA coding gene, sll1394 or slr1795, were generated and exposed to varying stress conditions. Strains were subjected to two light intensity experiments: one in moderate light and another in high-light, to test the contribution role of either MSRA in combating oxidative stress. Non-lethal levels of photosensitizers were also used in both experiments to promote ROS generation. Parameters such as growth rate and doubling time, alongside carotenoid and chlorophyll levels were determined and analyzed.

2. Analysis of the Moderate Light Experiment

This experiment was the first initial characterization of MSRs physiological functionality in PCC 6803. Due to uncertainty about the mutant strain's resilience to oxidative stress, the experiment was done using 150 µE m^{-2} s^{-1} of light. In addition, the concentrations of the photosensitizers were also below the lethal threshold for the wild type.

2.1) Light Condition

2.1.1) Doubling Time

Although no notable difference was seen on the growth curves produced in Excel/LibreOffice, calculations of lag phase (λ) and growth rate (mµ) with R and grofit revealed that there was indeed some variations.

Analysis of the general doubling time across all plate conditions, revealed that the mutant strains, Δsll1394 and Δslr1795, were growing faster than the wild type. A possible explanation for the differences in growth rate is that the wild type originated from an older batch of cells, whereas the mutants were transformed from a more recent batch. This could cause the wild type to have a longer lag

time in comparison to the mutant strains. A latter experiment done in high-light with all three strains showing the same lag time, confirms this hypothesis.

Another possible explanation for the difference in lag time may lie in a pre-adaptation to ROS in the MRSA deletion strains. Because the mutant strains were lacking either sll1394 or slr1795, they may have been more sensitive towards an attack by ROS; the mutant strains may have been genetically selected or physiologically pre-adapted to use anti-oxidizing mechanisms. With this pre-emptive protection in place, the mutant strains had advantage over the wild type, which was still establishing countermeasures. Between the mutant strains, it would seem that Δsll1394 grows slightly faster than Δslr1795 on most plates. This may indicate that absence of the sll1394 MSRA caused the cell to have a greater vulnerability towards ROS and therefore possesses more preventive measures against ROS than the Δslr1795 strain.

2.1.2) Plate Conditions

Among all of the plate conditions, a striking observation is that the wild type, as well as the mutant strains, has a shorter doubling time on rose bengal (with the exception of glucose + DCMU + RB) than on other plates, including plain BG11 plates. There can be several hypotheses for this. First off, rose bengal (RB) is a photosensitizer which promotes generation of singlet oxygen ($^1O_2$) under illumination. The presence of $^1O_2$ may have triggered the production of antioxidizing agents, such as carotenoids and α-tocopherols, which countered/minimized its oxidizing effects (Krieger-Liszkay, 2004). Addition of glucose to these 0.1/1.0uM RB plates, makes the strains grow mixotrophically, leading to the down regulation of PSII activity; which minimizes the generation of $^1O_2$.

The sites where the ROS were generated may also shed light as to why the strains grew faster on plates containing RB. Most $^1O_2$ is produced by PSII where it can be rapidly quenched by localized antioxidants or pigments, (Latifi *et. al.*, 2008); giving the cell more time to invest in growth rather than defense. In comparison, superoxide anion generated by methyl viologen (MV) (and further to hydrogen peroxide and hydrogen radical) occurs in PSI and/or later in the cytosol. Not only do the cells need to produce antioxidizing agents, they also need to produce or activate enzymes that neutralize these three types of ROS. For example, superoxide anion and hydrogen peroxide have been known to oxidize methionine to methionine sulfoxide reductase. This requires the activation/production of MSR and the thioredoxin system to safely reduce MetSO back to Met. All these factors force the cell to invest more resources on defense and repair rather than growth; hence the slower doubling time of the wild type and the mutant strains.

However, the difference between the doubling time of the strains on plates with MV and RB is not that very large; at least for the mutant strains with (5-6 hours difference). Interestingly enough, addition of DCMU seem to have slowed down the growth for both the mutant strains and the wild type. By inhibiting PSII and hindering the transfer of electrons from plastoquinone A to B, DCMU might have given the strains an added protection from ROS, but slowed down their overall growth at the same time.

2.2) Dark Condition

Unlike the data collected from the light condition, the doubling time of the strains in the quasi-dark condition seems to be more homogenous. The doubling time is longer compared to the light condition but this is expected when the strains are growing on glucose which down-regulates PSII; and with minimal light. There are exceptions however; on the Glu + DCMU + 1 uM of RB plates, Δslr1795 seem to be growing slightly faster than the other two strains**.** The doubling time variation might have occurred when the strains were taken out of the aluminum foil for imaging, thus exposing them to higher light for a short duration of time.

3. Analysis of the High-Light Intensity Experiment

In order to test if higher light intensities (ca. 1500 µE m^{-2} s^{-1}) would cause differences in growth and physiological adaptation between wild type and MSRA deletion strains, a second experiment was performed. The increased light exposure was intended to induce larger photodamage and challenge PCC 6803s defenses (NPQ, carotenoids, HLI genes, tocopherols, SOD, catalases, peroxidase/ peroxiredoxins, etc) against high-light and oxidative stress (Latifi, *et al.,* 2008; Maeda *et al.,* 2005; Krieger-Liszkay, 2004). The high-light treatment would generate higher levels of ROS, which would potentially lead to the oxidation of methionine to methionine sulfoxide. In addition, inducing high-light intensity may also activate latter mechanisms; such as transcription of photoprotective genes (e.g. HLI genes); increase in synthesis of proteins required in CO_2 fixation; or up-regulation of repair genes involved in ROS scavenging (e.g. MSR) (Hihara *et. al.,* 2001; Latifi *et. al.,* 2008) that may prolong the cells' survivability.

In contrast to the moderate light experiment, where strains where scraped off from plates, in the high-light experiment cells were first grown in liquid BG11 in order to have actively growing cells, before they were spotted on agar plates. The increased temperature (30^{o}C), however, managed to affect some of the cultures. There was a large variation in the formation of colonies with samples spotted from cell suspensions with an OD_{730nm} below 1.0. Therefore, only the growth parameters of cultures with an OD_{730nm} = 1.0 for each strain in all plate conditions, were analyzed.

3.1) Light Condition

Unlike the previous experiment done in 150 µE m^{-2} s^{-1} of light, strains grown on plates containing glucose displayed an initial growth phase, followed by a decrease in the apparent cell density and the recovery phase after 70 hours. On the first exponential phase, it seems that most strains had little to no significant difference on all the plate conditions in this experiment. This suggests that either that (1) all three strains are equally stressed, regardless of what photosensitizers used; or (2) PCC 6803 truly has many layers of defense against ROS or methionine oxidation that ensures its survivability without MSRA.

Each of the mutant strains also possessed one active MRSA, which may have been enough to reduce any oxidized methionine. In addition, the gene coding for MRSB is also still active on both mutant strains, contributing to yet another layer of defense against oxidative stress.

Interestingly, addition of glucose may have given the Δsll1394 strain a growth advantage between 50-70 hours of incubation in high-light. Lack of the sll1394 gene and down-regulation of PSII due to the photoheterotrophic metabolism of glucose, might have triggered the early release of antioxidizing agents/enzymes; or secondary responses such as up-regulation of repair genes when exposed to high-light (Hihara *et. al.,* 2001). However, like the other two strains, the Δsll1394 strain also showed a decrease in apparent cell number after 70 hours. During this decrease in cell density, it can be assumed that the rate of damage is finally higher than the cells capability for defense and repair (Murata *et al.,* 2007). The strains do recuperate after 100 hours; suggesting that other genes might have been activated to assist in repair and/or proliferation.

3.1.1) Recovery Phase

Upon closer inspection of the growth curves, data seem to suggest that MSR encoded by sll1394 may play a role in the cells recovery phase. On the glucose plate, the Δsll1394 seems to remain in the stationary phase (around 120-150 hours) longer than the wild type and the Δslr1795 strain. A longer stationary phase of the Δsll1394 strain can be seen on the glucose + 0.1um of RB plate, only this time it occurred around 140-170 hours.

The prolonged stationary phase may indicate that the lack of sll1394 MSRA influences the cell during its repair phase. Even in the presence of slr1795 MSRA that could potentially compensate for the loss of sll1394. If sll1394 is more highly expressed than sll1795 or the gene products have different catalytic targets, or catalytic activity could not be tested during the duration of this project. One possible approach to resolve this question is to run an enzyme assay on each of the purified MSRA- enzymes to check for catalytic activity (Brunell *et. al.,* 2010). Nevertheless, this prolonged lag time may be the reason why the Δsll1394 strain seems to recuperate and continue to grow after ca. 170 hours while the other two strains started to slowly die or stayed stationary at 250 hours.

3.1.2) Self-shading

Strains exposed to high-light intensity displayed rings formations on the spotted colonies. These ring formations are considered to be a consequence of the spotting process and drying of the spot, which leaves a denser outer ring. The novel observation here is that the inner part dies in high light. As to why this occurs, this may have been caused by a photoprotective mechanism often referred to as self-

shading. Self-shading is a mechanism wherein cells are in close proximities and form a shield against high-light. The more cells are condensed on one area (cells on the outer ring), the lower average light intensity each individual cell has to endure.

The self-shading characteristic of the colonies was observed on all plate conditions; however, the ring formations were most noticeable on plates containing glucose and glucose + DCMU. Both glucose and DCMU indirectly protect the cells from oxidative stress by down-regulating and/or inhibiting PSII; eventually giving the strains a growth advantage over the other strains grown in their absence. More cellular growth results in denser outer rings. This was most noticeable on strains grown under glucose + DCMU, which formed pronounced rings. DCMU greatly minimizes ROS generation by PSII inhibition, thereby giving the cells more time for growth than defense.

3.2) Dark Condition

Strains growing in the quasi-darkness environment showed very little to no observable difference in growth; with the exception of strains on the glucose + 0.1um of MV and RB plate. This was an expected outcome since ROS generation by light is almost nonexistent. Similar growth characteristics for wild type and MSRA deletion strains on all different plates also indicates that the loss of MSRA has no significant influence in the cell physiology during the dark. Each of the MSRA could have also compensated each other's absence.

4. Chlorophyll and Carotenoid levels

In order to assess how high-light influenced the levels of chlorophyll and carotenoids within the wild type and the MSRA deletion strains, four plates that showed obvious visual differences in pigmentation were analyzed. The spectra gathered from these plates, revealed that the mutant strains had higher carotenoids-chlorophyll a ratios; which could indicate that they were more stressed than the wild type.

Inspection of the spectra with the least pigmented cultures on the MV plate with concentration of 1.0 uM, revealed no notable difference between the wild type and the mutant strains. All three strains seem to have the similar spectra, suggesting that absence of MSRA does not play a critical role in the defense against oxidative stress.

Data gathered from the spectra of cultures grown on glucose and 1.0 uM of RB, revealed that the Δsll1394 strain seems to contain more carotenoids in comparison to the other two strains. This indicates that the lack of the 1394 gene exposed the mutant strain to more oxidative stress; thus producing more carotenoids to either quench excitation and/or scavenged generated singlet oxygen. The protection provided by these increased levels of carotenoids, may have been another factor that increases Δsll1394s survivability on the high-light experiment (Maeda *et. al.,* 2005).

Analysis of the glucose + DCMU + 0.1 uM of MV plate containing the strains with self-shading behavior, showed that there is a clear difference in the absorption spectra between the Δsll795 strain and the other two strains. Not only does the Δslr1795 strain have elevated carotenoid levels , but it also contained less phycobilins than the other strains. Down-regulation of phycobilin production might have been another photoprotective mechanism initiated by the cell to avoid excess light energy. Whether this behavior is unique to the Δslr1795 strain in the said plate condition, or if it is also present in other plate conditions/strains, requires more pigment analysis.

In summary, measurements of the chlorophyll and carotenoid levels of strains with varying degree of pigmentation, gave a promising insight into the role of carotenoids in compensating for the loss of individual MSRA genes. Further experiments still need to be performed to determine this hypothesis in detail.

5. Future Research

Now that we have determined how much oxidative stress the mutant strains can sustain, further experiments can be performed. Ideally, we would like to find conditions where the MRSA mutant strains will grow slow/die. An example could be the repetition of the moderate and high light experiments, but with added parameters to the plate conditions to further compromise the cells many layers of defense. Another example would be the generation of a double deletion strain which might give a better characterization of MSRAs importance in the cell, than partial absence of the gene with the potential to compensate each others' function.

5.1) Double Deletion Strain

Initially, it was planned to generate a double deletion strain of the MSRA genes during the last phase of the project. However, due to the challenges encountered during the vector generation phase and transformation into PCC6803, this was not achieved.

Now that it has been determined that PCC6803 can survive with just one active MSRA on non-lethal levels of photosensitizers and on moderate to high-light intensities, it may be a good idea to generate a double deletion strain in the future. This new strain may hopefully demonstrate how the complete absence of both MSRA enzymes will influence the cells growth rate, reparative capabilities, and overall survivability.

5.2) Plate Conditions

The growth experiment performed on the wild type in the presence of photosensitizers, showed that the growth on non-lethal levels of 2 uM for MV and 5 uM for RB is possible. Being careful to stay under these lethal concentrations, while still ensuring the promotion of ROS, it was determined that future experiments should be performed with 0.1 uM to 1.0 uM of either RB or MV, or both.

5.2.1) Increased Toxicity Levels

Seeing that both the wild type and the mutant strains seem to cope with the existing concentrations levels of RB and MV, it might be a good idea to include another set of plate conditions with increased concentrations of these photosensitizers. The new concentrations could be around, 1.5 uM for MV, and 2.5uM for RB. These new concentrations may generate enough ROS to bypass the cells defense, specifically superoxide dismutase and catalase-peroxidases and their cofactors. The double deletion strain, if generated, should experience elevated stress levels in comparison to the individual deletion strains and the wild type .

5.3) Additional measurements

5.3.1) Varying Light Intensities

Another experiment that could be performed, are high light recovery studies. For example, strains grown on glucose could first be exposed to high-light intensity for 100 hours (wherein most cells have decreased in cell density) before being transferred to quasi- darkness. In doing so, we greatly minimize the generation of ROS, stimulating the cells focus solely on repair rather than preventing damage. Strains with longer lag times during this repair phase, could either have more ROS damage received, or be less efficient repairing cell damage due to individual/ complete absence of MSRA. Studies using similar methods have been reported by Hihara *et. al.,* 2001 to investigate gene regulation after high-light stress.

Chapter 5: Conclusion

To our knowledge, this is the first characterization of the function of MSRA in *Synechocystis* sp. PCC6803s physiology. Both moderate light and high-light experiments have revealed interesting observations. For one, partial absence of MSRA displayed no significant difference between the wild type and the mutant strains in terms of survivability against oxidative damage. This was mainly because of the cells' many layers of preventive measures against oxidative stress. Glucose and DCMU also helped protecting strains by down-regulating or inhibiting PSII; thus minimizing ROS generation.

The main challenge now lies in bypassing the cells' robust defense mechanism against oxidative stress without fully killing the strain. However, in the high-light experiment, the Δsll1394 strain MSRA's functionality began to reveal itself. Lack of this gene appears to results in a strain that was more stressed, thereby triggering both early preventive measures, and maintenance mechanisms. This was most evident in plates with either glucose or 0.1uM of RB, or both. Growth curves for Δsll1394 strain in these plates seem to suggest that it grows slightly faster on the initial exponential phase, but this maybe due to the early preventive measures taken by the cells. The lack of the gene is more apparent during the decrease in cellular density and in the recovery phase, wherein the Δsll1394 strain took a longer time to repair itself before being able to grow again. Increased carotenoid levels in the Δsll1394 strain, and the presences of self shading, seem to have also supported its survivability; indicating that this particular strain was indeed experiencing slightly more oxidative stress than the other two.

In summary, thought-provoking observations into the role of MSRAs start being revealed in the presented study. However, further experiments need to be performed to give a better characterization of MSRAs functionality in *Synechocystis* sp. PCC6803. These experiments could be the generation of a double deletion strain and modification of the stress factors.

References

Allakhverdiev S.I and Murata N. (2004). "Environmental stress inhibits the synthesis de novo of proteins involved in the photodamage–repair cycle of Photosystem II in Synechocystis sp. PCC 6803". Biochimica et Biophysica Acta, **1657**: 23– 32.

Barely M.E., Bekker A. and Krapež B. (2005). "Late Archean to Early Paleoproterozoic global tectonics, environmental change and the rise of atmospheric oxygen". Earth and Planetary Science Letters, **238**: 156-171.

Berlett B.S. and Stadtman E.R. (1997). "Protein oxidation in aging, disease, and oxidative stress". Journal of Biological Chemistry, **272:** 20313—20316.

Blankenship R.E. (2014). Molecular Mechanisms of Photosynthesis -2nd ed. Chichester, UK. Wiley Blackwell.

Boschi-Muller S., Gand A. and Branlant G. (2008). "The methionine sulfoxide reductases: catalysis and substrate specificities. Arch". Biochem. Biophys, **474**, 266–273.

Brunell D., Weissbach H., Hodder P. and Brot N. (2010). "A High-Throughput Screening Compatible Assay for Activators and Inhibitors of Methionine Sulfoxide Reductase A". Assay Drug Dev Technol, **5:** 615-620.

Castano A.P., Demidova T.N. and Hamblin M.R. (2004). "Mechanisms in photodynamic therapy: Part one - Photosensitizers, photochemistry and cellular localization". Photodiagnosis and Photodynamic Therapy, **1:** 279-293.

Davies M.J. (2005). "The oxidative environment and protein damage". Biochim. Biophys. Acta, **1703**: 93–109.

Fujii T., Yokohama E.I., Inoue K. and Skurai, H. (1990). "The sites of electron donation of Photosystem I to methyl viologen". BBA- Bioenergetics, **1015:** 41-48.

Gibsons Assembly. New England Biolabs 2012, USA, Accessed 20. August 2014. https://www.neb.com/protocols/2012/12/11/gibson-assembly-protocol-e5510

Grigorieva G. and Shestakov S. (1981). "Transformation in the cyanobacterium *Synechocystis* sp. 6803". FEMS Microbiology Letters, **13:** 367-370.

Havaux M., Guedeney G., He, Q. and Grossman, AR. (2003). "Elimination of high-light-inducible polypeptides related to eukaryotic chlorophyll a/b-binding proteins results in aberrant photoacclimation in Synechocystis PCC6803". Biochemica et biophysica Acta, **1557:** 21-33.

Hihara Y., Kamei A., Kanehisa M., Kaplan A. and Ikeuchi M. (2001). "DNA microarray analysis of cyanobacterial gene expression during acclimation to high-light". Plant Cell, **13:** 793-806.

Hill R. and Bendall F. (1960). "Function of the two cytochrome components in chloroplasts: A working hypothesis". Nature, **186:** 136-137.

Holland H.D. (2006). "The oxygenation of the atmosphere and oceans". Phil. Trans. R. Soc. B,**361**: 903–915.

Hoshi T. and Heinemann S.T. (2001). "Regulation of cell function by methionine oxidation". Journal of Physiology, **53.1**: 1-11.

Ikeuchi M. and Tabata S. (2001). "*Synechocystis* sp. PCC 6803 – a useful tool in the study of the genetics of cyanobacteria". Photosynthesis Research, **70:** 73-83.

Imlay J.A (2003). "Pathways of Oxidative Damage". Annu Rev Micobiol, **57:** 395-418.

Kahm M., Kschischo M., Hasenbrink G., Lichtenberg-Fraté H. and Ludwig J. (2010). "grofit: Fitting Biological Growth Curves with R". Journal of Statistical Software, **33:** 1-21.

Kaneko T., Sato S., Kotani H., Tanaka A., Asamizu E., Nakamura Y., Miyajima N., Hirosawa M., Sugiura M., Sasamoto S., Kimura T., Hosouchi T., Matsuno A., Muraki A., Nakazaki N., Naruo K., Okumura S., Shimpo S., Takeuchi C., Wada T., Watanabe A., Yamada M., Yasuda M. and Tabata S. (1996). "Sequence analysis of the genome of the unicellular cyanobacterium *Synechocystis* sp. strain PCC6803. II. Sequence determination of the entire genome and assignment of potential protein-coding regions". DNA Res, **3:** 109–136.

Kasting J.F. (1993). "Earth's early atmosphere". Science, **259**: 920–926.

Kirilovsky D. (2007). "Photoprotection in cyanobacteria: the Orange Carotenoid Protein (OCP)-related nonphotochemical-quenching mechanism". Photosynth Res, **93:** 7–16.

Krieger-Liszkay A. (2004). "Singlet oxygen production in photosynthesis". Journal of Experimental Botany, **56:** 441.

Kumar R.A., Koc A., Cerny R.L. and Gladyshev V.N. (2002). "Reaction mechanism, evolutionary analysis, and role of zinc in Drosophila methionine-R-sulfoxide reductase". J. Biol. Chem, **277**: 37527–37535.

Latifi A., Ruiz M. and Zhang C.C. (2008). "Oxidative stress in cyanobacteria". FEMS Micobiol Rev, **33:** 258-278.

Maeda H., Skuragi Y., Bryant A. and DellaPenna D. (2005). "Tocopherols Protect Synechocystis sp. Strain PCC 6803 from Lipid Peroxidation". Plant physiology, **138**: 1422-1435.

Mehler A.H. (1951). "Studies on reactions of illuminatedchloroplasts. I. Mechanisms of the reduction of oxygen andother hill reagents". Arch Biochem Biophys, **33:** 65–77.

Montmerle T., Augereau J.C., Chaussidon M., Gounelle M.C., Marty B. and Morbidelli A. (2006). "Solar System formation and early evolution: The first 100 million years". Earth Moon and Planets, **98**: 39-95.

Mullineaux C.W. (1999). "The thylakoid membranes of cyanobacteria: structure, dynamics and function". Australian Journal of Plant Physiology,**26:** 671-677.

Murata N., Takahashi S., Nishiyama Y. and Allakhverdiev S.I.(2007). "Photoinhibition of photosystem II under environmental stress". Biochimica et Biophysica, **1767:** 414–421.

Nishiyama Y., Allakhverdiev S.I., Yamamoto H., Hayashi H. and Murata N. (2004). "Singlet oxygen inhibits the repair of photosystem II by suppressing the translation elongation of the D1 protein in Synechocystis sp. PCC 6803". Biochemistry, **43:** 11321–11330.

Pospíšil P. (2009). "Production of reactive oxygen species by photosystem II". Biochimica et Biophysica Acta, **10:** 1151–1160.

Rippka R., Deruelles J., Waterbury J.B., Herdman M. and Stanier R.Y. (1979). "Genetic assignments, strain histories and properties of pure cultures of cyanobacteria". J Gen Microbiol, **111:** 1–61.

Stanier RY. and Cohen-Bazire G. (1977). "Phototrophic prokaryotes: the cyanobacteria". Annual Review of Microbiology, **31**: 225-274.

Summerfield T.C., Crawford T.S., Young R.D., Chua J.P.S., Macdonald R.L., Sherman L.A. and Eaton-Rye J.J. (2013). "Environmental pH affects photoautotrophic growth of synechocystis sp. PCC 6803 strains carrying mutations in the lumenal proteins of PSII". Plant and Cell Physiological, **54:** 859-874.

Szabó I., Bergantino E. and Giacometti G.M. (2005). "Light and oxygenic photosynthesis: energy dissipation as a protection mechanism against photo-oxidation". EMBO Repo, **7:** 629–634.

Tichy M. and Vermaas W. (1999). "In Vivo Role of Catalase-Peroxidase in *Synechocystis* sp. Strain PCC 6803". Journal of bacteriology, **181**: 1875–1882.

Laugier E., Tarrago L., Santos V.D., Eymery F., Havaux M. and Rey P. (2010). "Arabidopsis thaliana plastidial methionine sulfoxide reductases B, MSRBs, account for most leaf peptide MSR activity and are essential for growth under environmental constraints through a role in the preservation of photosystem antennae". The Plant Journal, **61**, 271-282.

Lowther W.T., Brot N., Weissbach H., Honek J.F. and Matthews B.W. (2000). "Thiol-disulfide exchange is involved in the catalytic mechanism of peptide methionine sulfoxide reductase". Proc. Natl Acad. Sci. U S A, **97**: 6463–6468.

Niedzweidzki D.M. and Blankenship R.E. (2010). "Singlet and triplet excited state properties of natural chlorophylls and bacteriochlorophylls". Photosynth. Res., **106**: 227-238.

Tarrago L., Laugier E. and Rey P. (2009). "Protein-Repairing Methionine Sulfoxide Reductases in Photosynthetic Organisms: Gene Organization Mechanisms, and Physiological Roles". Mol. Plant, **2:** 202 -217.

Qiaquick PCR purification kit. QIAGEN 2013, Germany, Accessed 5. May 2015**.** http://www.qiagen.com/no/products/catalog/sample-technologies/dna-sample-technologies/dna-cleanup/qiaquick-pcr-purification-kit

Appendix

A. Moderate Light Experiment

A.1) Light Condition

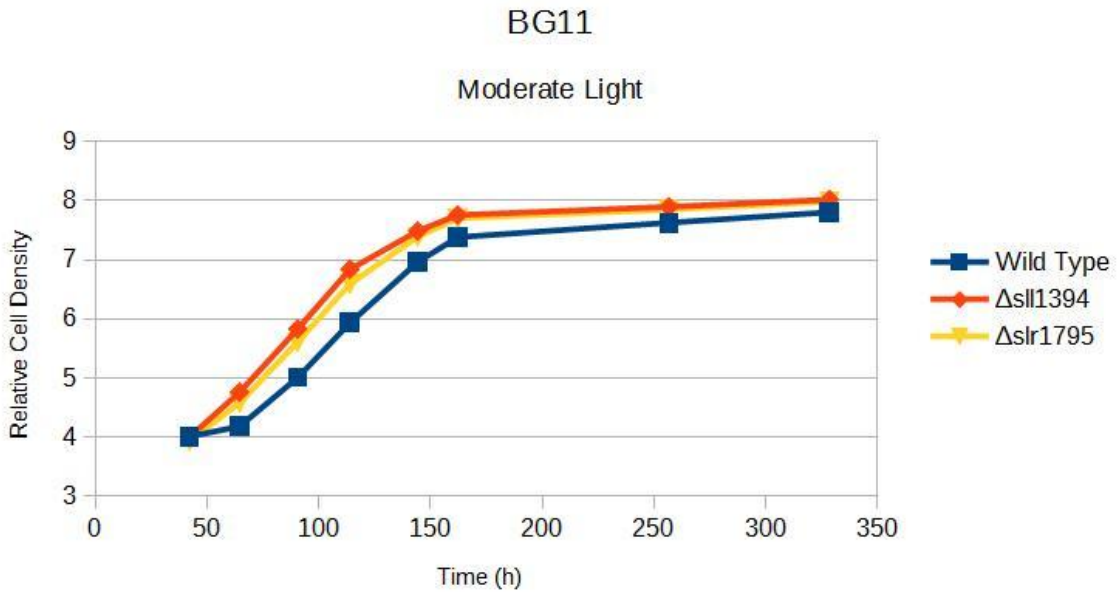

Figure Appendix 1: Averaged growth curve of strains with an $OD_{730\ nm}$ of 1.0 grown on BG11.

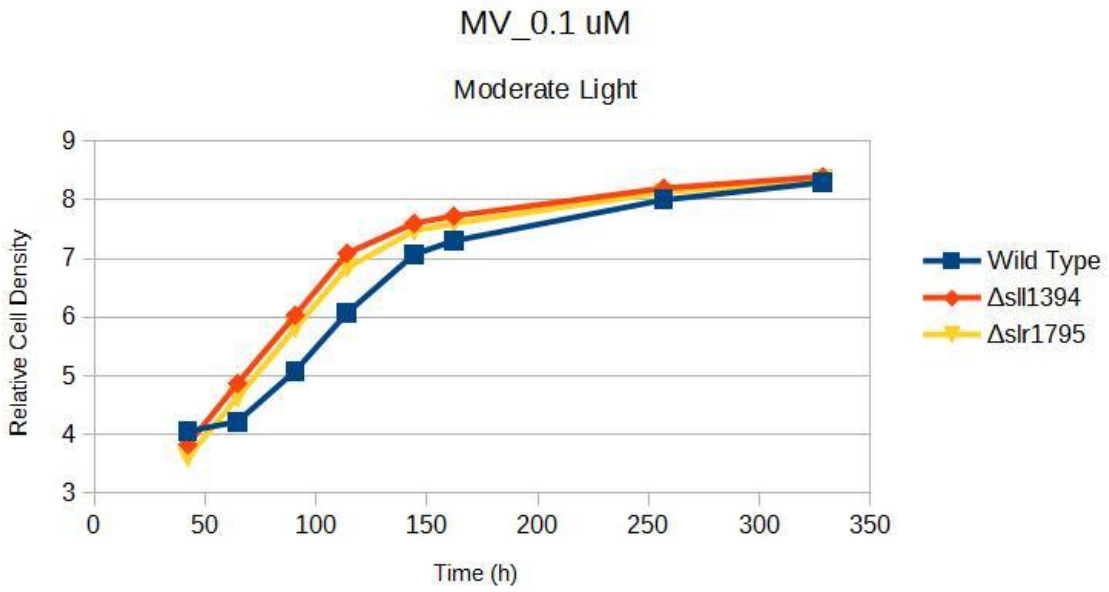

Figure Appendix 2: Averaged growth curve of strains with an $OD_{730\ nm}$ of 1.0 grown on 0.1 uM of MV.

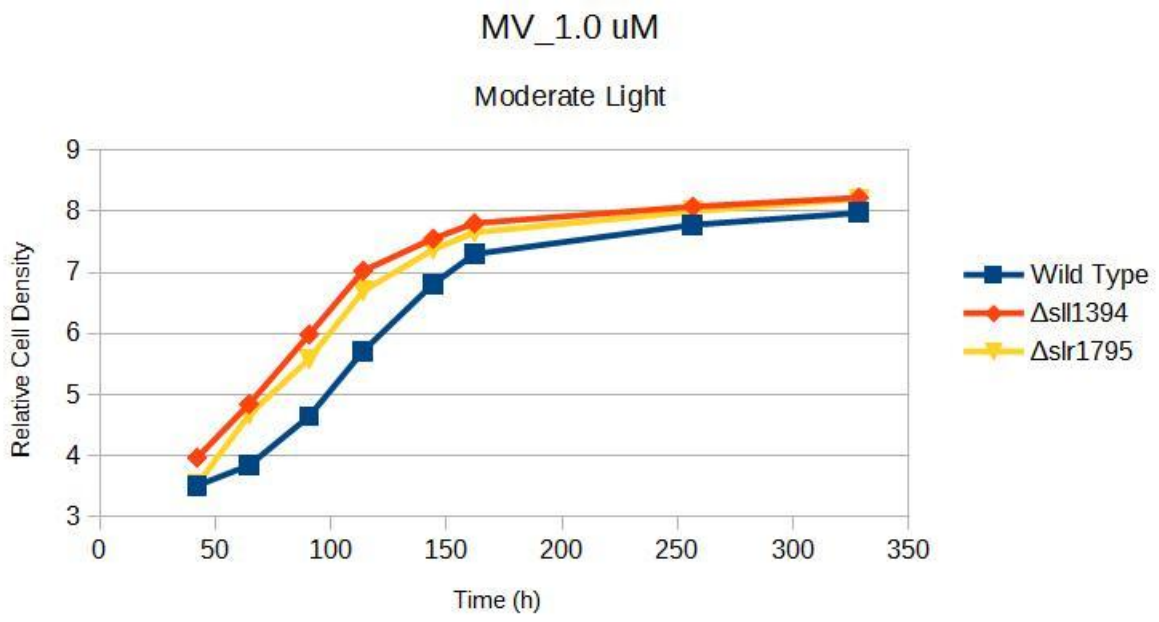

Figure Appendix 3: Averaged growth curve of strains with an $OD_{730\ nm}$ of 1.0 grown on 1.0 uM of MV.

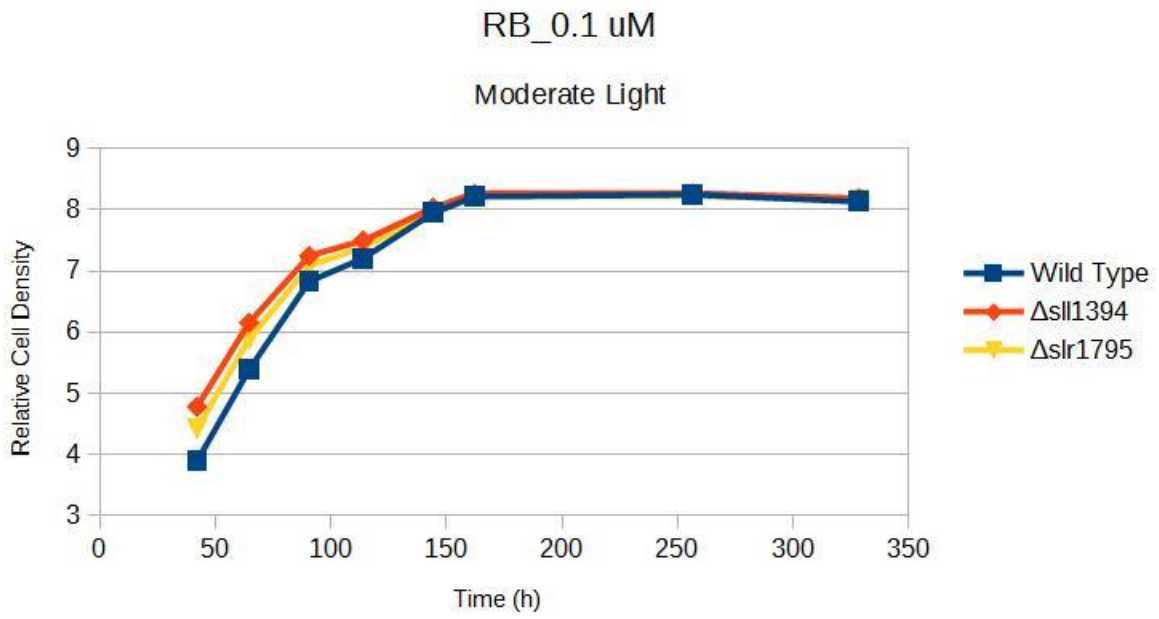

Figure Appendix 4: Averaged growth curve of strains with an $OD_{730\ nm}$ of 1.0 grown on 0.1 uM of RB

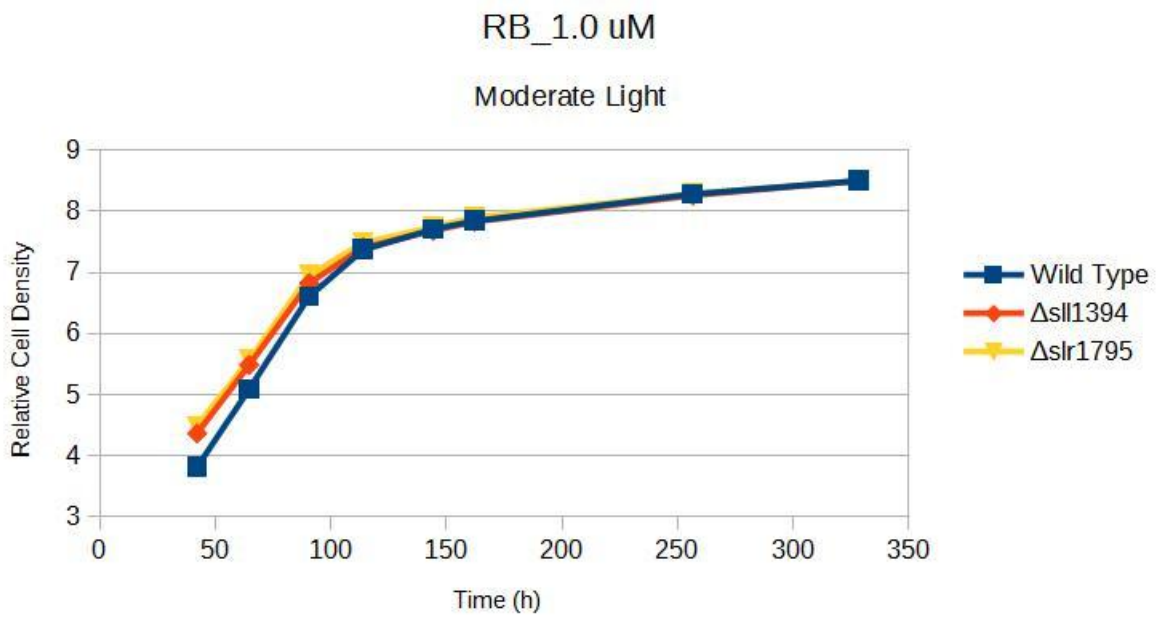

Figure Appendix 5: Averaged growth curve of strains with an $OD_{730\ nm}$ of 1.0 grown on 1.0 uM of RB.

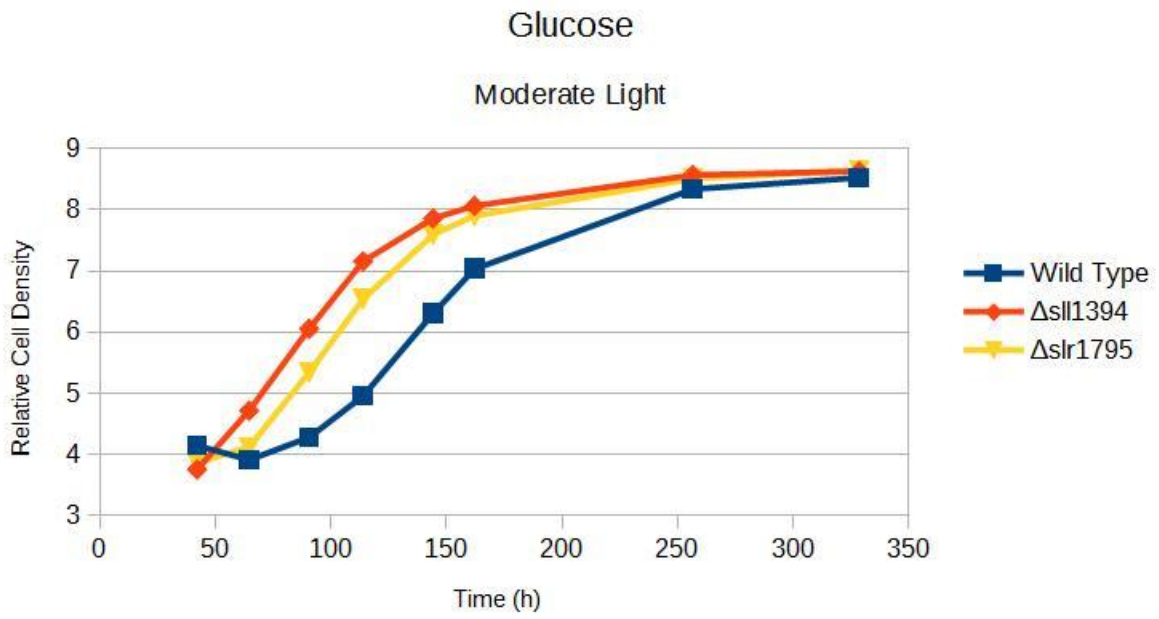

Figure Appendix 6: Averaged growth curve of strains with an $OD_{730\ nm}$ of 1.0 grown on Glucose.

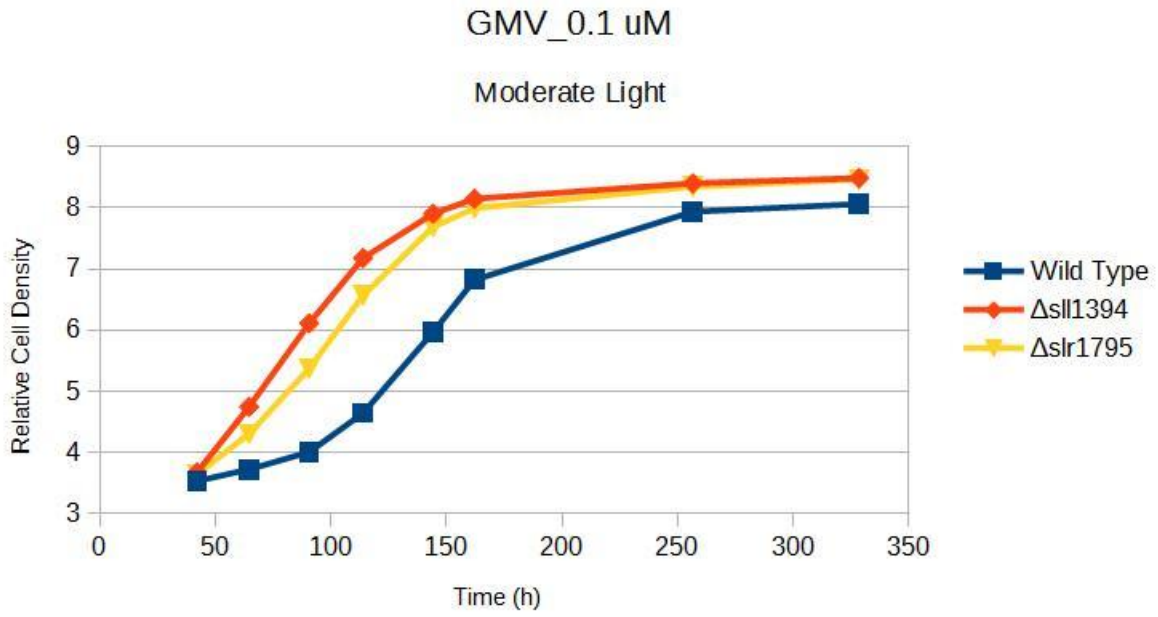

Figure Appendix 7: Averaged growth curve of strains with an $OD_{730\ nm}$ of 1.0 grown on Glucose + 0.1 uM of MV.

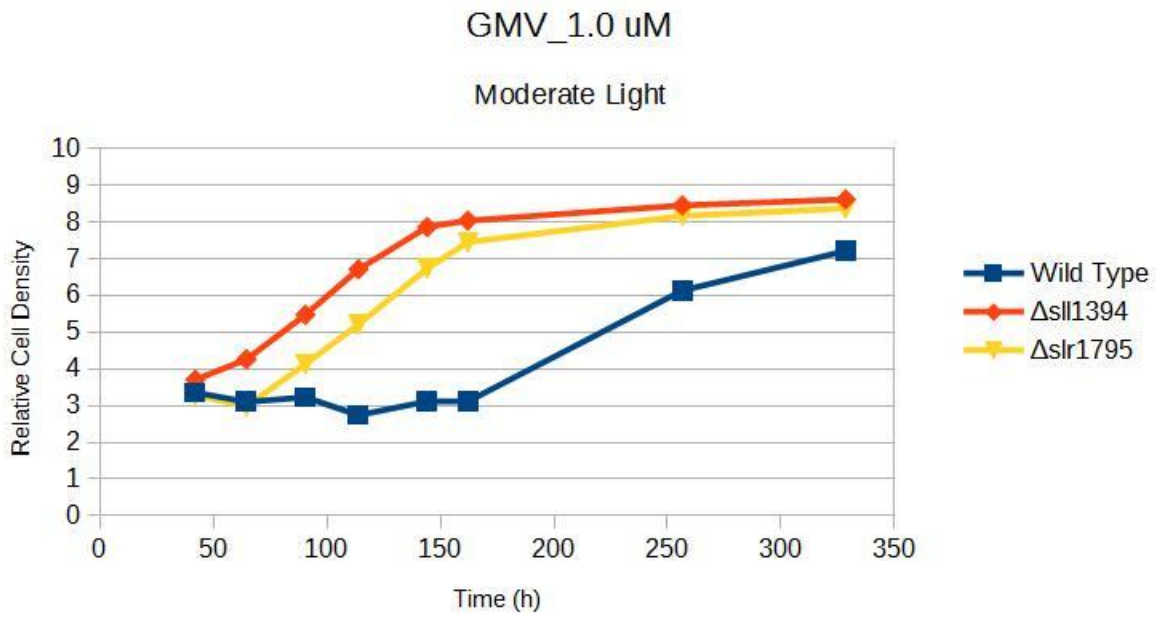

Figure Appendix 8: Averaged growth curve of strains with an $OD_{730\ nm}$ of 1.0 grown on Glucose + 1.0 uM of MV.

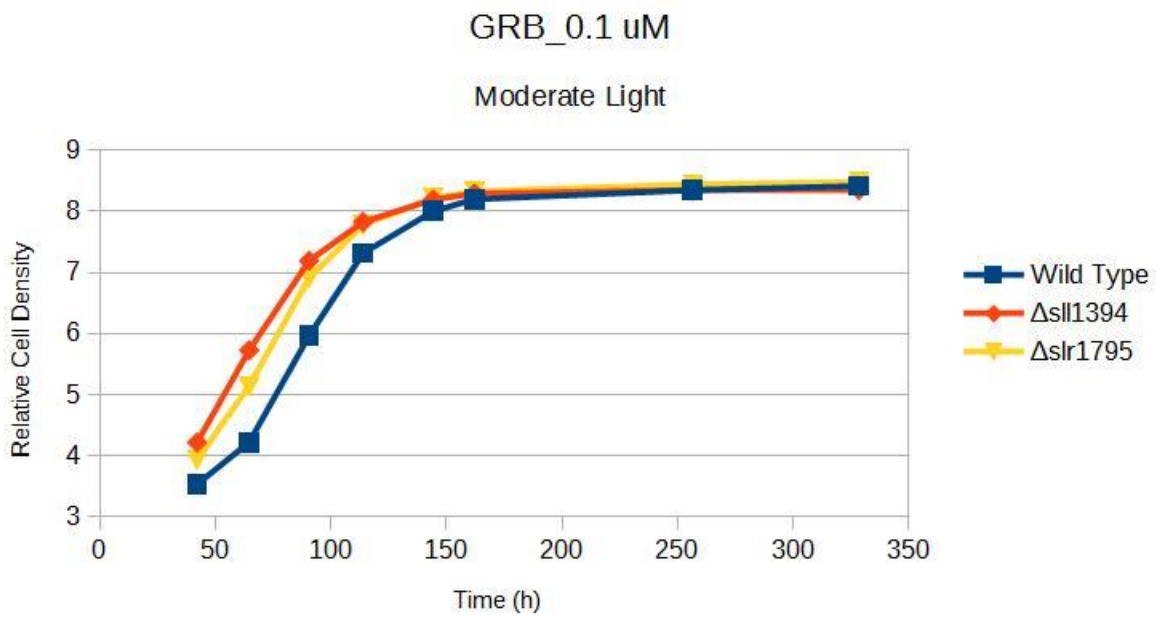

Figure Appendix 9: Averaged growth curve of strains with an $OD_{730\ nm}$ of 1.0 grown on Glucose + 0.1 uM of RB.

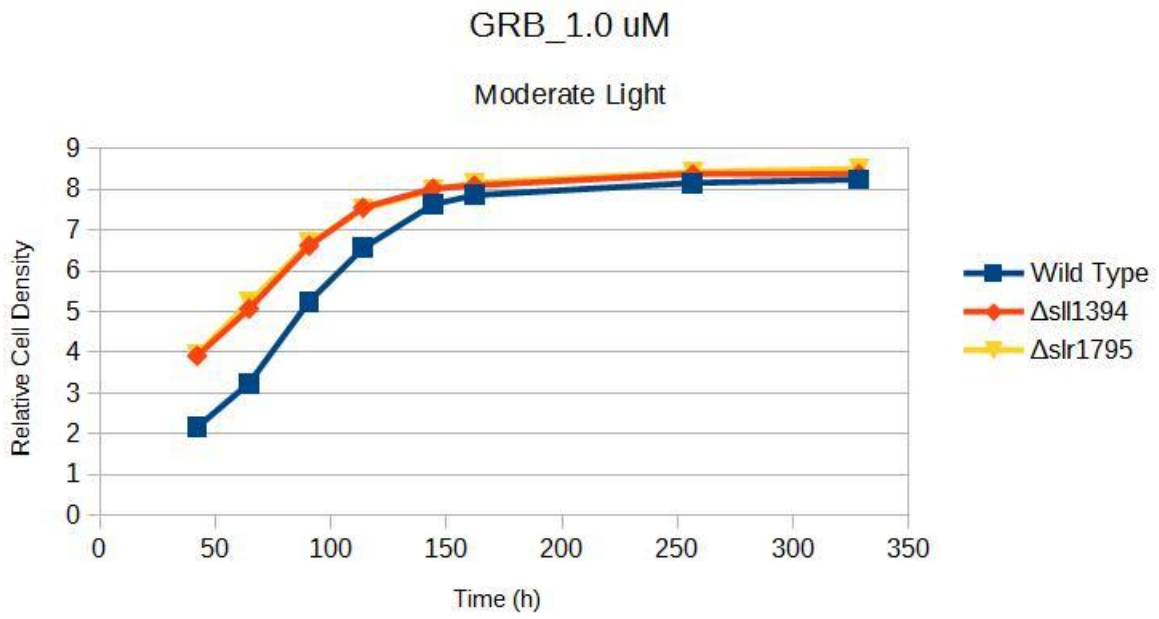

Figure Appendix 10: Averaged growth curve of strains with an $OD_{730\ nm}$ of 1.0 grown on Glucose + 1.0 uM of RB.

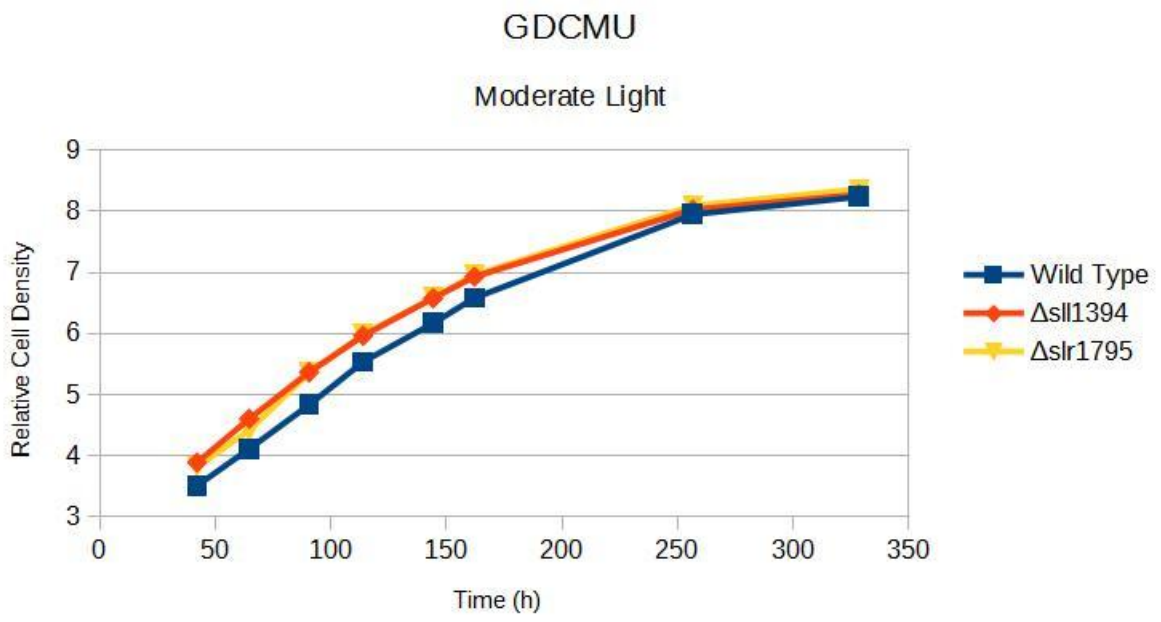

Figure Appendix 11: Averaged growth curve of strains with an $OD_{730\,nm}$ of 1.0 grown on Glucose + DCMU.

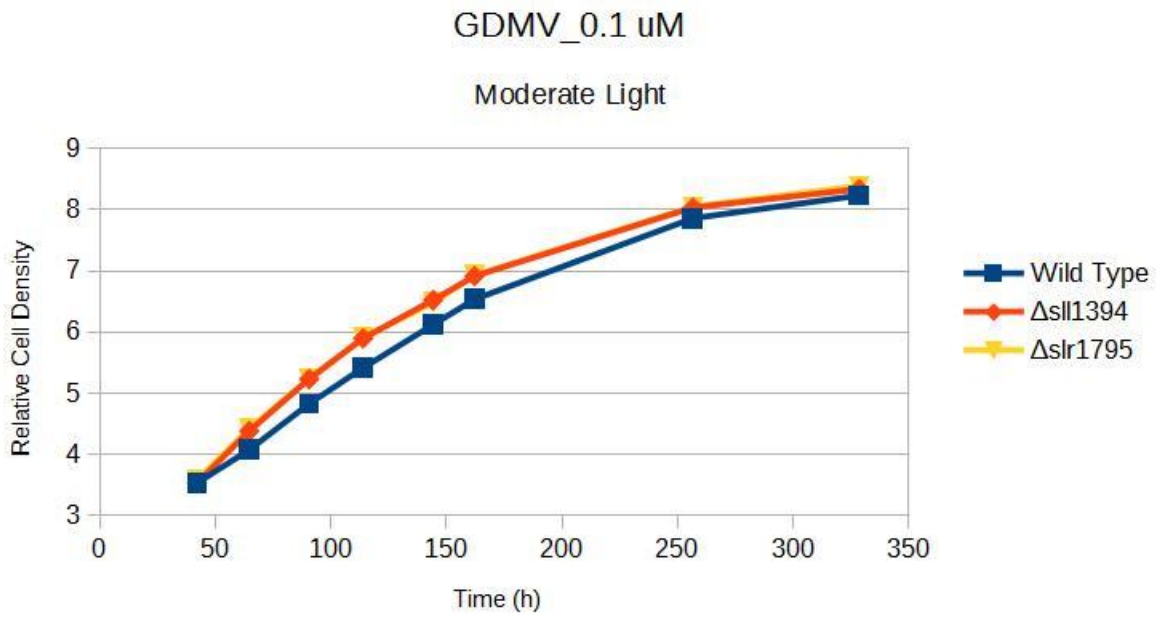

Figure Appendix 12: Averaged growth curve of strains with an $OD_{730\,nm}$ of 1.0 grown on Glucose + DCMU + 0.1 uM of MV.

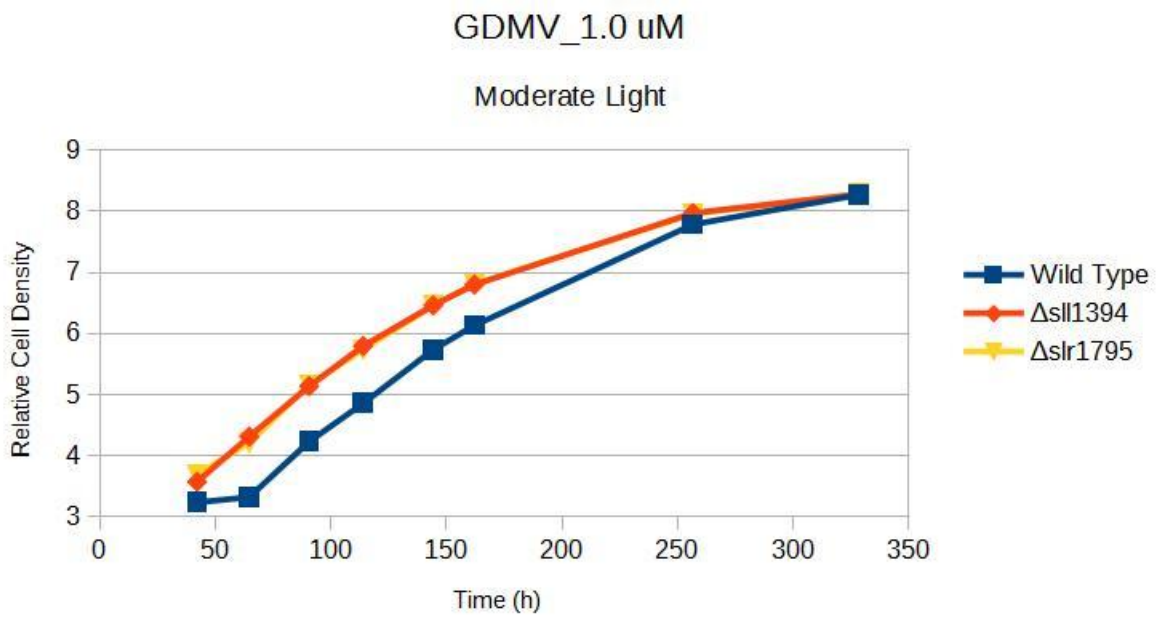

Figure Appendix 13: Averaged growth curve of strains with an $OD_{730\,nm}$ of 1.0 grown on Glucose + DCMU + 1.0 uM of MV.

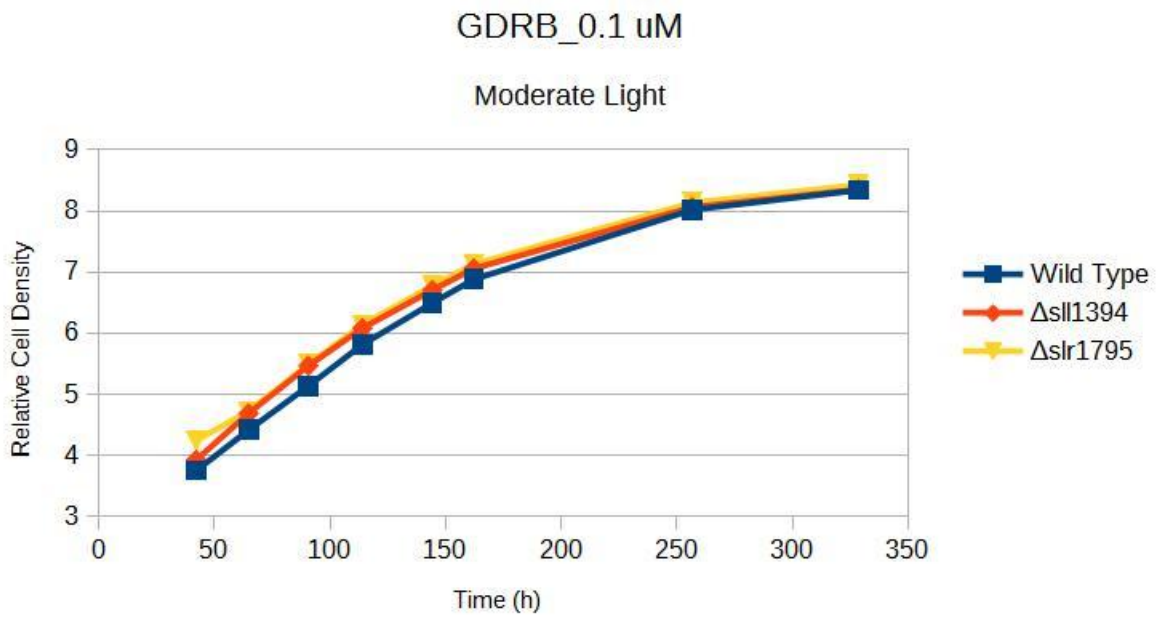

Figure Appendix 14: Averaged growth curve of strains with an $OD_{730\,nm}$ of 1.0 grown on Glucose + DCMU + 0.1 uM of RB.

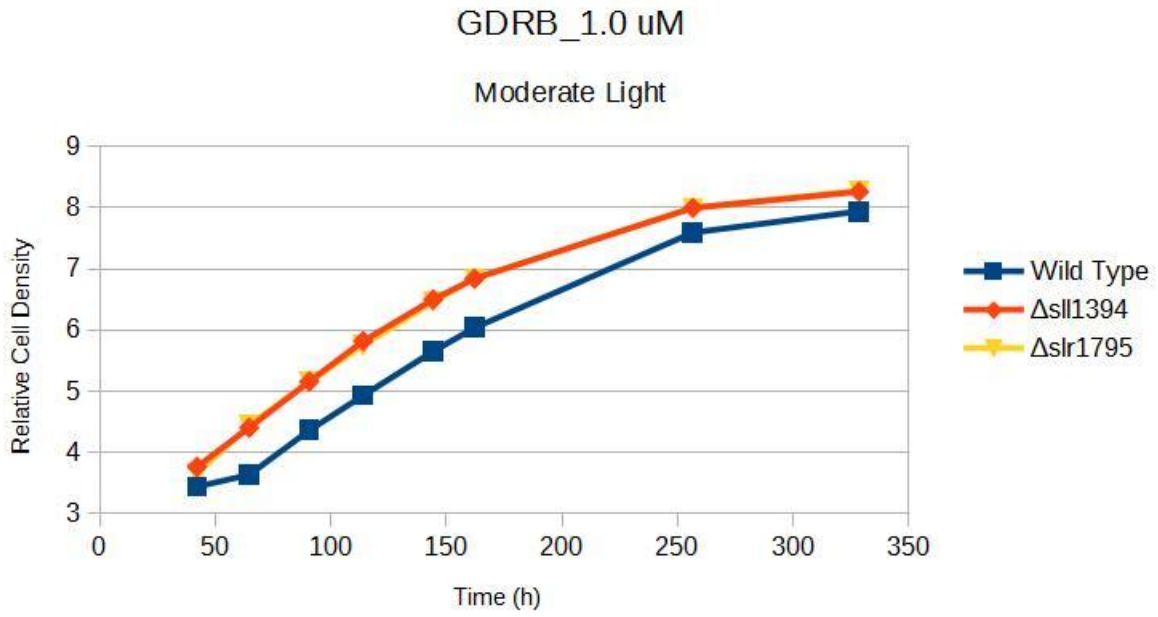

Figure Appendix 15: Averaged growth curve of strains with an $OD_{730\,nm}$ of 1.0 grown on Glucose + DCMU + 1.0 uM of RB.

A.2) Dark Condition

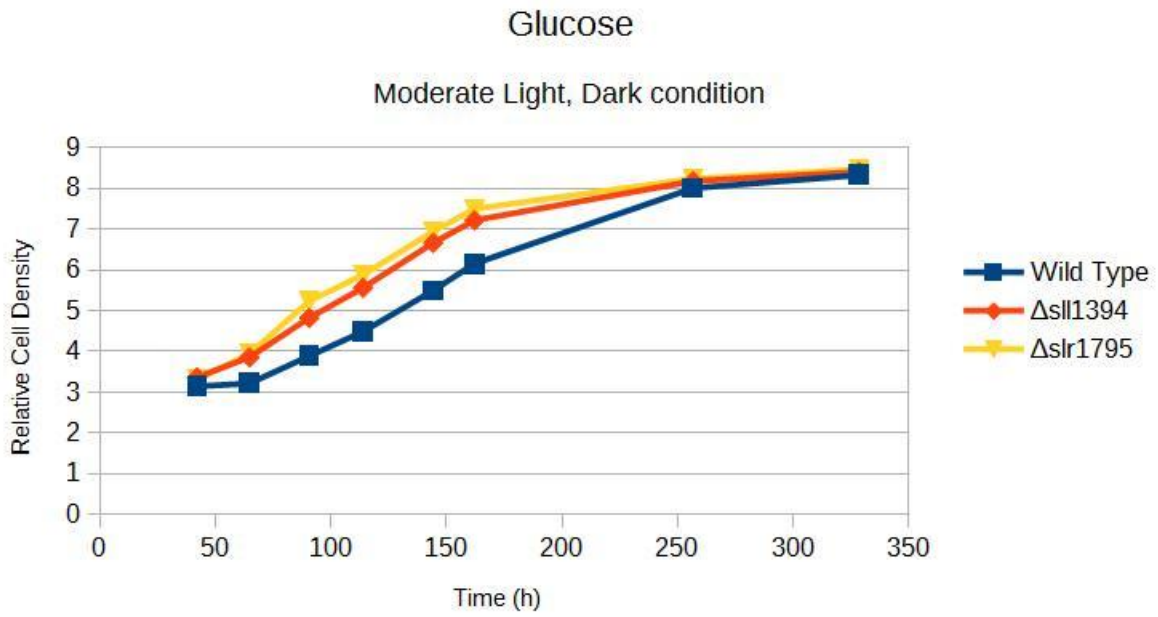

Figure Appendix 16: Averaged growth curve of strains with an $OD_{730\,nm}$ of 1.0 grown on Glucose.

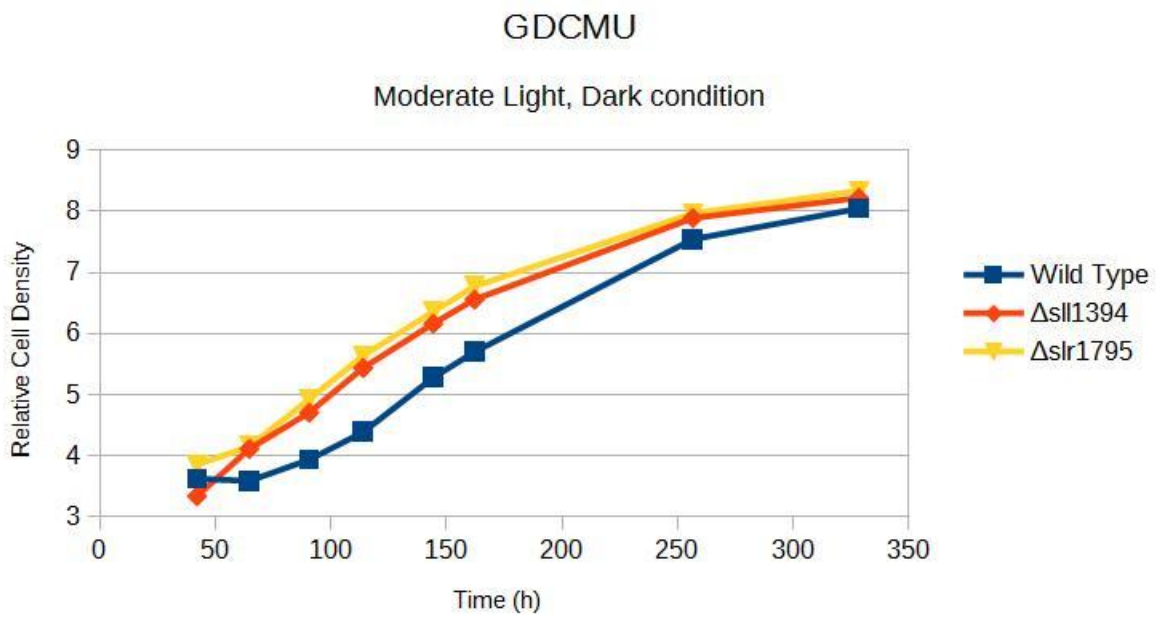

Figure Appendix 17: Averaged growth curve of strains with an $OD_{730\,nm}$ of 1.0 grown on Glucose + DCMU.

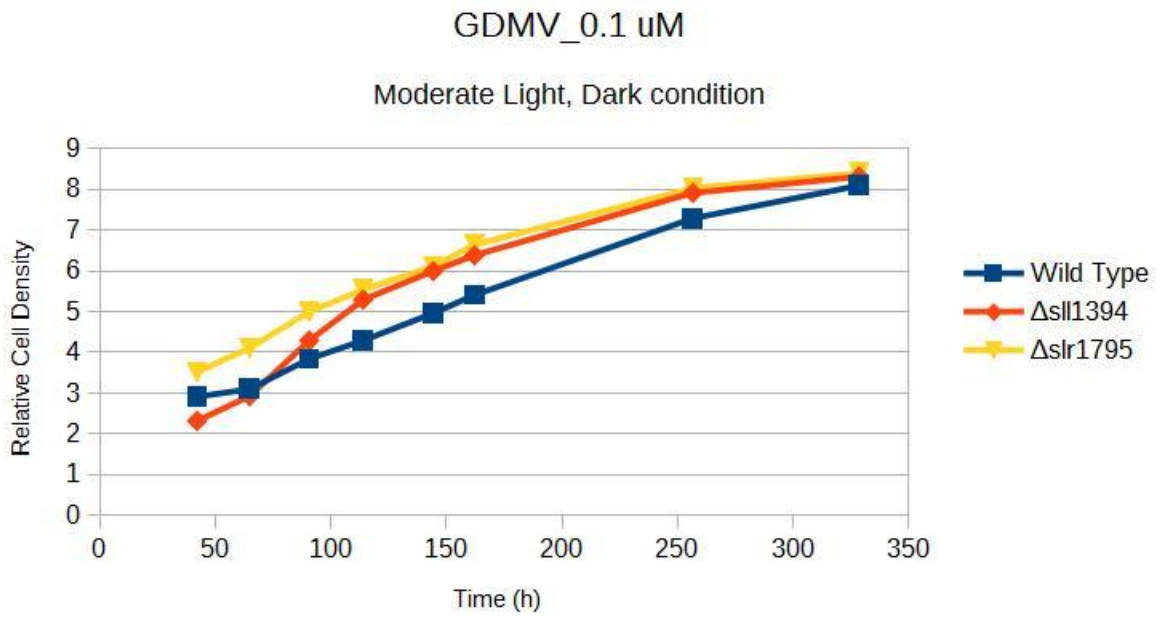

Figure Appendix 18: Averaged growth curve of strains with an $OD_{730\,nm}$ of 1.0 grown on Glucose + DCMU + 0.1 uM of MV.

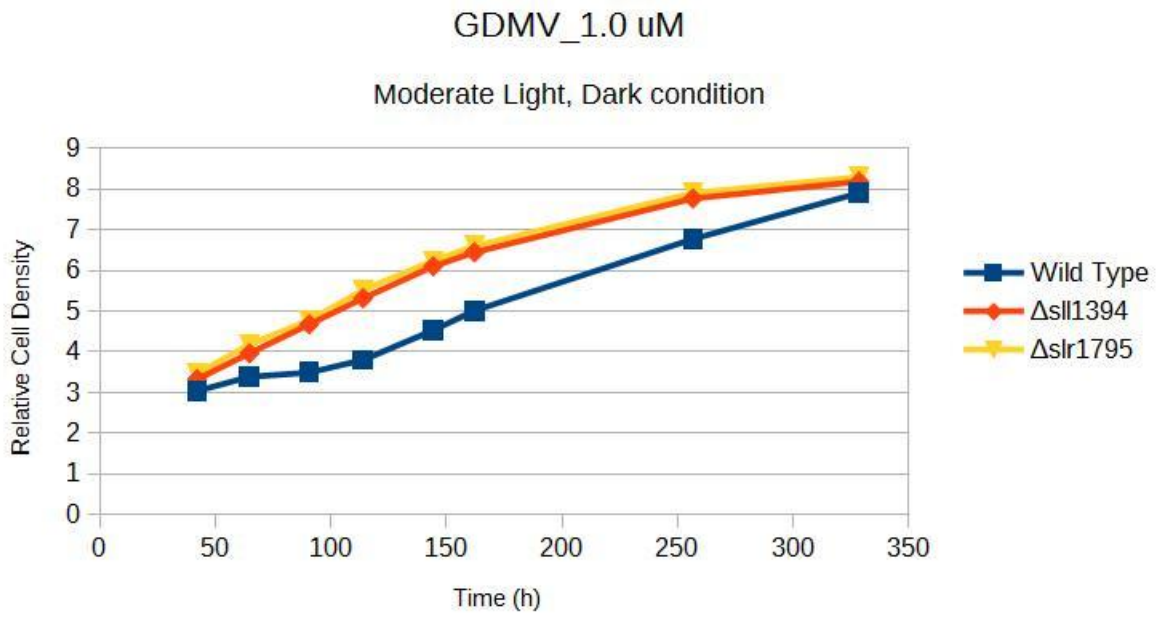

Figure Appendix 19: Averaged growth curve of strains with an $OD_{730\,nm}$ of 1.0 grown on Glucose + DCMU + 1.0 uM of MV.

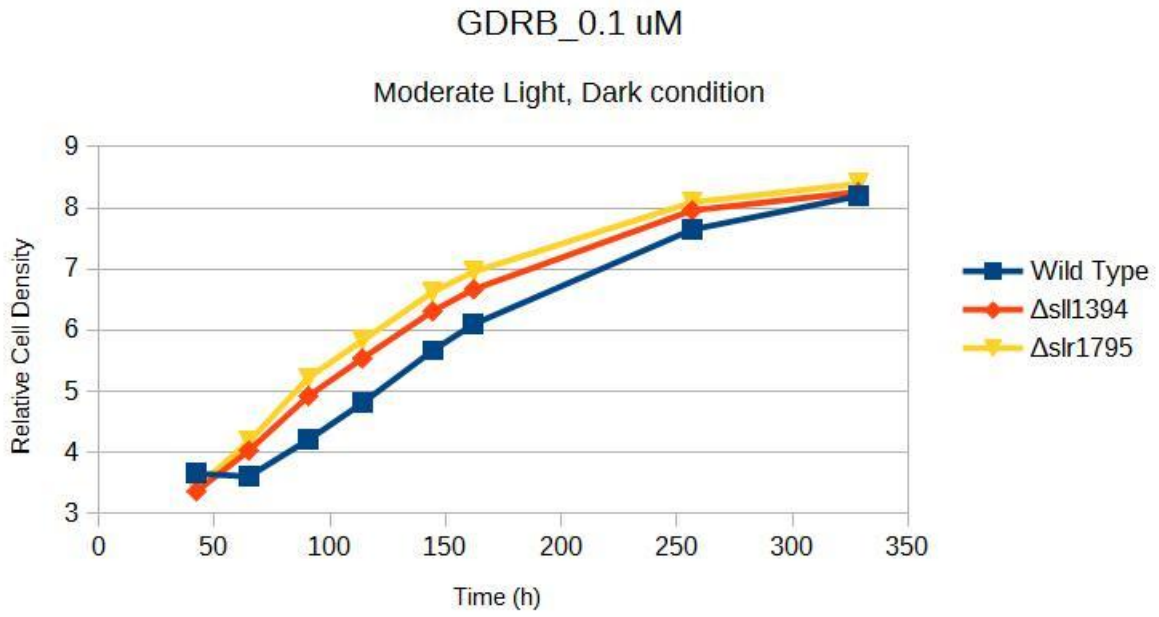

Figure Appendix 20: Averaged growth curve of strains with an $OD_{730\,nm}$ of 1.0 grown on Glucose + DCMU + 0.1 uM of RB.

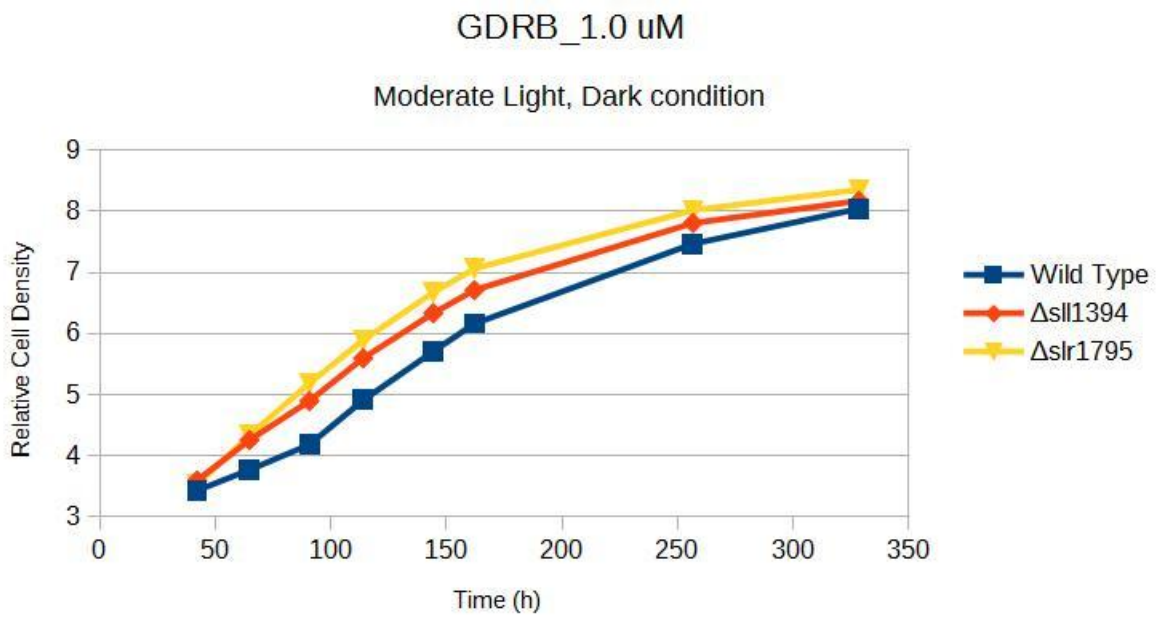

Figure Appendix 21: Averaged growth curve of strains with an $OD_{730\,nm}$ of 1.0 grown on Glucose + DCMU + 1.0 uM of RB.

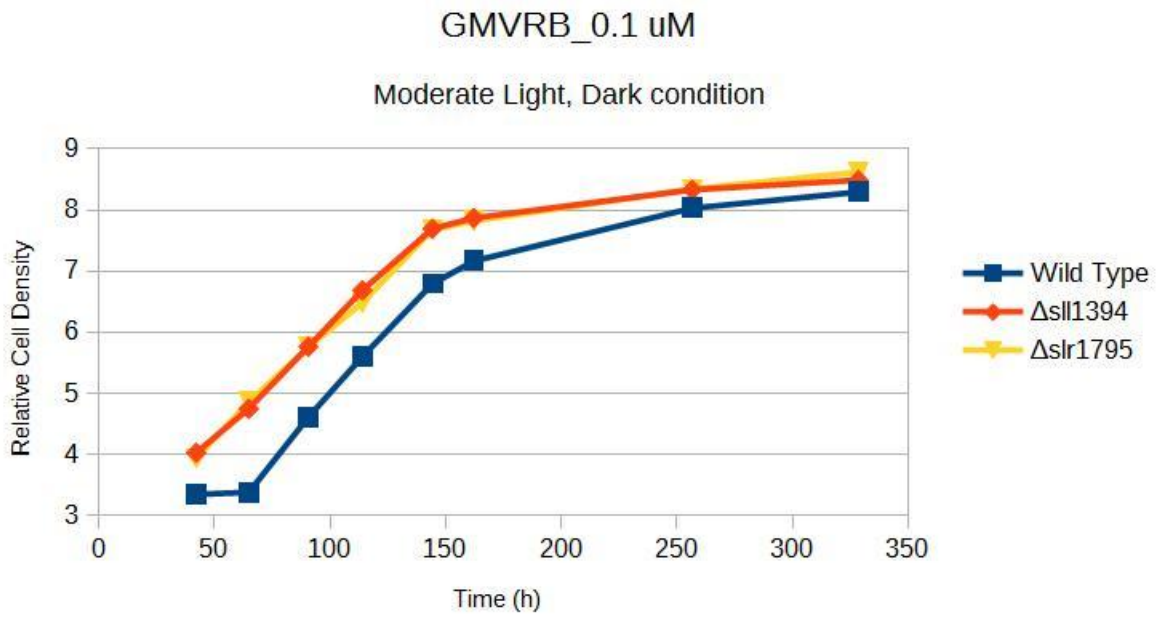

Figure Appendix 22: Averaged growth curve of strains with an $OD_{730\,nm}$ of 1.0 grown on Glucose + 0.1 uM of MV and RB.

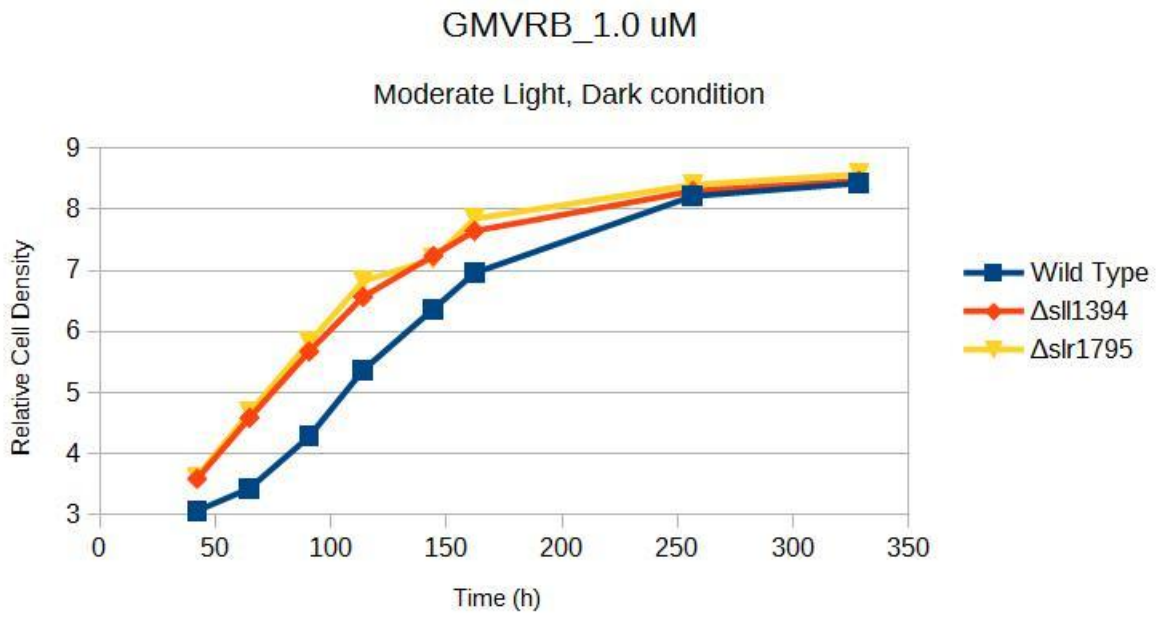

Figure Appendix 23: Averaged growth curve of strains with an $OD_{730\,nm}$ of 1.0 grown on Glucose + 1.0 uM of MV and RB.

B. High-Light Experiment

B.1) Light Condition

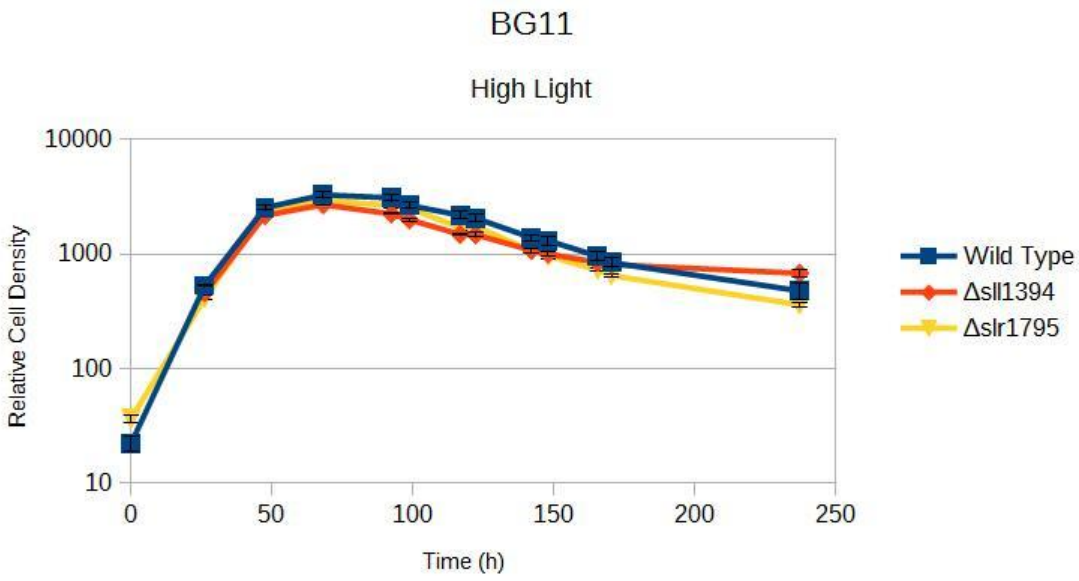

Figure Appendix 24: Averaged growth curve of strains with an $OD_{730\,nm}$ of 1.0 grown on BG11.

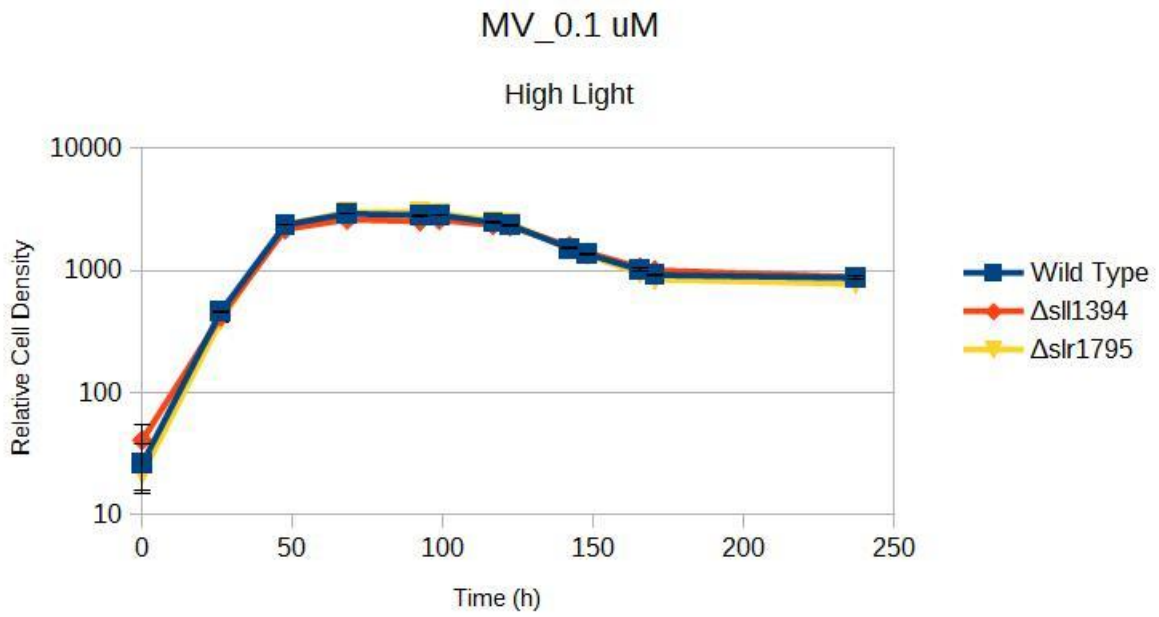

Figure Appendix 25: Averaged growth curve of strains with an $OD_{730\,nm}$ of 1.0 grown on 0.1 uM of MV.

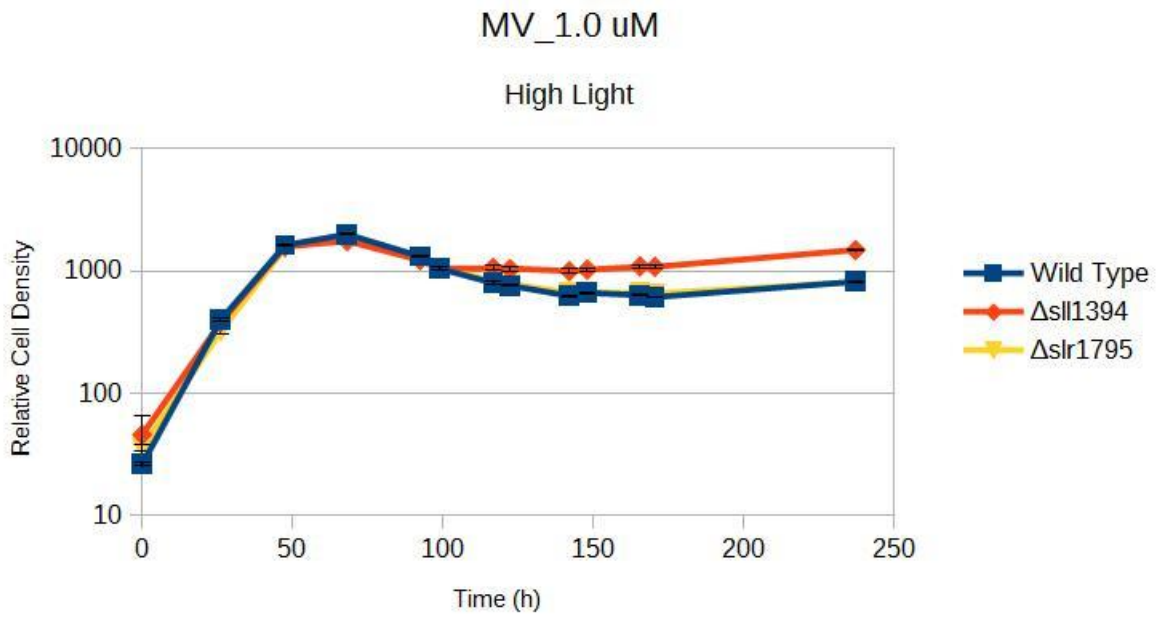

Figure Appendix 26: Averaged growth curve of strains with an $OD_{730\,nm}$ of 1.0 grown on 1.0 uM of MV.

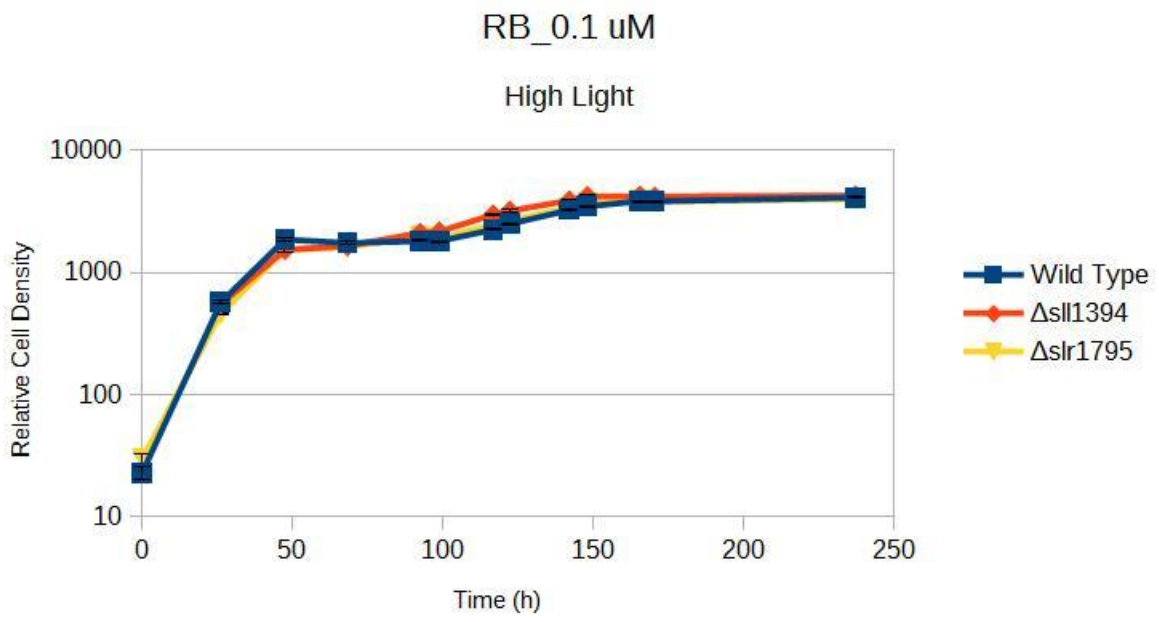

Figure Appendix 27: Averaged growth curve of strains with an $OD_{730\,nm}$ of 1.0 grown on 0.1 uM of RB.

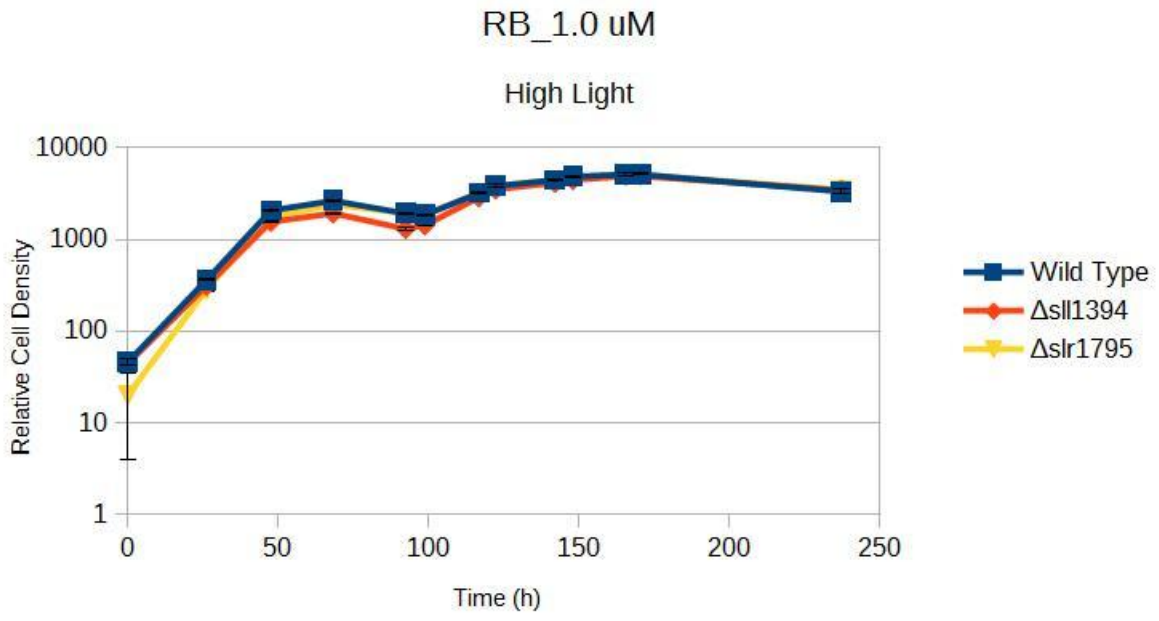

Figure Appendix 28: Averaged growth curve of strains with an $OD_{730\,nm}$ of 1.0 grown on 1.0 uM of RB.

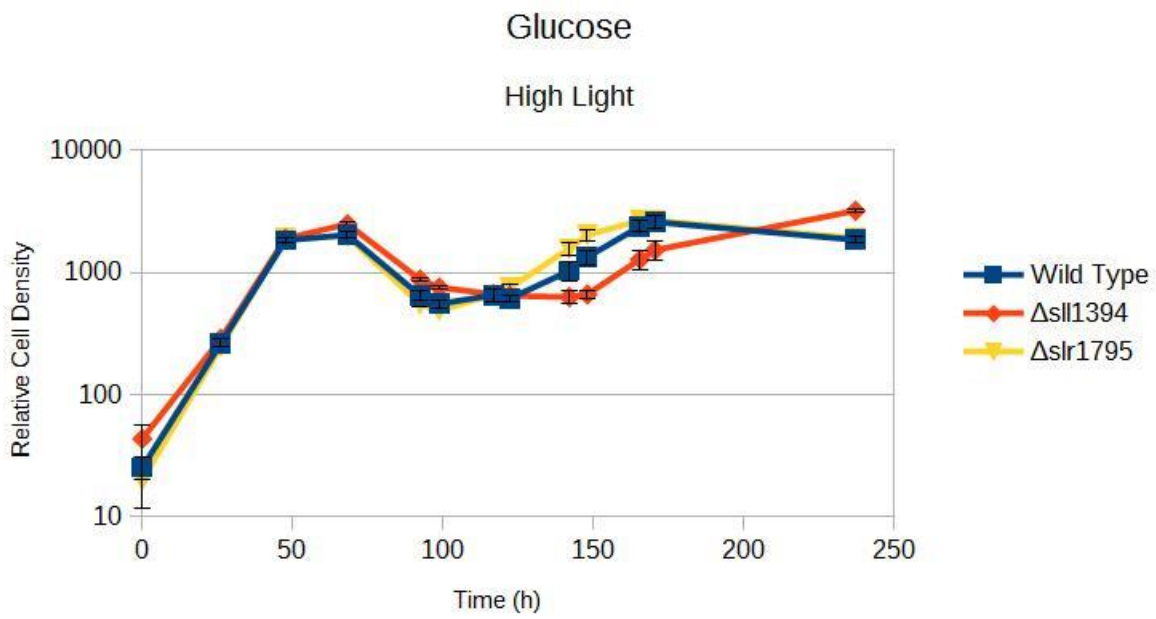

Figure Appendix 29: Averaged growth curve of strains with an $OD_{730\,nm}$ of 1.0 grown on Glucose.

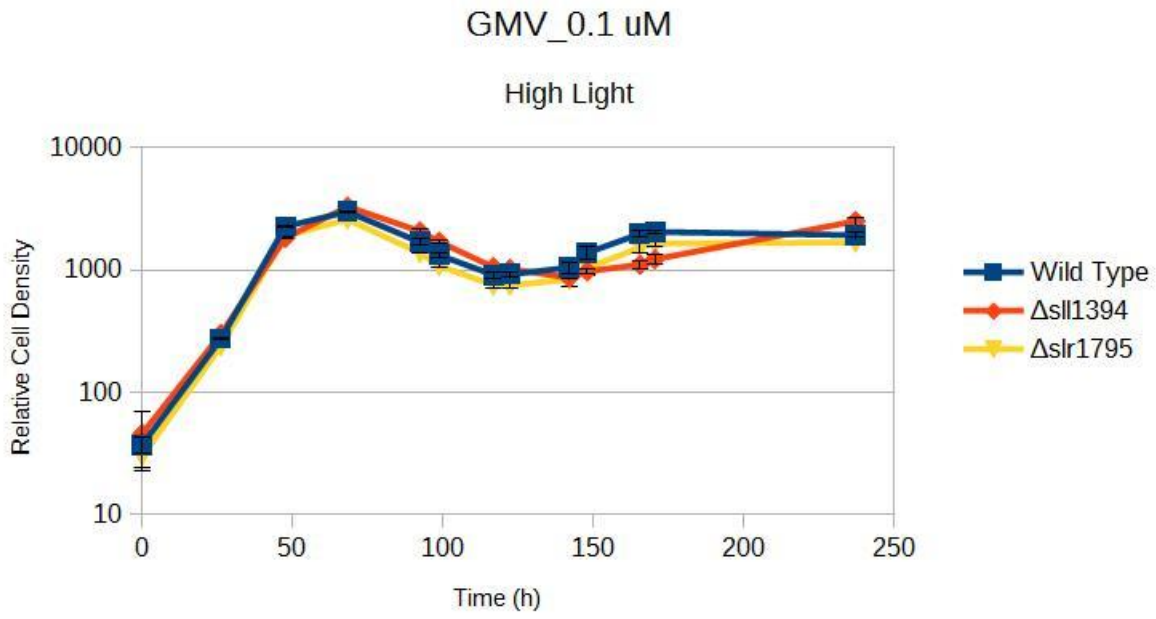

Figure Appendix 30: Averaged growth curve of strains with an $OD_{730\,nm}$ of 1.0 grown on Glucose + 0.1 uM of MV.

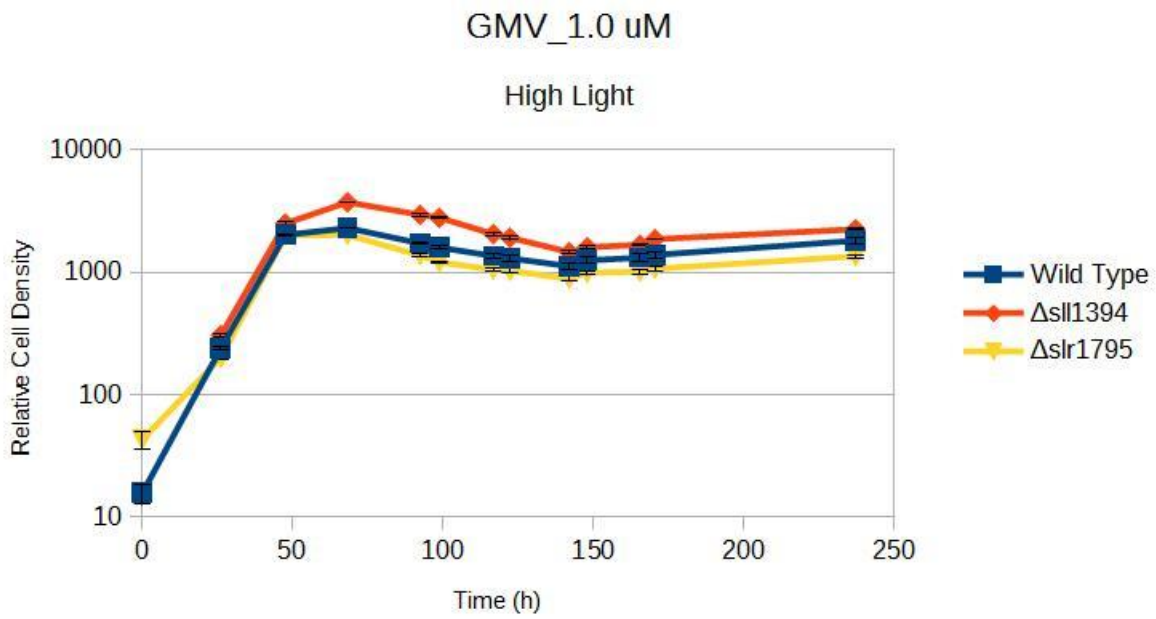

Figure Appendix 31: Averaged growth curve of strains with an $OD_{730\,nm}$ of 1.0 grown on Glucose + 1.0 uM of MV.

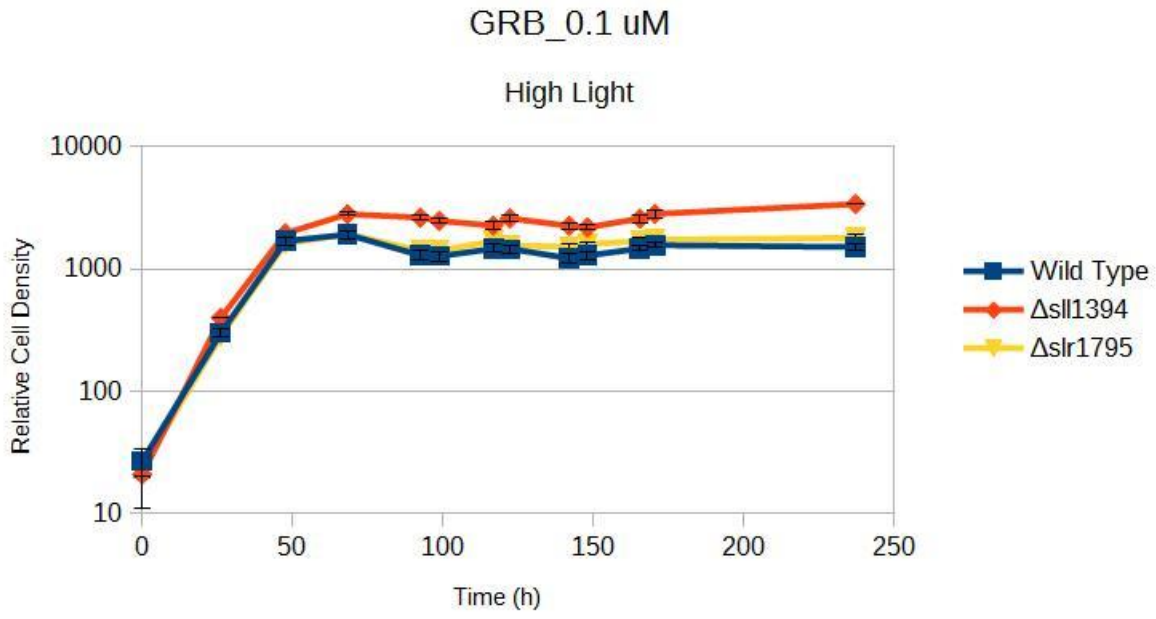

Figure Appendix 32: Averaged growth curve of strains with an $OD_{730\,nm}$ of 1.0 grown on Glucose + 0.1 uM of RB.

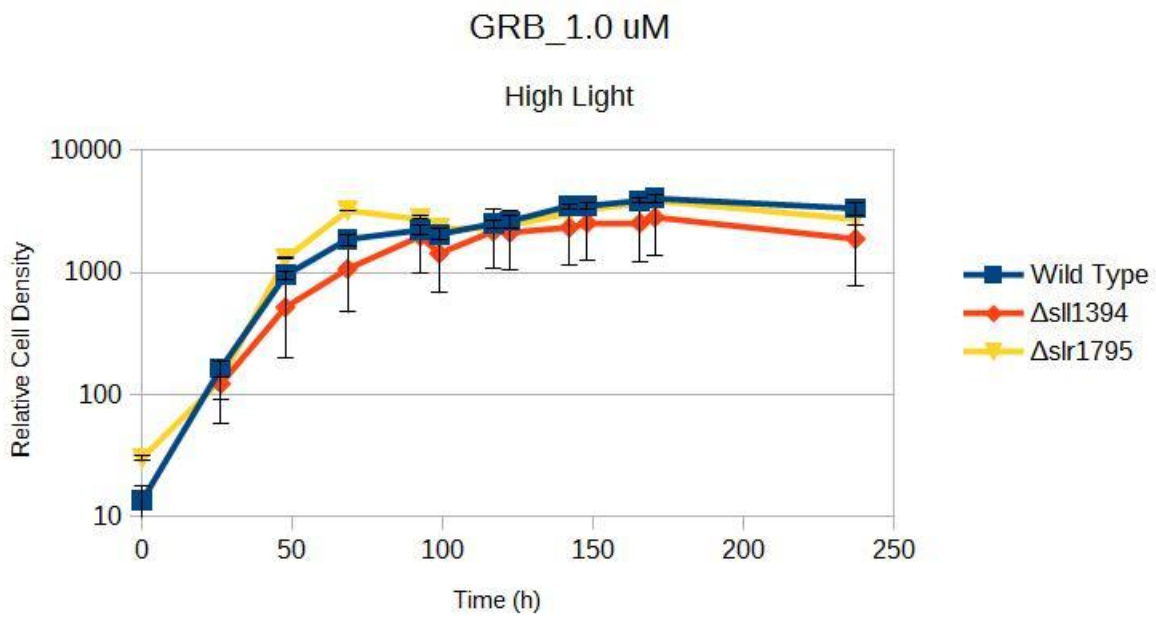

Figure Appendix 33: Averaged growth curve of strains with an $OD_{730\,nm}$ of 1.0 grown on Glucose + 1.0 uM of RB.

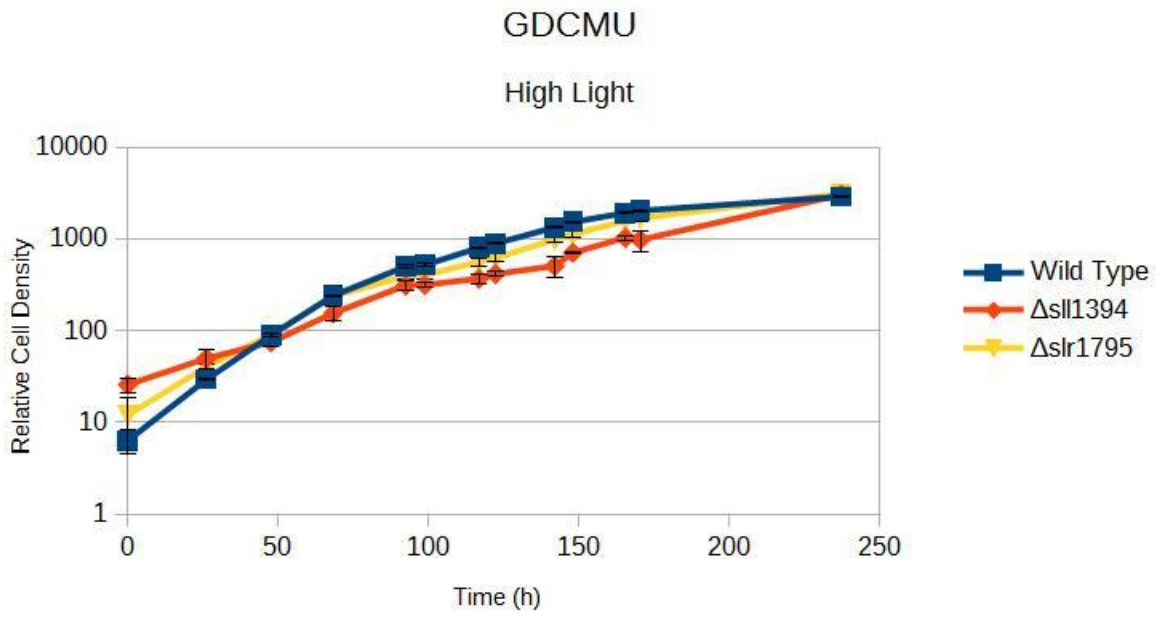

Figure Appendix 34: Averaged growth curve of strains with an $OD_{730\,nm}$ of 1.0 grown on Glucose + DCMU.

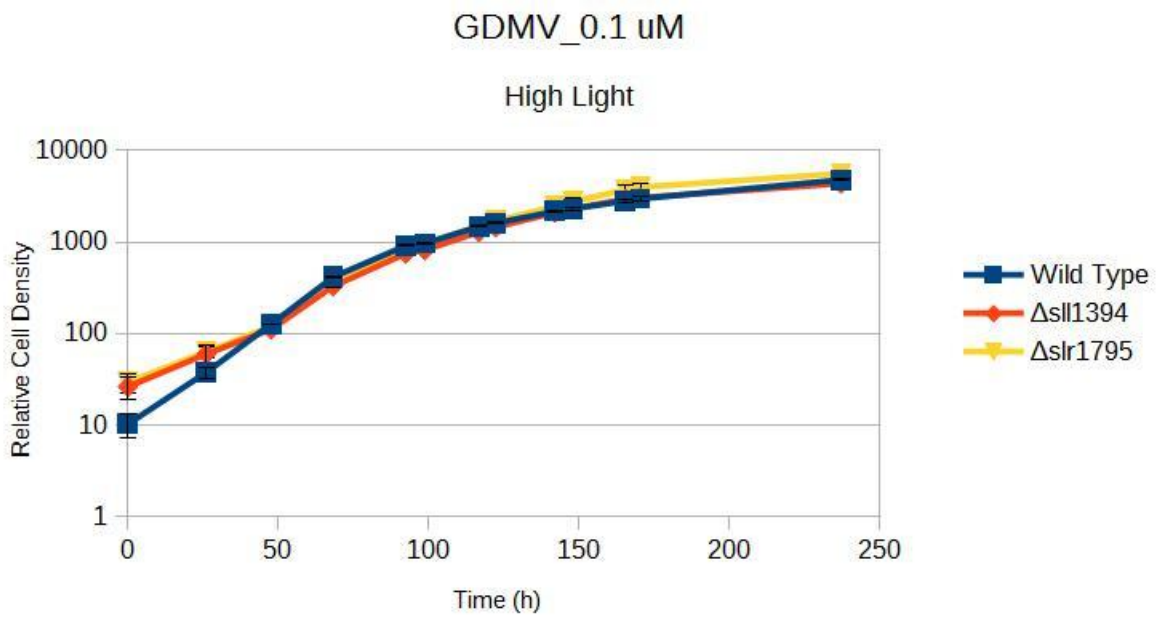

Figure Appendix 35: Averaged growth curve of strains with an $OD_{730\,nm}$ of 1.0 grown on Glucose + DCMU + 0.1 uM of MV.

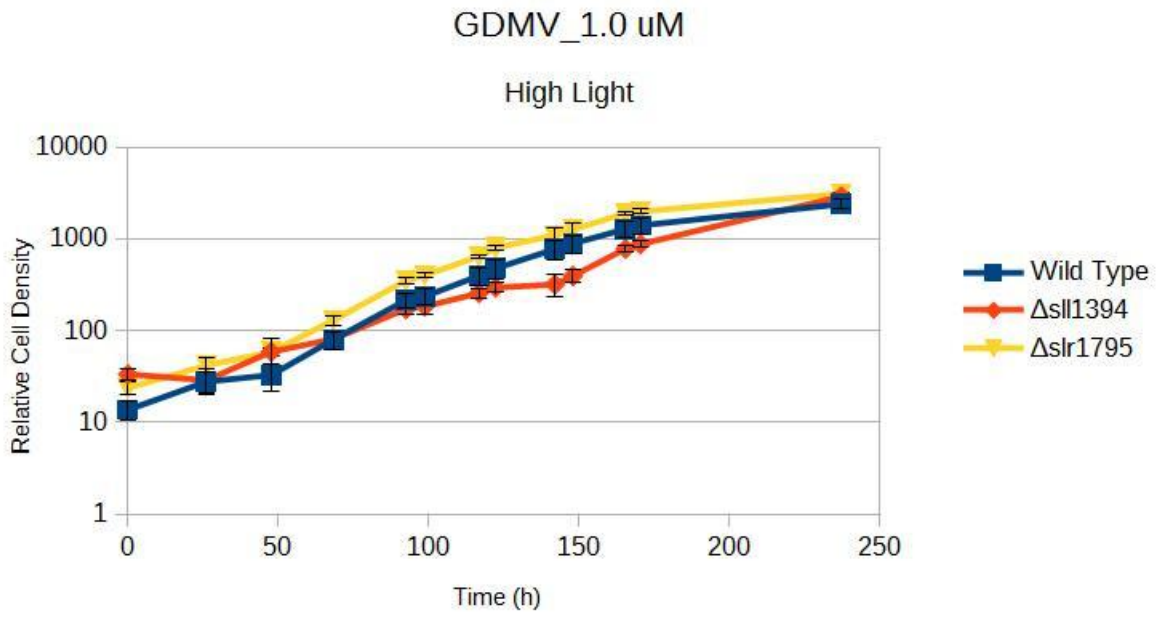

Figure Appendix 36: Averaged growth curve of strains with an $OD_{730\,nm}$ of 1.0 grown on Glucose + DCMU + 1.0 uM of MV.

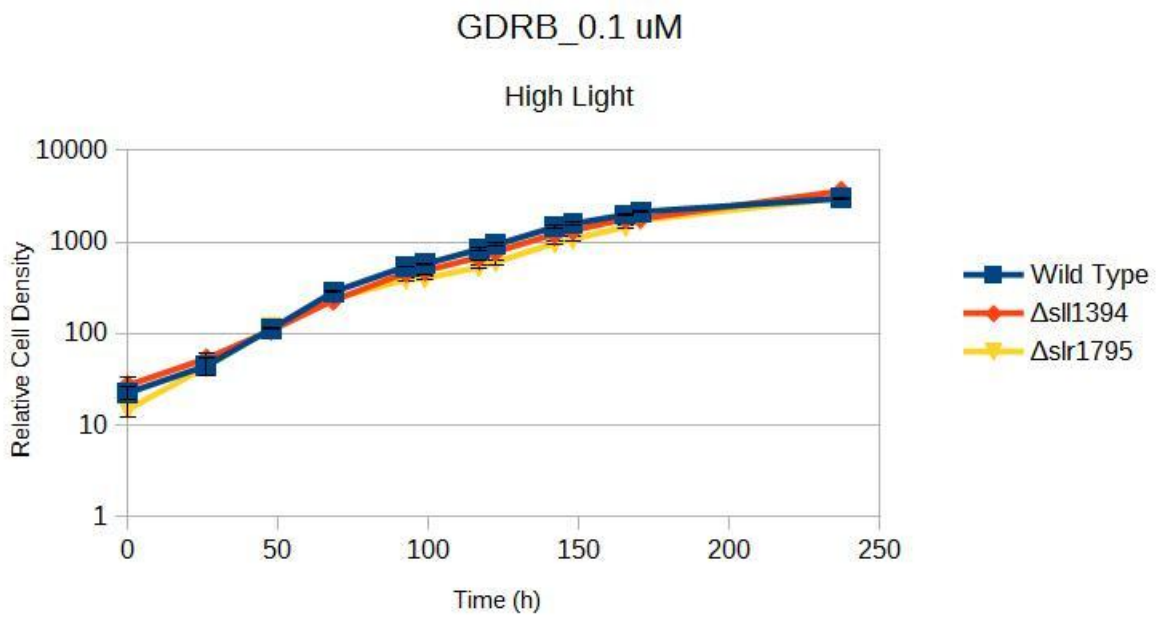

Figure Appendix 37: Averaged growth curve of strains with an $OD_{730\,nm}$ of 1.0 grown on Glucose + DCMU + 0.1 uM of RB.

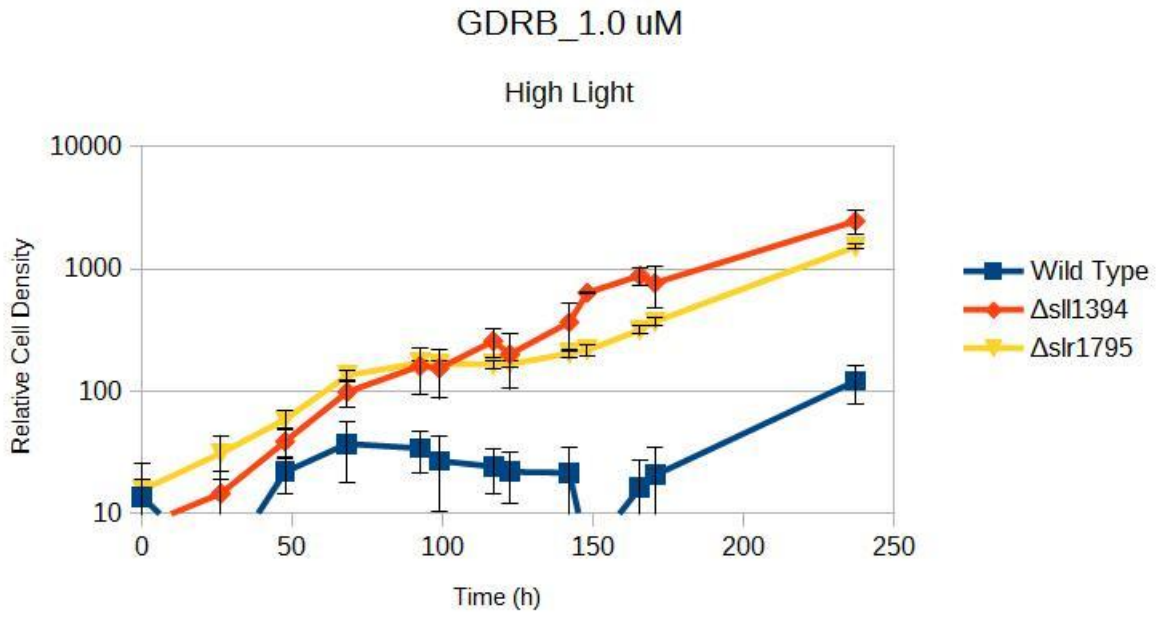

Figure Appendix 38: Averaged growth curve of strains with an $OD_{730\,nm}$ of 1.0 grown on Glucose + DCMU + 1.0 uM of RB.

B.2) Dark Condition

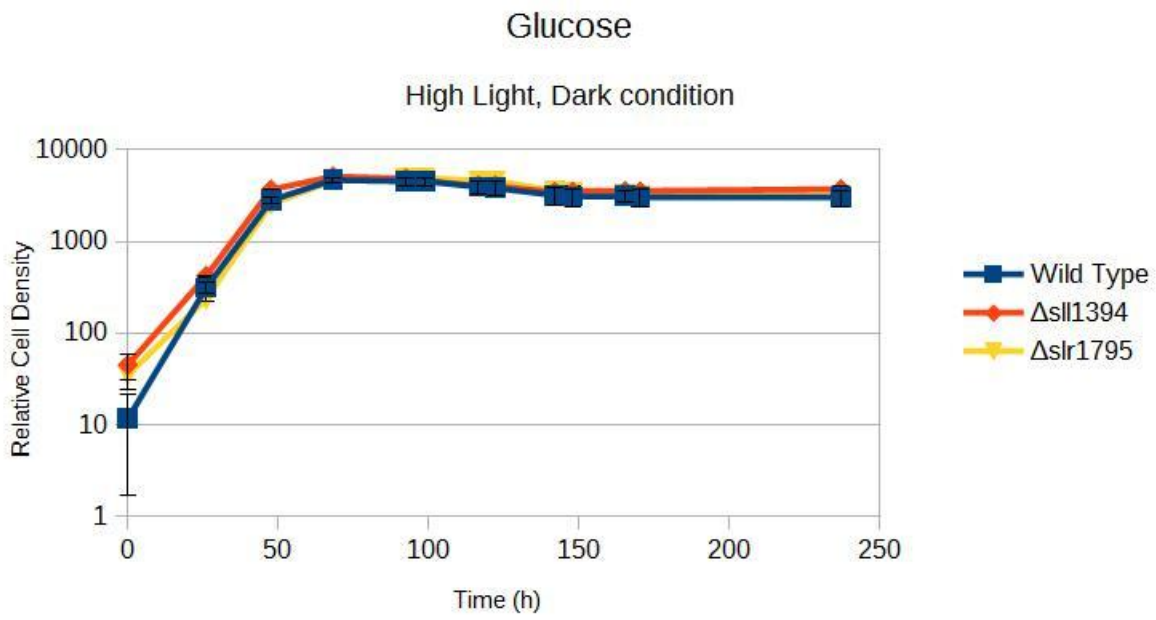

Figure Appendix 39: Averaged growth curve of strains with an $OD_{730\,nm}$ of 1.0 grown on Glucose.

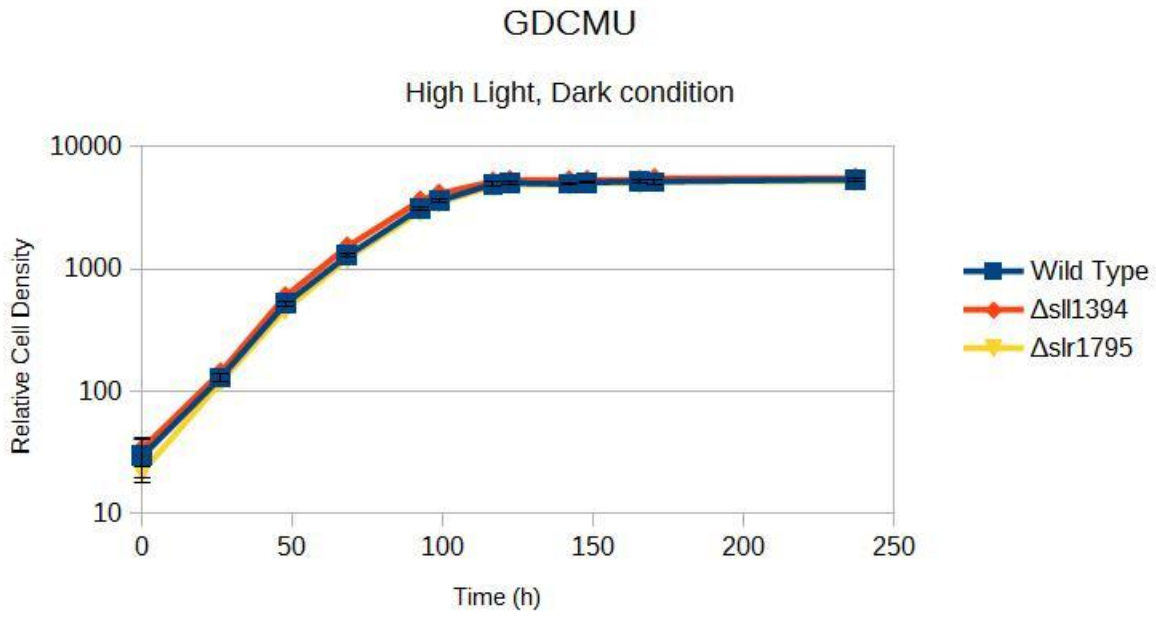

Figure Appendix 40: Averaged growth curve of strains with an $OD_{730\,nm}$ of 1.0 grown on Glucose + DCMU.

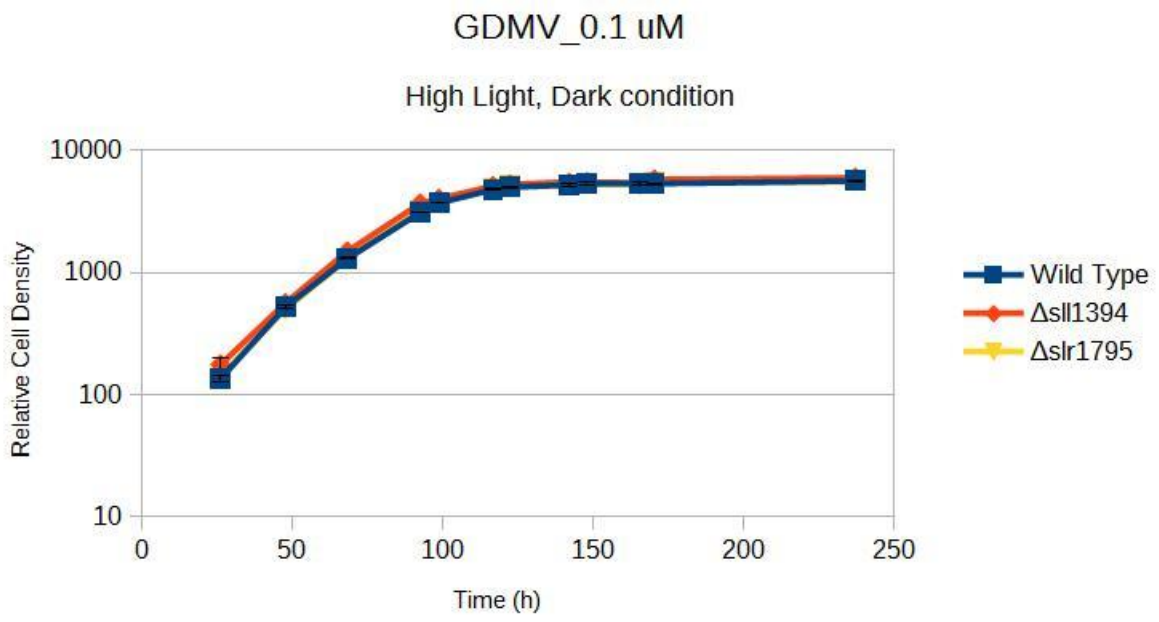

Figure Appendix 41: Averaged growth curve of strains with an $OD_{730\,nm}$ of 1.0 grown on Glucose + DCMU + 0.1 uM of MV.

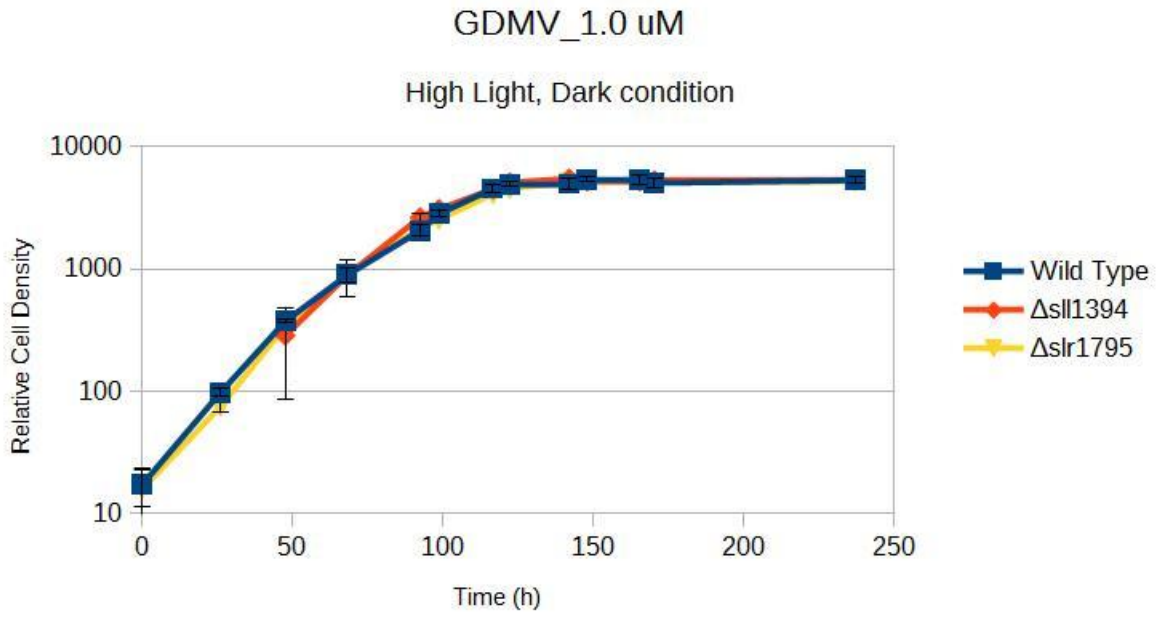

Figure Appendix 42: Averaged growth curve of strains with an $OD_{730\,nm}$ of 1.0 grown on Glucose + DCMU + 1.0 uM of MV.

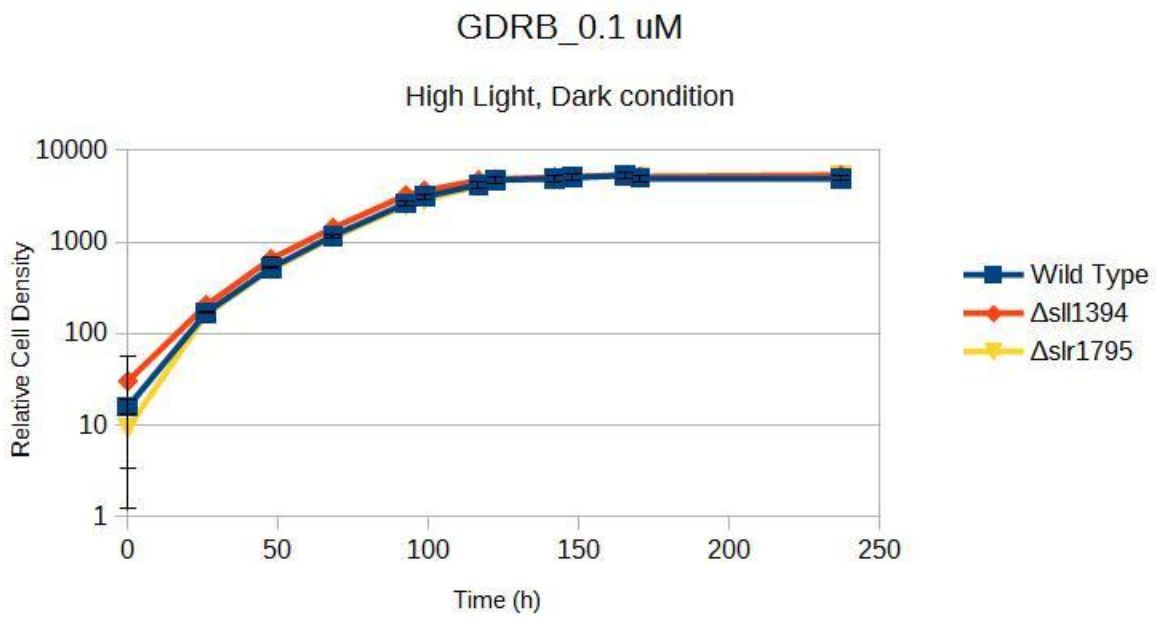

Figure Appendix 43: Averaged growth curve of strains with an $OD_{730\,nm}$ of 1.0 grown on Glucose + DCMU + 0.1 uM of RB.

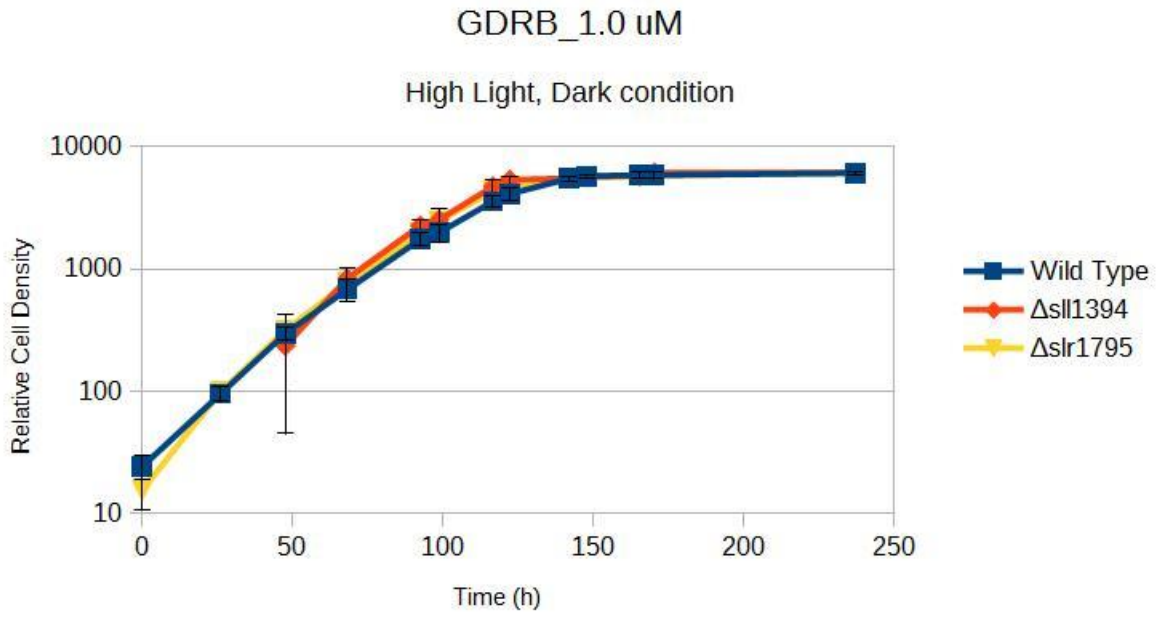

Figure Appendix 44: Averaged growth curve of strains with an $OD_{730\,nm}$ of 1.0 grown on Glucose + DCMU + 1.0 uM of RB.

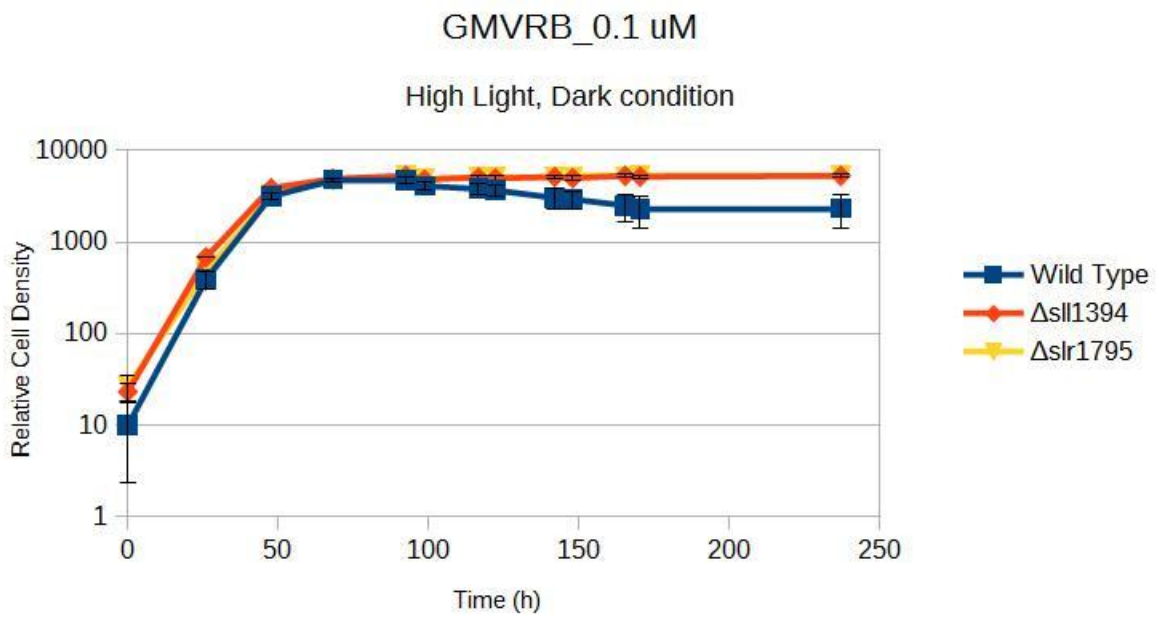

Figure Appendix 45: Averaged growth curve of strains with an $OD_{730\,nm}$ of 1.0 grown on Glucose + 0.1 uM of MV and RB.

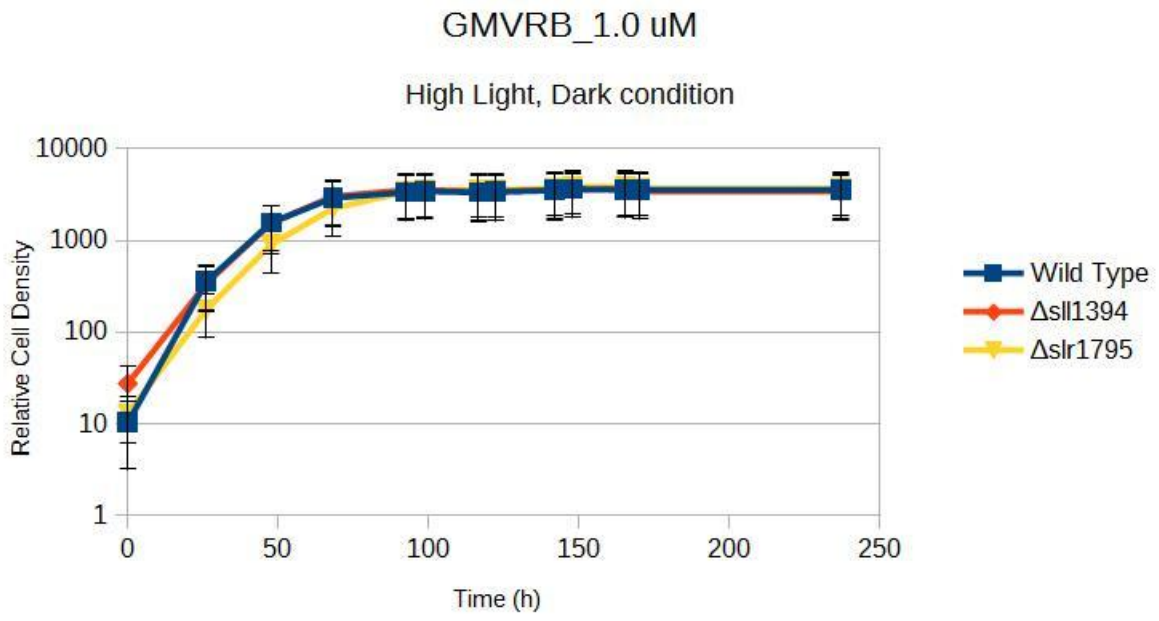

Figure Appendix 46: Averaged growth curve of strains with an $OD_{730\,nm}$ of 1.0 grown on Glucose + 1.0 uM of MV and RB.